MCR-76-387
NAS8-31574

Interim Report

September 1976

Payload/Orbiter Contamination Control Requirement Study

- SPACELAB CONFIGURATION CONTAMINATION MODEL

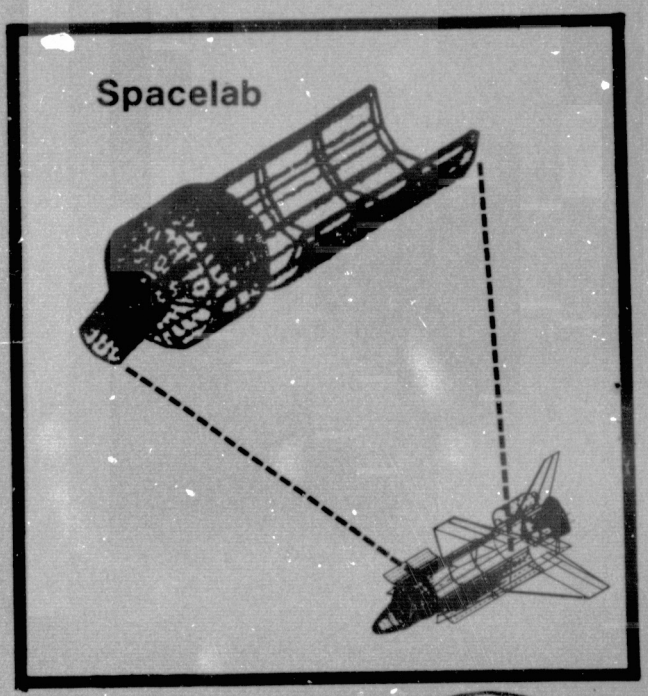

MARTIN MARIETTA

MCR-76-387
September 30, 1976

TECHNICAL REPORT

PAYLOAD/ORBITER CONTAMINATION CONTROL REQUIREMENT STUDY SPACELAB CONFIGURATION CONTAMINATION MODEL

INTERIM REPORT

CONTRACT NAS8-31574 EXHIBIT A

AUTHORS

L. E. BAREISS
M. A. HETRICK
E. B. RESS
D. A. STRANGE

PREPARED FOR

GEORGE C. MARSHALL SPACE FLIGHT CENTER
MARSHALL SPACE FLIGHT CENTER, ALABAMA 35812

BY

MARTIN MARIETTA AEROSPACE, DENVER DIVISION
P. O. BOX 179, DENVER, COLORADO 80201

CONTENTS

CONTENTS - CONTINUED

CONTENTS - CONTINUED

CONTENTS - CONTINUED

1. INTRODUCTION

The purpose of the overall study effort conducted under the NAS8-31574 contract was to continue the assessment of the Spacelab carrier induced contaminant environment and to determine the Spacelab's ability to meet established contamination control criteria for the Space Transportation System (STS) Program. The primary areas of on-going activity of the contracted study included updating, refining and improving the Spacelab Contamination Computer Model and contamination analysis methodology; establishing the resulting adjusted induced environment predictions for comparison with the applicable criteria; determining Spacelab design and operational requirements necessary to meet the criteria; conducting mission feasibility analyses of the combined Spacelab/Orbiter contaminant environment for specific proposed missions and payload mixes; and establishing a preliminary Spacelab mission support plan as well as model interface requirements between Martin Marietta and Marshall Space Flight Center (MSFC) facilities.

This interim report presents only a summary of those activities conducted to date with respect to the modeling, analysis and predictions of the induced environment including any modifications in approach or methodology utilized in the contamination assessment of the Spacelab carrier, Separate reports have been prepared to cover both the mission support plan and the model interface requirements. The emphasis in this report has been placed on the Spacelab modeling efforts which covers a period of effort of 15 months and is an extension of previous studies conducted for Spacelab that has spanned a time period of over two years. Topics presented in an earlier interim report have been included herein for completeness. The level of detail of this report has been based upon the most current available Spacelab data and on-going configuration and material modifications which will be expanded upon in the text. In this light, certain assumptions are currently being used in the analysis in order to bridge the gap between previous known configuration and available test data as well as anticipated data to be supplied when available by the National Aeronautics and Space Administration (NASA), the European Space Agency (ESA), or other European agencies. These are described herein with the thought that modifications will be necessary when the anticipated data is received.

The basic approach to this modeling study has been essentially two-fold. The first of these was conducted through

utilization of the Spacelab Contamination Computer Model in its current stage of development to support Spacelab design and development from a contamination viewpoint by establishing design and operational requirements early enough in the program for possible implementation. Secondly, the development and refinement of the computer model and methodology was continued with the ultimate goal of establishing a streamlined mission simulation model which could be used with minimum turn-around time, manual interpolations and calculations to accurately predict contamination impacts for specific Spacelab mission profiles and payload mixes in total.

Information and data set forth in this report includes: 1) descriptions of the modeled Spacelab configurations (subsection 2.1.1); 2) descriptions and evaluations of the major Spacelab contaminant sources (subsection 2.1.2); 3) explanation of the major updates and modifications that have occurred in the Spacelab modeling during this contract period and detailed assessments of the model improvement studies conducted (subsections 2.2 and 2.3 respectively); 4) a complete presentation of the current Spacelab induced environment predictions (subsection 2.4); and finally; 5) an evaluation of Spacelab's compliance with the existing contamination control criteria and the resulting Spacelab design and operational requirements necessary to insure that Spacelab contamination does not compromise the scientific and operational objectives of the Space Transportation System-Spacelab (STS-SL) Program presented in subsections 2.5 and 2.6.

The important conclusion which can be drawn from this study is that it is apparent from the analysis herein that many of the criteria are exceeded under the conditions evaluated. Spacelab design recommendations have been made, where feasible, to meet the criteria, but design alone does not necessarily satisfy all of the requirements. In certain cases; mission dependent recommendations such as orbital altitude, attitude, covers, etc. are necessary in order that Spacelab meet the intent of the criteria.

2. SPACELAB MODELING AND ANALYSIS

2.1 Major Model Parametric Considerations - A primary design goal for the various Spacelab configurations is to insure that the Spacelab/Orbiter systems and scientific instrument mission objectives are not compromised by the induced molecular and particulate contaminant environment emanating from the Spacelab carrier. To accomplish this, a rigorous computer modeling and analysis study has been conducted over the past 2½ years to establish the predicted on orbit contaminant environment levels under variable orbital conditions as well as to determine Spacelab contamination related design and operational requirements necessary to meet the maximum allowable induced environment levels or criteria as set forth in Volume X of JSC 00770[1]. These criteria have also been recommended for application as a design goal for Spacelab by ESA in ECR 00049[2]. The criteria state that it is a design and operational goal for Spacelab to control:

a. in an instrument field-of-view particles of 5 microns in size to one event per orbit;

b. induced water vapor column density to 10^{12} molecules/cm^2 or less;

c. return flux to 10^{12} molecules/cm^2/s;

d. continuous emissions or scattering to not exceed 20th magnitude/s^2 in the UV range; and

e. to control to 1% the absorption of UV, visible, and IR radiation by condensibles on optical surfaces.

This set of criteria, which is compatible with the contamination control criteria imposed upon the Orbiter[1], has been utilized as the baseline from which to make Spacelab design and development decisions throughout this report. It should be mentioned that other versions of the Spacelab contamination control criteria were evaluated during this contract, but for various reasons were not accepted by the program. Therefore, the above requirements are considered as the baseline criteria currently deemed acceptable by the National Aeronautics and Space Administration (NASA) and the European Space Agency (ESA). These criteria have been used as a basis in the modeling activities to establish a compatible model output format which facilitates the understanding of the criteria implications and aids in the performance of contamination evaluation studies.

Because of the dependence of the current model format upon the above contamination control criteria, it is important to note the additional assumptions and interpretations that are required to make the abbreviated criteria statements more applicable and useful in design and development evaluation. These interpretations will demonstrate the reasoning behind certain modeling decisions and approaches discussed in ensuing sections of this report. In his memo of May 24, 1976[3], R. Naumann of the Marshall Space Flight Center (MSFC), chairman of the Contamination Requirements Definition Group (CRDG) presented the necessary additional interpretations of these criteria that were established by the cognizant scientific user community. Included therein were:

a. The molecular column density of 10^{12} H_2O molecules/cm^2 is measured along any vector within 60° of the +Z axis originating at the Prime Measurement Point (PMP) X_o = 1107, Y_o = 0, Z_o = 507). It is further assumed that this represents the worst case situation.

b. The return flux of 10^{12} molecules/cm^2/s refers to the total flux on an unshielded surface (2 π steradian acceptance) oriented in the +Z direction at the PMP under worst case situation.

c. The 1% change in optical properties refers to the objective of an optical system that would typically have a dielectric surface at ambient temperature ($\sim 300^{\circ}K$) that is located at the PMP, is oriented along the +Z axis and has an acceptance of 0.1 steradian. It is also assumed that this is for a 7 day mission with random orientation of the ambient drag vector.

d. The 1 particle per orbit larger than 5 microns entering an instrument field-of-view assumes a field-of-view of 1.5×10^{-5} steradian and is restricted to particles within 5 km of the spacecraft.

e. The background brightness of a 20th magnitude star per square arc second in the ultraviolet region is equivalent to 10^{-12} $B_{\odot}$ at 360 nanometers.

As mentioned, the primary analytical tool utilized in this study was the Spacelab Contamination Computer Model which was developed to geometrically synthesize the contaminant sources, susceptible surfaces, transport mechanisms and establish the

predicted induced contaminant environment of the Spacelab carriers modeled. The general modeling considerations and approaches employed herein are identical to those in previous studies (References 4, 5, 6 and 7) combined with the model refinements and improvements discussed throughout this report. In the subsections that follow, a brief description of the current Spacelab modeled configurations and contaminant sources is presented along with those identified modifications, refinements and updates that have been incorporated during this contract period. The modifications reflect the most current established technology; the most recent available Spacelab source, configuration and thermal data; and where applicable, the results of the model improvement studies (subsection 2.3.1) conducted during this contract.

2.1.1 Modeled Spacelab Configurations - The current Spacelab Contamination Computer Model developed primarily for static design and development analysis consists of three unique Spacelab configurations deemed representative of the assorted module and pallet hardware combinations that will be utilized throughout the Spacelab Program. The Spacelab Contamination Computer Model has been formatted with certain basic elements similar to a more sophisticated dynamic program identified by the acronym VOLCAN (Vent, Outgassing and Leakage Contamination Analysis). VOLCAN, which is presently in the development phase, will have the flexibility to accept any vehicle configuration such as the Shuttle Orbiter (developed under separate contract to Johnson Space Center (JSC)) and to dynamically synthesize the contaminant environment for any given space vehicle mission parameters. In conjunction with the Spacelab and Orbiter segments, VOLCAN can be used for total combined Spacelab/Orbiter mission evaluation studies.

The current Spacelab configurations modeled include: 1) the long module/one pallet (LMOP); 2) the short module/three pallet (SMTP); and 3) the five pallet (FIVP) configurations. Geometrical data utilized in establishing the necessary model input parameters for these configurations was obtained from Reference 8. Contained therein was high resolution data for the LMOP Spacelab from which the SMTP and FIVP configurations were constructed. Figure 1 illustrates the basic LMOP configuration elements utilized in the geometric modeling. Note that the axis system and station numbers (X_o, Y_o, Z_o) presented are consistent with those of the Shuttle Orbiter coordinant system which is a baseline for this report. The primary purposes for developing the geometric configurations are to establish the spatial relationships between all Spacelab contaminant sources and surfaces and to obtain viewfactors (i.e.; the percentage of mass leaving

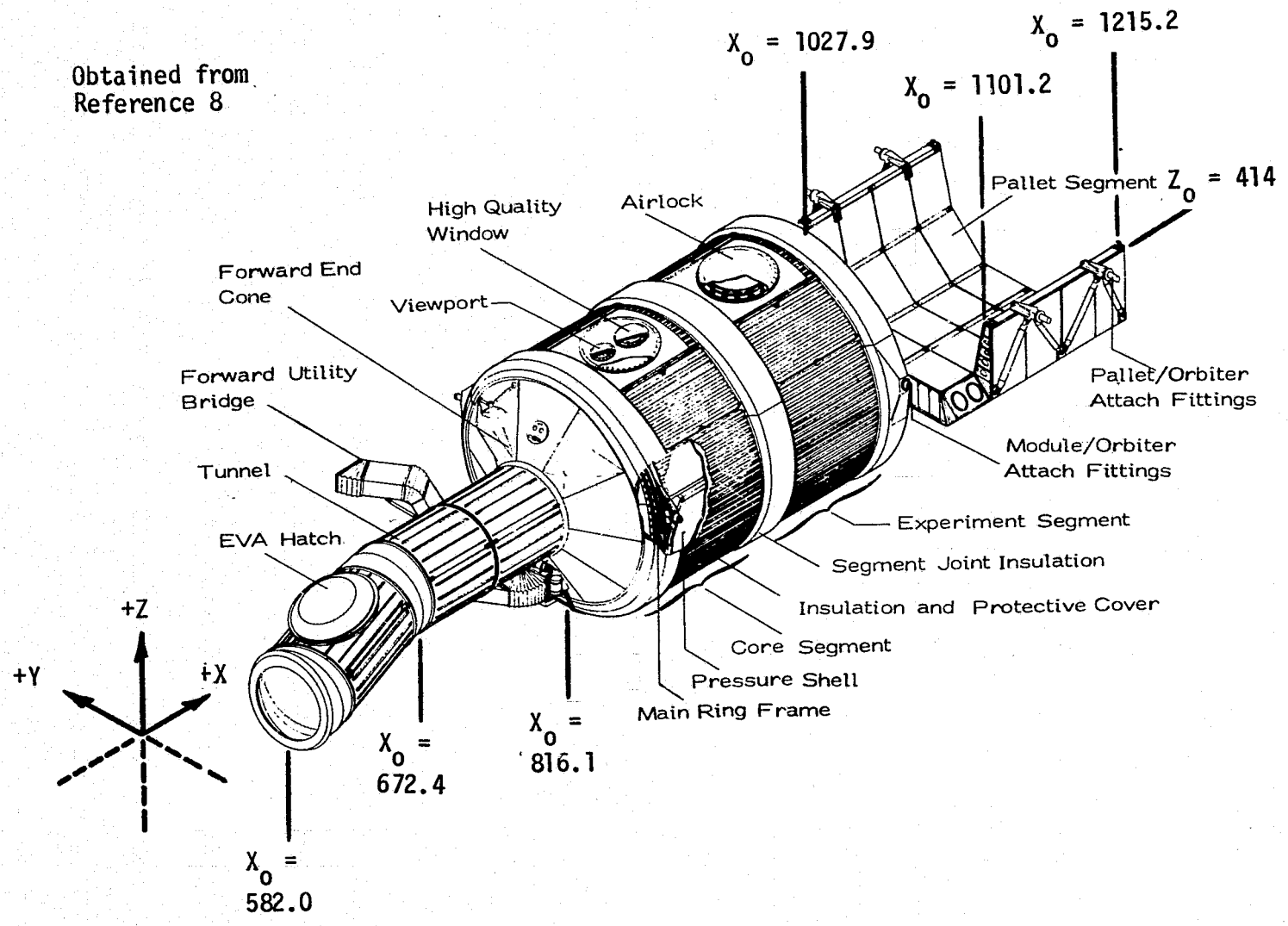

Figure 1. Baseline Long Module/One Pallet Reference Spacelab Configuration (LMOP)

a Lambertian source or surface capable of reaching another point or surface based upon geometry and surface shadowing between sources and receivers) which, when input into the model, formulate the basis for describing the Spacelab induced contaminant environment.

The three geometric configurations were segmented nodally and displayed graphically by the computer as depicted in Figures 2 through 4. The nodal breakdown of each configuration is used as the prime reference system between the configuration and contaminant source parametric data such as materials mass loss characteristics and surface temperature profiles discussed later. A specially modified Martin Marietta Thermal Radiation Analysis System (TRASYS-II)[9] is utilized to establish the necessary geometrical relationship input data to the Spacelab Contamination Computer Model, however, almost any properly modified configuration model can probably be used in its place. Once the required relationships are established, this segment of the model is no longer needed. However, any changes in geometrical relationships between surface and sources, require new relationships to be established from the TRASYS II program.

In order to establish consistency between the three modeled configurations, they were each located within the Orbiter payload bay envelope between X_o = 582.0 and X_o = 1215.2, as depicted in Figure 5. It is realized that hardware locations within the bay will vary depending upon center-of-gravity considerations, but the envelope utilized establishes a consistent base and allows adequate volume between X_o = 1215.2 and X_o = 1307 for auxiliary Orbital Maneuvering System (OMS) propellant tanks required for certain Spacelab missions. The payload bay surfaces (representative of the Orbiter payload bay liner) are included in the model for surface shadowing characteristics only and are not presently considered as contaminant sources in the Spacelab model predictions.

The Spacelab Contamination Computer Model not only considers contaminant transport directly between a source and a receiving surface but also evaluates the physics of the contaminant cloud in the near vicinity of the Spacelab. The major items included therein are the phenomena of the column density or "thickness" of the induced environment through which a payload must view and the return flux (or backscatter) of released contaminant molecules to a surface of interest resulting from molecular collisions with the ambient atmosphere. To evaluate these phenomena, seventeen (17) lines-of-sight for each Spacelab

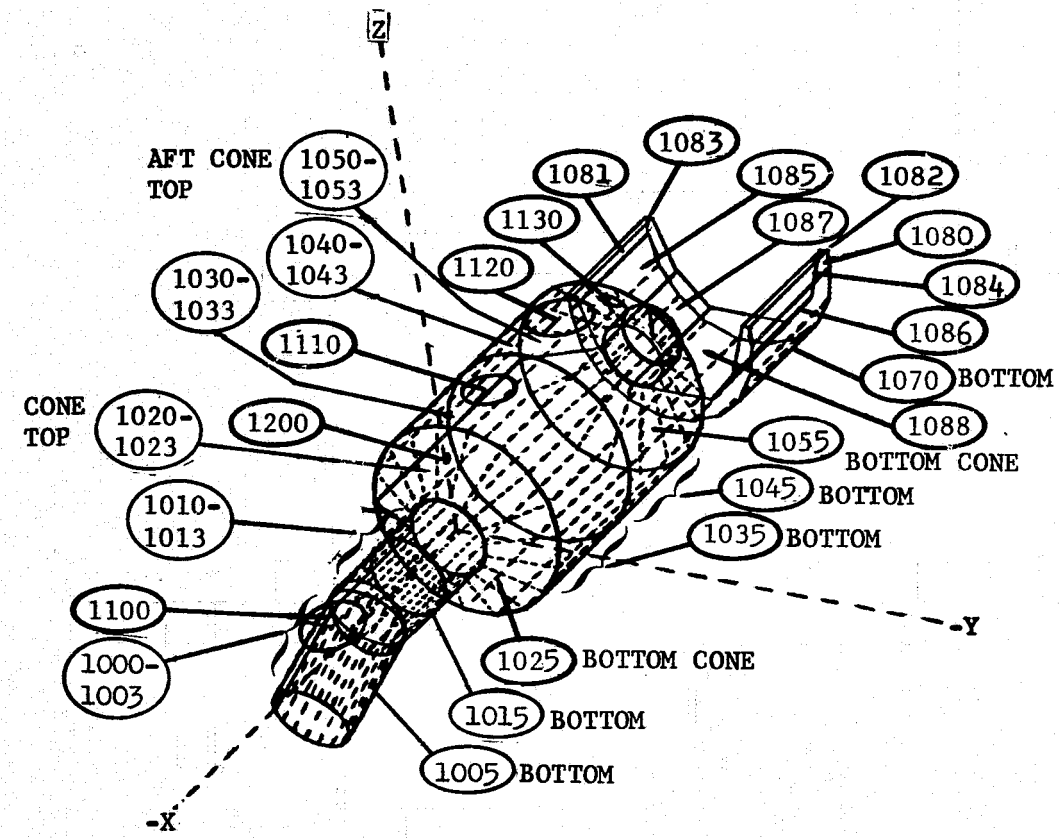

Figure 2. Primary LMOP Nodal Surface Number Assignments

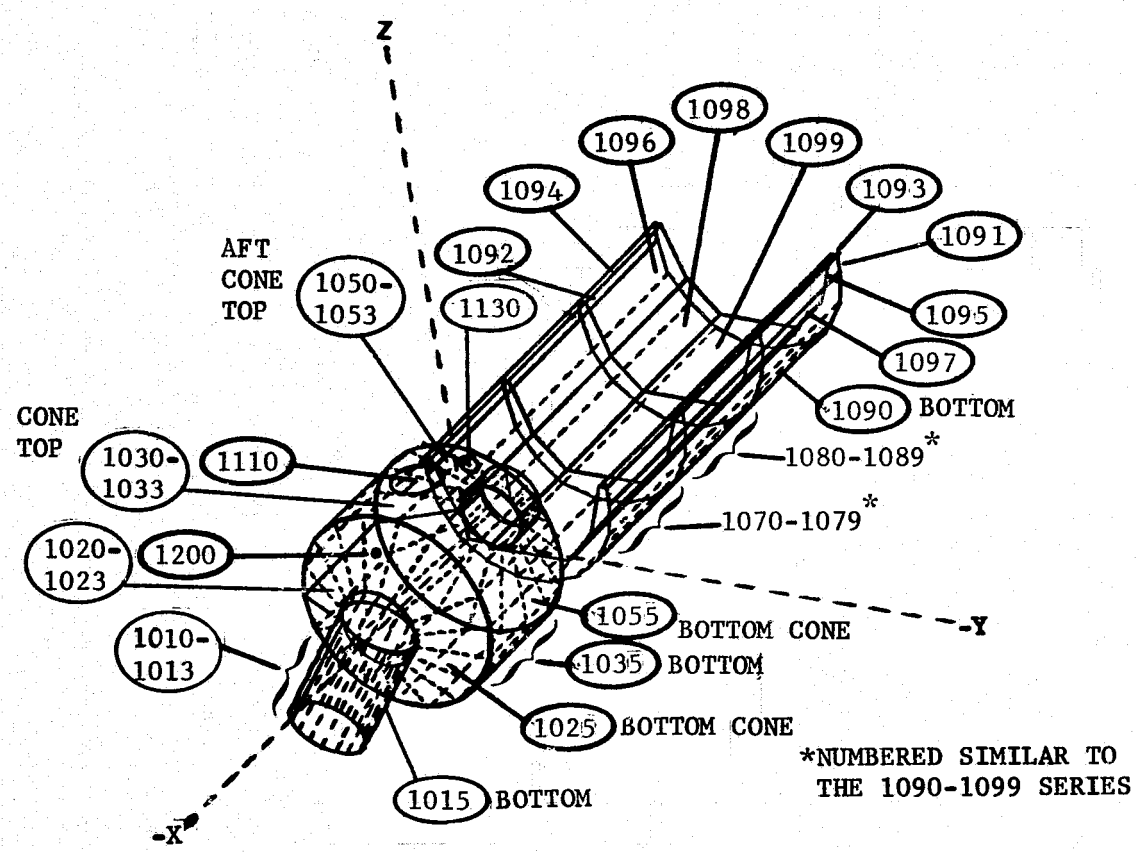

Figure 3. Primary SMTP Nodal Surface Number Assignments

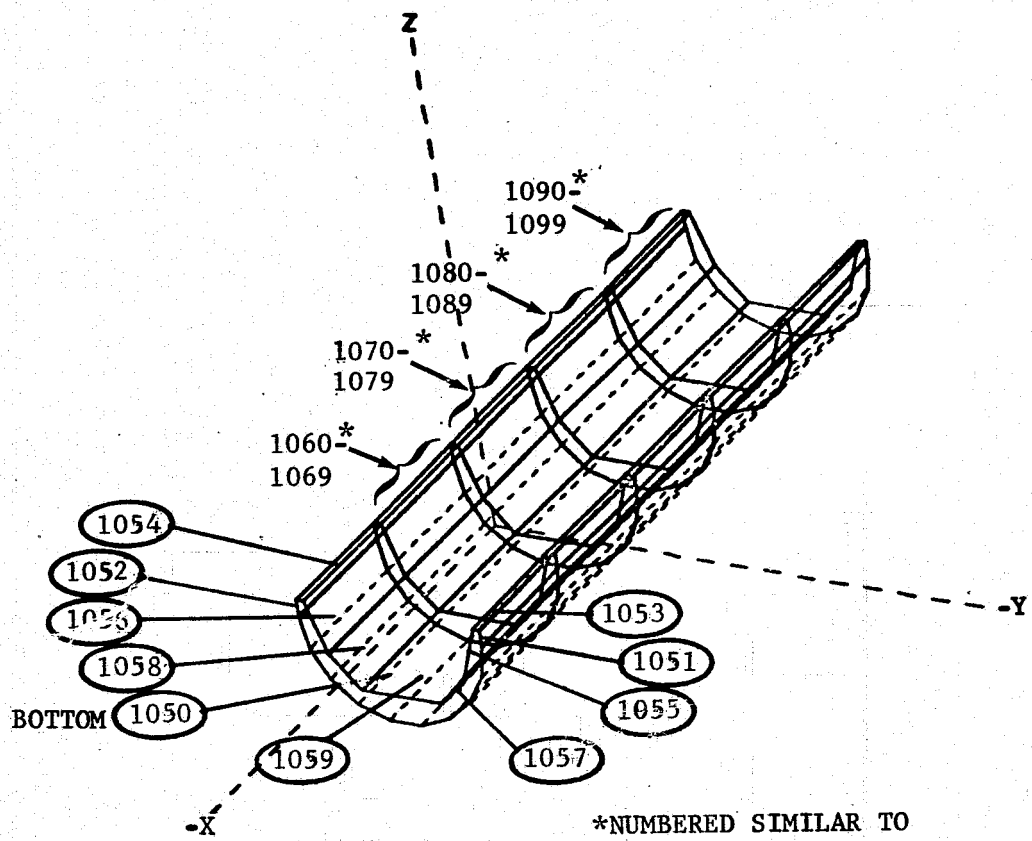

Figure 4. Primary FIVP Nodal Surface Number Assignments

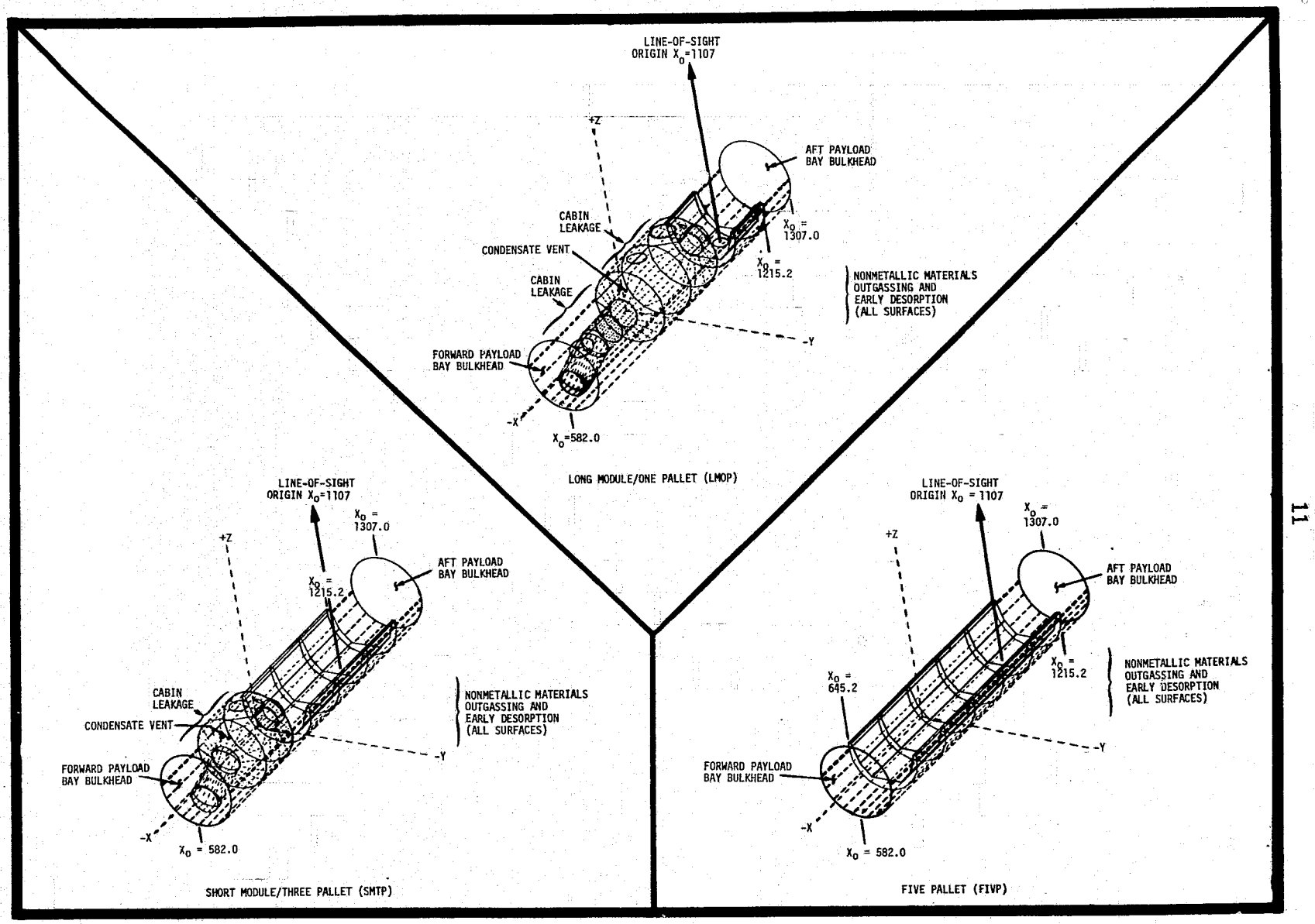

Figure 5. Modeled Spacelab Configurations and Contaminant Sources

configuration have been geometrically modeled. Along each of these lines-of-sight, a series of pseudo surfaces were input to the model as point receivers with all of the lines-of-sight originating at X_o = 1107, Y_o = 0 and Z_o = 507 (see Figure 5). This point of origination is consistent with the Prime Measuring Point (PMP) advocated by the Contamination Requirements Definition Group (CRDG) at MSFC for contamination control criteria evaluation. The lines-of-sight currently modeled were selected to uniformly encompass a 120 degree conical viewing volume around the +Z axis above the Spacelab configurations as illustrated in Figure 6 for the SMTP. This is also consistent with the CRDG interpretation of the contamination control criteria and encompasses the majority of viewing requirements of Spacelab payloads to be flown.

Although the three modeled Spacelab configurations are fairly similar in geometry and total surface area as well as the number of modeled lines-of-sight, the need for the present level of resolution and complexity of the Spacelab models can be graphically demonstrated by plotting the predicted number column densities for one of the Spacelab contaminant sources along the modeled lines-of-sight from the PMP as a function of viewing direction in the XZ plane. Figure 7 presents such an example for the nonmetallic materials outgassing source which is discussed in detail in subsections 2.1.2 and 2.4.1. Depicted in Figure 7 is a family of curves indicating the variation of total outgassing number column density for the maximum Spacelab thermal profiles for the three modeled Spacelab configurations. As can be seen, even though outgassing is modeled as a uniform Lambertian source, the column density variation can be as much as 100% for the Spacelab LMOP configuration. This variation can be even greater for less symmetric vehicles such as the Shuttle Orbiter, point sources such as the evaporator and the 38 RCS engines on the Orbiter and for vehicles which are coated with assorted nonmetallic materials that have different outgassing characteristics rather than the single material as assumed for all of the Spacelab surfaces.

The observed variation of column density with viewing angle is a function of Spacelab geometry, surface shadowing and surface temperature considerations and is not due to the cosine influence of the angles the lines-of-sight make with the +Z axis. If this latter point were true, the curves of Figure 7 would tend to increase in value toward the aft viewing directions displaying symmetry with the forward viewing directions. It should also be noted that if the line-of-sight origin were positioned at a

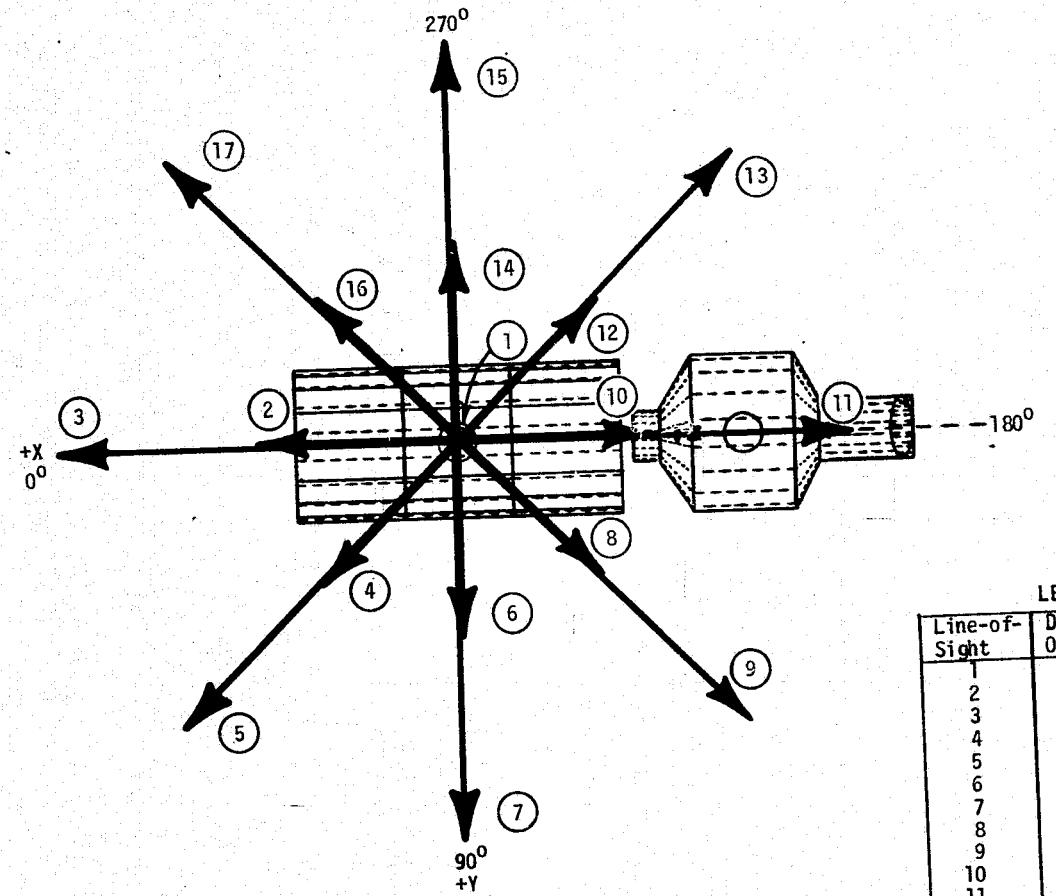

LEGEND

Line-of-Sight	Degrees Off +Z	Degrees Off +X
1	0	0
2	30	0
3	60	0
4	30	45
5	60	45
6	30	90
7	60	90
8	30	135
9	60	135
10	30	180
11	60	180
12	30	225
13	60	225
14	30	270
15	60	270
16	30	315
17	60	315

Figure 6. Modeled Lines-of-Sight for the SMTP Spacelab Configuration

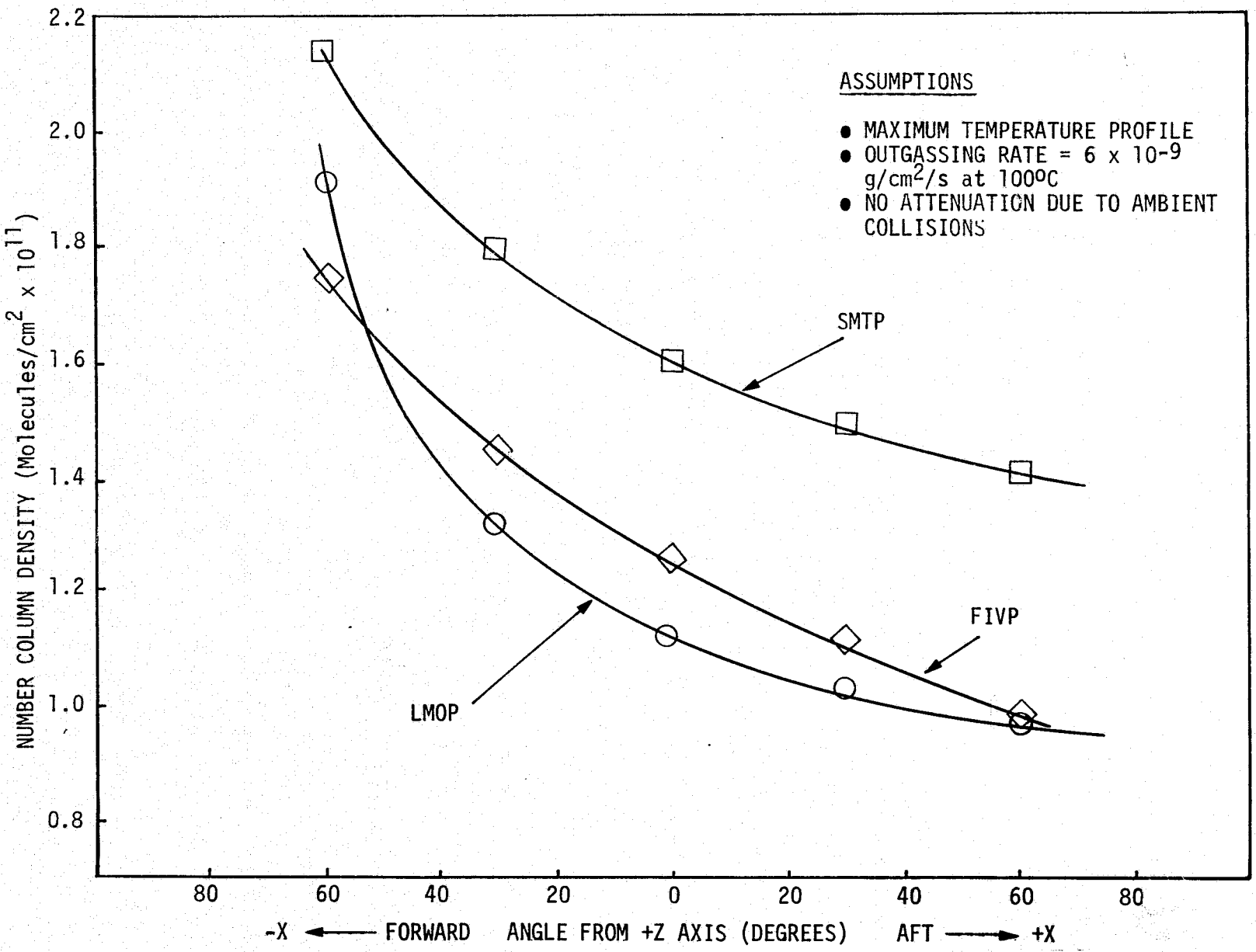

Figure 7. Variation in Total Column Density for Outgassing as a Function of Viewing Angle from the PMP

location other than the PMP or if other contaminant sources were evaluated, the absolute values and shapes of the curves would be totally different.

Some efforts have recently been made by Robertson[10,11] to evaluate the induced contaminant environment of a space vehicle by assuming a spherical spacecraft emitting contaminants at a constant mass loss rate uniformly in all directions. Such an approach can be taken without the use of a computer but in its simplicity, the resolution of the resulting predictions can suffer significantly. The methodology and physics employed by Robertson are sound within the limitations of the assumptions and are similar to those utilized in the Spacelab Contamination Computer Model. However, the approach has limitations such as the inability to vary source rates at different locations based upon temperature, time or material type and the inability to consider geometric and surface shadowing characteristics. Therefore the column density predictions resulting from such a simplified approach are forced to equal a constant value regardless of viewing direction. Where a particular value determined by such a technique might fall with respect to the model predictions for a particular spacecraft is unknown and becomes a strong function of systems information inferred or extrapolated to the simplified spherical case. Even if such a value were to fall within the range of predictions as presented for Spacelab in Figure 7, it would still be in variance by at least 50% for certain viewing directions. A 50% variance in making a design and development decision such as how much of a spacecraft should be covered with a given nonmetallic material or in the decision to change a given material could result in a significant cost consideration to a program such as the Spacelab Program.

The standard method to alleviate these shortcomings is the development of a configuration or system dependent model such as those that have been developed by other systems-evaluators (e.g.; thermal, power, flight operations, etc.). This supports the need for a somewhat more flexible approach such as the Spacelab Contamination Computer Model which establishes a consistent base for all pertinent systems data to the level of refinement necessary to insure the accuracy and resolution of the induced environment predictions for Spacelab design and development decisions. The configuration, nodal selection and line-of-sight complexities in the model have been established through considerable experience with spacecraft systems with this thought in mind without inducing unnecessary over complexity in understanding or running of the model.

2.1.2 Spacelab Contaminant Sources - The modeled Spacelab carrier configurations currently have four major contaminant sources identified which have been evaluated in detail. These include: 1) external nonmetallic materials outgassing (i.e.; the long term mass loss of the material upon exposure to space vacuum); 2) early desorption from external surfaces (i.e.; the initial high mass loss of adsorbed and absorbed volatiles, gases and liquids); 3) cabin atmosphere leakage from pressurized tunnel and module segments; and 4) the Spacelab Condensate Vent (SCV). A fifth source, the Avionics Bay Vent (ABV) which was previously analyzed has apparently been deleted from the system. For information concerning this potential contaminant source and its impacts, reference can be made to the previous Spacelab contamination modeling report[6] in which the ABV was analyzed in detail. Figure 5 should be consulted for the locations of the modeled contaminant sources for each of the three Spacelab configurations.

These sources are treated as closed form mathematical expressions which physically approximate the contaminant emission processes involved. Table I presents a parametric summary of the methodology and assumptions utilized in the modeling of these sources while the following paragraphs expand upon the primary considerations involved in determining the major expressions and relationships. It should be noted that through the modeling activities, the major contaminant transport mechanism of concern to Spacelab and its payloads is the phenomena of return flux through ambient interaction since most Spacelab/payload sensitive surfaces will not have direct line-of-sight to the contaminant sources.

a. Outgassing - Nonmetallic materials outgassing is modeled as a continuous Lambertian contaminant source with an emission rate that is a direct function of surface temperature (T in ^{o}C) and time (t in hours) of exposure to the vacuum of space. Available data from ESA[12] indicates that the final selection of the major external Spacelab Thermal Control Surface (TCS) material is yet to be made although two candidates (Z202 and S13G-Lo with various primers) are currently being considered. Reference 13 indicates that the solar oriented surfaces of Spacelab will be entirely coated with a white thermal control coating.

Due to the fact that materials mapping of the Spacelab external nonmetallics is not yet available, the model currently assumes that all Spacelab surfaces are coated with a material that just meets the implied outgassing

Table I. Summary Table for Major Spacelab Sources

Major Sources	Modeled Location	Duration/ Frequency	Flowrate	Constituents	Plume Shape Function	Velocity	Size Parameter
Outgassing	All External Spacelab Surfaces	Continuous	$6 \times 10^{-9} e^{-t/4100} e^{(T-100)/29}$ $g/cm^2/s$	Hydrocarbon Chain Fragments, RTV's, etc.	$\cos \theta / r^2$	$12.9 \sqrt{T(^oK)}$ m/s	Molecular Average M = 100
Early Desorption	All External Spacelab Surfaces	Continuous for the First 100 Hours On Orbit	$[2.16e^{-0.14t} + 1.74e^{-0.055t}] e^{(T-100)/29} \times 10^{-7}$ $g/cm^2/s$	Water, Light Gases, Volatiles	$\cos \theta / r^2$	$30.4 \sqrt{T(^oK)}$ m/s	Molecular Average M = 18
Cabin Atmosphere Leakage	Pressurized Module/ Tunnel Surfaces (Excluding Igloo)	Continuous	1.35 kg/day	O_2 N_2 CO_2 H_2O	$\cos \theta / r^2$	$2220 \sqrt{\frac{1}{M}}$ m/s	Molecular Average M = 29
Spacelab Condensate Vent	Module Forward End Cone - Venting 45^o Off +Z Towards -X in the X, Z Plane	Once Every Seven Days for 32 Minutes	0.91 kg/minute (35 kg/dump)	Water	Empirical 65^o Half Angle	7 m/s	Particles 30 μ to 900 μ Radius

M = Molecular Weight
T = Temperature (^oC unless noted)
t = Time (hours) of Vacuum Exposure

θ = Angle (degrees) Off Surface Normal or Plume Centerline
r = Distance (cm) from Emitter to Receiver

rates of a material qualified under the recognized materials screening criteria[14,15]. Reference should be made to subsection 2.2.1 for an evaluation of this parameter. The modeled baseline outgassing rate at 100°C is 6.0×10^{-9} g/cm^2/s and varies with surface temperature as $e^{(T-100)/29}$ where T equals the temperature in °C.

Outgassing rates and early desorption rates (discussed later) are input into the model at the 100°C reference temperature and then adjusted internally in the model for individual nodal surface temperature. Based upon observed inflight Skylab data, the outgassing rate is modeled to also vary with exposure time as $e^{-t/4100}$. This equates to a near constant rate with time over a seven to thirty day Spacelab mission.

Identification of the constituents of nonmetallic materials outgassing has been accomplished in part through extensive ground based thermal vacuum testing and the resulting acquired mass spectroscopy data. Such data for "typical" silicon-based external spacecraft thermal control coating materials like S13G or S13G-Lo indicate the primary outgassing products to be various forms of the methylpolysiloxane polymer which has the general cyclic formula:

$$\left[(CH_3)_2\ SiO\right]_n$$

A single link of this polymer has a molecular weight of 74 AMU. Linear methylpolysiloxane combines the above form with two end links having the formula:

$$(CH_3)_3\ SiO_{\frac{1}{2}}$$

One of these end links has a molecular weight of 89 AMU, and for any complete linear methylpolysiloxane molecule there are only two of the 89 AMU links for n number of the 74 AMU links. Therefore, for any "typical" methylpolysiloxane polymer outgassing mass spectrum, the 74 AMU peak predominates. However, outgassing does not occur in single chain links only as can be seen in Figure 8 which is a typical example of acquired field emission mass spectrum data for an outgassing material such as methylpolysiloxane.

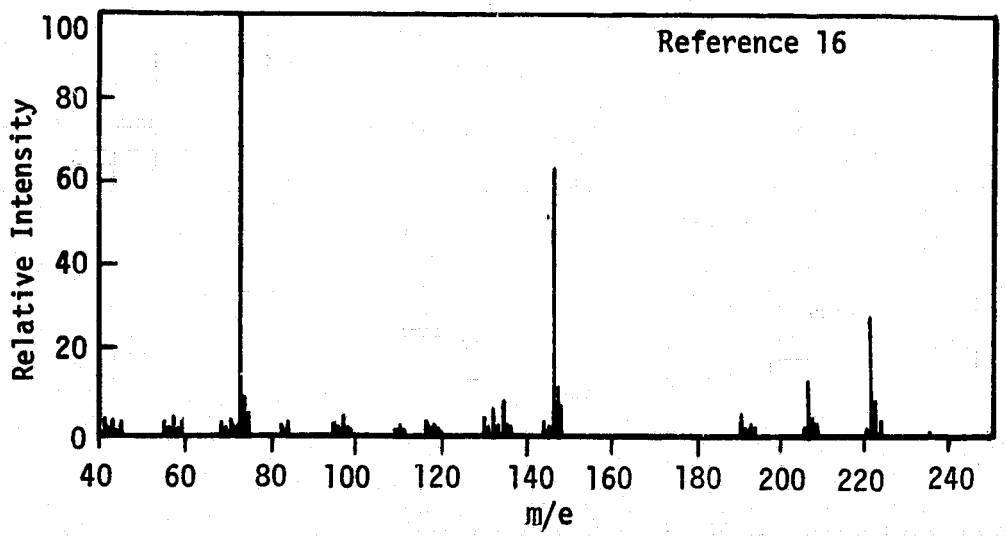

Figure 8. Typical Methylpolysiloxane Outgassing Mass Spectrum

As illustrated, the 74 AMU mass predominates but reduced numbers of links of AMU 148 and 222 show up in the spectrum so that the average molecular weight lies between 74 and 148, favoring the lower AMU somewhat and falling near an average molecular weight of 100.

Further investigation of other polymers indicates that those having smaller link masses than the methylpolysiloxane have a higher percentage of two and three link masses in their mass spectra and the larger link polymers tend to have even a higher percentage of single links. The result is that the average molecular weight of outgassed molecules from "typical" aerospace nonmetallic materials appears to be near 100 AMU and consequently this value is utilized in the Spacelab contamination modeling and analysis activities.

b. Early Desorption - A similar approach is utilized in modeling the phenomena of early desorption, however, in contrast to outgassing; the early desorption rate decays rapidly upon initial exposure to space vacuum. Generally, the early desorption rate will fall below the outgassing mass loss rate in 50 to 60 hours and essentially disappear in 100 hours. This is modeled based upon the expression $2.16e^{-0.14t} + 1.74e^{-0.055t}$ with t in hours of vacuum exposure. This equates to an early desorption rate at 100°C of 1.5×10^{-7} g/cm^2/s at 10 hours into the decay curve. The 10 hour point has been selected for

modeling early desorption herein to present worse case predictions for payloads at the point when activation of susceptible instruments might be expected to commence. An average molecular weight of 18 is assumed in the modeling for the early desorption species at this 10 hour point in the mission.

c. Cabin Atmosphere Leakage - Cabin atmosphere leakage is limited to the pressurized volumes of the LMOP and SMTP Spacelab configurations. For those pressurized volumes which include the module and tunnel segments only, leakage is modeled as a Lambertian source being emitted uniformly from their external surfaces. Molecular velocities are based upon the internal cabin atmosphere gas temperature of 25°C. Leakage is modeled as a constant steady state source for the LMOP and SMTP pressurized volume surfaces having the following mass fraction of molecular constituents:

Constituent	Mass Fraction	
N_2	0.75	Average Molecular Weight = 29
O_2	0.23	
CO_2	0.01	
H_2O	0.01	

Data on leakage of N_2 from the Spacelab Igloo module is currently to be determined by ESA. When received, this source can be easily incorporated into the model. Evaluation of this source is quite necessary due to its proximity to many of the pallet mounted Spacelab payloads.

d. Spacelab Condensate Vent - The SCV final design is yet to be determined, however, indications are that it will be similar to the Skylab contingency condensate vent which was tested in situ during the Skylab Contamination Ground Test Program (SCGTP) at Martin Marietta, Denver Division. The parameters in Table I for the SCV reflect the SCGTP results. The SCV was previously analyzed extensively in Reference 5 based upon these parameters. Since no additional design data has been supplied by ESA, the evaluation was not modified. It suffices to say that since the current design allows a large portion of the SCV vent plume to impinge upon structural surfaces of the Orbiter payload bay that the vent should be relocated to a more optimum location. Further analysis is pending a response by ESA.

2.1.3 Primary Contaminant Transport Considerations - In addition to the aforementioned modeling considerations for configurations and sources, basic parametric and methodological assumptions are employed in the Spacelab contaminant transport modeling and analysis which warrent mentioning. These include approaches to determining contaminant return flux, mean free path influence upon molecular column density and deposition upon sensitive surfaces. These will be discussed in the ensuing paragraphs.

2.1.3.1 Return Flux Determination - Due to the geometries of the Spacelab carriers, the primary transport mechanism of contaminant species between sources and receivers is the phenomena of return flux or backscattering of emitted molecules resulting from collisions with the ambient atmosphere. Direct line-of-sight source-to-surface transport and self scattering of contaminant molecules have been considered in the modeling (see subsections 2.3.1.5 and 2.3.1.2, respectively) and are of concern to Spacelab and its payloads under isolated conditions.

The relationship for modeling the return flux (RF) to a surface of interest along with the assumptions employed in the contamination modeling is:

$$RF = N_A V_A \sigma_A \cdot NCD \cdot \frac{\Omega}{\pi} \cdot \cos \alpha$$

where,

N_A = ambient density, molecules/cm^3 (medium density profile as function of altitude assumed)

V_A = orbital velocity, 7.65×10^5 cm/s assumed

NCD = molecular column density, molecules/cm^2 (calculated by the model)

Ω = sensitive surface geometric acceptance angle, steradians (0.1 and 2π assumed)

σ_A = scattering cross section of colliding molecules, cm^2 (8.3×10^{-14} cm^2 assumed for outgassing/ambient collisions and 3.1×10^{-14} cm^2 assumed for early desorption/ambient and leakage/ambient collisions)

α = angle ambient drag vector makes with surface normal (0 degrees assumed)

An important factor in the calculation of the return flux of contaminant molecules through collisions with the ambient

atmosphere is the "collision sphere of influence" or scattering cross section of the interacting molecules. Ideally, one would employ an experimentally determined scattering cross section for each interacting pair combination. As indicated in Table II, scattering cross sections have been measured for only a few polyatomic collisions similar to what may be anticipated for the Spacelab contaminant molecules interacting with ambient species.

Table II. Scattering Cross Sections for Various Polyatomic Collisions[17,18]

Colliding Substances	σ Total Scattering Cross Section	v Incident (km/sec)	$\delta_x + \delta_y$ Effective Scattering Diameter (Å)	Ref.
H_2O/H_2O*	$6.15 \pm .65 \times 10^{-14}$ cm^2	.60	28	17
NH_3/H_2O	$3.85 \pm .53 \times 10^{-14}$ cm^2	.63	22	17
	$3.70 \pm .46 \times 10^{-14}$ cm^2	.67	21.6	17
H_2O/H_2O	$3.2 \pm .3 \times 10^{-14}$ cm^2	.92	20	18
	$3.1 \pm .3 \times 10^{-14}$ cm^2	.96	19.9	18
	$3.07 \pm .3 \times 10^{-14}$ cm^2	1.00	19.8	18
CO_2/N_2	$4.04 \pm ? \times 10^{-14}$ cm^2	.45	22.6	18
CO_2/O_2	$3.97 \pm ? \times 10^{-14}$ cm^2	.45	22.4	18

*Snow et al (Reference 18) contends there was a "systematic error" in the H_2O/H_2O scattering experiments of Kydd (Reference 17).

There are no generally accepted values for total scattering cross sections for most of the space borne contaminants. In particular, outgassing can be composed of plastisizers, additives, polymerized fragments, etc. Therefore, the size of each outgassing molecule can vary greatly depending on the material involved and the environment seen. Polymers have physical dimensions in the range from 10Å to 10,000Å. Under the influence of solar ultraviolet, formation and breaking of molecular chains can lead to a different distribution of molecular weights and sizes. Volatile Condensible Material (VCM) tests generally provide enough time and a closed environment for the outgassed species to form droplets, thus the diameters of 10,000Å measured in the laboratory[19] are probably too high for space application.

In lieu of specific experimental data, there are certain assumptions and available data which can be utilized to infer the scattering cross sections. One approach is to use the hard sphere interaction model which assumes the cross section is a circle whose radius is the sum of the effective radii of the colliding molecules. This is analytically expressed as

$$\sigma = \pi \cdot \frac{d_{eff}^2}{4} = \frac{\pi(d_x + d_y)^2}{4}$$

where d_x and d_y represent diameters of the two interact- species.

As described in molecular theory texts such as Reference 20, the microscopic structure of a molecule including its potential or force fields (and subsequently its "diameter") can be deduced from macroscopic measurements such viscosity, heat conduction, or pressure-temperature variations. As indicated in Table III, molecular diameters have been inferred from viscosity measurements for several simple gases and hydrocarbons. It is important to note that diameters deduced from viscosity measurements of water do not correlate with those deduced from actual scattering observations (refer to Table II).

Table III shows, as one would expect, a general increase in diameter as the molecule becomes more complex. Unfortunately, there do not appear to be any diameters reported in the literature for the complex space type contaminants such as the methylpolysiloxanes. Robertson[10] in his report on spacecraft self-contamination assumes a value of 6.56Å. Scialdone[21] of GSFC and Harvey[22] of Lincoln Laboratory both use a development by Mirtov[23] which defines a relative mean free path as a function of the satellite and desorbed molecular velocities. This treatment does not account for the mass or diameter of the colliding molecules.

Based upon the assumption that the viscosity diameters depicted in Table III are representative of Spacelab contaminant species, the average hydrocarbon (outgassing) diameter would be near 7.5Å for an average molecular weight of approximately 90 and the early desorption/leakage diameter would be approximately 3.3Å. This latter value of 3.3Å is also assumed to be valid for the viscosity diameter of the ambient atmosphere which is composed primarily of atomic oxygen and diatomic nitrogen. Utilizing these values from literature, the outgassing/ambient and early desorption or leakage/ambient viscosity diameter sums $(d_x + d_y)$ would be 10.8 and 6.6Å, respectively.

Table III. Equivalent Molecular Diameters from Viscosity[20]

	Molecular Gas	Temperature °K	Molecular Weight	Diameter (d) Å
Characteristic of Early Desorption/Leakage	N_2	91.5	28	4.132
	O_2	113	32	3.853
	CO_2	190	44	4.485
	H_2O	380	18	2.975
Characteristic of Hydrocarbons (Outgassing)	$n\text{-}C_4H_{10}$	410	58	5.609
	$i\text{-}C_4H_{10}$	313	58	5.995
	$n\text{-}C_5H_{12}$	345	72	6.475
	$n\text{-}C_6H_{14}$	413	86	6.633
	$n\text{-}C_7H_{16}$*	282	100	9.967
	$n\text{-}C_8H_{18}$	320	114	8.363
	$n\text{-}C_9H_{20}$	240	128	9.483
	Cyclohexane	324	84	6.839
	C_6H_6	440	78	5.915

*From second virial coefficient.

Scattering test data from References 17 and 18 for various polyatomic gas collisions at relative velocities near 1×10^5 cm/s indicate scattering cross sections of $3.1 \pm 0.3 \times 10^{-14}$ cm^2 for the molecular species tested (see Table II). This indicates that an effective diameter sum deduced from actual scattering experiments is 19.9Å which is approximately three times the corresponding average viscosity diameter of 6.6Å for similar collisions (i.e.; $\delta_x + \delta_y = 3(d_x + d_y) = 19.9$Å). This distinguishes between molecular sizes based solely upon viscosity or intermolecular potential energy theory, and the effective molecular sizes based upon scattering phenomena which is applicable to return flux modeling. This apparent increase in molecular size during the collision process is a result of the "sphere of influence" created by the charge, polarizability and internal energy of the dipole molecules. Applying this relationship to the outgassing/ambient collision process results in an effective scattering cross section of $\sigma = \frac{\pi}{4}(3 \times 10.8\text{Å})^2 = 8.3 \times 10^{-14}$ cm^2 representing an effective total diameter of approximately 32 to 33Å. Application of this phenomena to

outgassing molecules appears valid when considering that the outgassing constituents will most likely be ionized and dipole in nature. As stated previously, this scattering cross section as well as the 3.1×10^{-14} cm^2 cross section utilized in the modeling for leakage and early desorption/ambient collisions is based upon test data for relative molecular velocities near 10^5 cm/s. The cross section is known to be velocity dependent so that an orbital velocity of 7.65×10^5 cm/s may alter the effective scattering cross section. It is known that as the relative velocities increase between the molecules, the cross sections become smaller. Plotting the data in Table II as a function of relative velocity indicates a trend toward a smaller σ of 1.2×10^{-14} cm^2 at orbital velocity. With such limited data it is difficult to verify the slope or shape of the curve at Spacelab velocities. For Spacelab velocities, the scattering cross sections would not be expected to be decreased significantly over those observed in the available test data. Velocities much higher than expected for Spacelab would be required to reduce the scattering cross section where the effective diameters of collision approach those of the viscosity measurements.

It should also be pointed out that in each of these scattering events there is a significant probability that the collision will be elastic and that internal energy modes will be excited. For example, data is available that indicates approximately 6% of the collisions with water molecules will excite the ν_3 stretch vibrational mode of the H_2O. When this excited state collapses, energy is radiated at 2.7 μ and could provide a mechanism for measuring return flux. It is recommended that further evaluation be conducted into the subject of return flux and that limited laboratory testing be conducted to establish scattering cross sections for the major Spacelab molecular sources at relative velocities in the 7 to 8×10^5 cm/s range. Until such data is available, the model will assume the following scattering cross sections for determining return flux:

$$\sigma_{out} = 8.3 \times 10^{-14} \text{ cm}^2$$
$$\sigma_{ED} = 3.1 \times 10^{-14} \text{ cm}^2$$
$$\sigma_{leak} = 3.1 \times 10^{-14} \text{ cm}^2$$

2.1.3.2 Mean Free Path Influence Upon Mass Column Density Calculations - The model is currently configured to consider the influence of contaminant mean free path upon predicted mass column densities and return flux only under specific situations. This influence is important under certain ambient drag vector

orientations and especially at lower altitudes where the mean free paths become increasingly smaller. Analytically, the mean free path can be determined by:

$$\lambda = \frac{4V_o}{\pi\left[3(d_o + d_A)\right]^2 N_A V_A} = \frac{4V_o}{\pi(\delta_o + \delta_A)^2 N_A V_A} = \frac{V_o}{\sigma_A N_A V_A}$$

where,

λ = mean free path, cm

d_o+d_A = viscosity diameter, cm

V_o = velocity of emitted molecule, cm/s

$\delta_o+\delta_A$ = effective scattering diameter, cm

V_A = ambient velocity, cm/s

N_A = ambient density, molecules/cm^3

σ_A = scattering cross section, cm^2

Now, direct flux to a point along a given line-of-sight would be:

$$\text{Flux} = OGR \bullet VF \bullet e^{-R/\lambda}$$

where,

OGR = surface mass loss rate, molecules/cm^2/s

VF = viewfactor between surface and point

R = distance from surface to point, cm

Utilizing this relationship would result in an effective reduction in the predicted column densities and return flux levels as the orbital altitude becomes lower. This is accounted for in the modeling of return flux at the lower orbital altitudes where the ambient drag vector orientation does not allow emitted contaminant molecules to travel far enough into the ambient "wind" to be returned to a surface of interest at the PMP. For outgassing, it is assumed that the return flux is attenuated to approximately zero at altitudes below 250 km while for the lighter species of leakage and early desorption it is assumed that this phenomena occurs below 200 km. At higher altitudes, it is assumed that this effect is negligible.

This ambient "sweeping" will also impact the molecular column density along a given line-of-sight for certain drag conditions by scattering contaminant molecules out of the line-of-sight

or by not allowing them to reach the line-of-sight. This phenomena is considered important for mission planning and evaluation. However, for the design and development activities conducted herein, the approach has been to establish the worst case conditions in order that upper design and operational limits can be determined. For ambient drag conditions where the contaminant molecules are scattered out of a line-of-sight, one must also consider those molecules being swept from other lines-of-sight into the line-of-sight in order to conserve mass. In addition, when the ambient drag vector is parallel to and in the same direction as the line-of-sight or at high orbital altitudes, little or no attenuation to the column density will be experienced. It is therefore, assumed that even though this attenuation will occur under certain conditions, that for design and development analyses there are situations where the contaminant mean free path does not influence the column density values. This philosophy is reflected in the predictions and evaluations contained later in this report.

2.1.3.3 Return Flux Deposition - Once the return flux levels are established for a surface of interest, the next step is to determine the amount of this material that will accommodate on the surface. At the present time, the percentage of outgassed material impinging upon a surface that accommodates (i.e.; the sticking coefficient) is determined by the temperature differential between the emitting surface and the surface which is receiving the outgassing flux divided by a constant that is characteristic of the outgassing material when the outgassing surface is warmer ($S = \Delta T/K$). K, which should be included in materials test data requested from ESA, is currently set at 200 (a value that was used successfully in the previous Skylab contamination modeling).

The lighter molecules of early desorption and leakage will not stick to the 300°K surface at the PMP as stipulated in the applicable criteria, but for colder surfaces in the cryogenic region the Langmuir-Knudsen relationship is utilized to determine deposition and the ensuing desorption rates.

It is recognized that the scattering event changes the energy and momentum of the contaminant molecule which probably makes it appear to have originated from a hotter source. Here again, experimental data is lacking which could be used to develop a more accurate formulation of the sticking coefficient.

2.2 Updated Modeling Considerations - Throughout the course of this contract period, several modifications were made to the basic model input data and refinements were conducted on the

analytical and modeling methodology. These all ultimately impacted the resulting induced environment predictions for the Spacelab contaminant sources. These modifications and/or refinements reflected either a change in current modeling philosophy or an actual adjustment to baseline input data. The modifications that have been completed include: 1) adjustments of the Spacelab external nonmetallic TCS material outgassing and early desorption rates to be equivalent to the maximum allowable implied mass loss rate of the applicable materials screening criteria; 2) maximum and minimum temperature profile updates for all three Spacelab configurations; 3) use of point receivers as opposed to segmented spheres along a line-of-sight to determine line-of-sight viewfactors and ultimately the line-of-sight molecular column densities; and 4) refinement of the Orbiter Orbital Maneuvering System (OMS) engine impact assessment upon Spacelab surfaces.

The following subsections contain a discussion of the incorporated modifications and the results of the evaluations conducted.

2.2.1 Spacelab External Materials Mass Loss Characteristics - As stated previously, the external surfaces of Spacelab are presently being planned to be covered with a white thermal control coating, although to date, this material or materials have not been expressly identified by ESA. Most recent data from ESA[12] indicates two candidate materials (Z202 and S13G-Lo with various primers) that are being considered, but insufficient additional data has been supplied to perform specific analysis without making gross assumptions for area of coverage, location, vacuum mass loss characteristics, etc.

During the previous Spacelab studies, a baseline assumption was made that the entire vehicle was to be coated with normal S13G white thermal control paint; however, existing S13G steady state outgassing rate data obtained during the Skylab Program varied between 10^{-8} g/cm^2/s and 2.7 x 10^{-12} g/cm^2/s at 100°C depending strongly upon the materials cure cycle and batch control. This data is no longer used in the modeling. To further complicate the issue, VCM data supplied by ESA on the above mentioned candidate materials indicate that the primer selection is critical to the acceptability of the surface coating (i.e.; preliminary analysis indicates that S13G-Lo with DC1200 or SS4155 primer would be acceptable while the same coating with SS4044 primer may not qualify based upon the ESA VCM data which implies that the first two of these have an outgassing rate of zero while the latter has a rate of 2.6 x 10^{-10} g/cm^2/s at 100°C). Additional

test data recently developed by the MSFC Materials and Processes Laboratory for S13G-Lo with no primer depicted an outgassing rate of 5.5×10^{-11} g/cm^2/s. It is apparent that this data cannot be directly compared to criteria acceptability due to the influence of the primer selected. In addition, there is no guarantee that S13G-Lo will be the final material selected for use by ESA.

Due to the apparent fluid posture of the thermal control coating decision and based upon the extreme variations in existing test data, a decision was made to conduct the ongoing modeling activities based upon the assumption that Spacelab would be completely coated with a nonmetallic material that meets the applicable materials screening criteria established for the Space Shuttle Program (50M02442[14] and SP-R-0022A[15]). Using these criteria, an implied maximum allowable materials outgassing rate can be determined for qualified materials. The pertinent requirements extracted from these criteria are summaried below:

a. 50M02442 Requirements (Paragraph 3.2)

   1) Weight loss rate during temperature cycling from 25°C to 100°C shall not exceed 0.2%/cm^2/hour when heated at a rate of 2°C/minute.

   2) Steady-state weight loss rate at 100°C shall not exceed 0.04%/cm^2/hour. Steady-state is defined as that point where the rate has been constant for 8 hours.

   3) Desorption of surface adsorbed atmospheric gases or other contaminants shall be included in the rates.

b. SP-R-0022A Requirements (Paragraph 7.4)

   1) The materials shall have a VCM (Volatile Condensible Material) content of $< 0.1\%$ by weight. The total weight loss of material shall not exceed 1.0% by weight.

   2) This is for a 24 hour test period for samples at 125°C.

To determine the implied allowable outgassing rate (OGR) from these criteria requires that the basic parameter of surface density be established for the material as applied to a space

vehicle. This parameter is, of course, a variable with each material and application; therefore a nonmetallic material assumed to be "typical" of aerospace thermal control coatings was chosen for the analysis.

The selected material was S13G white thermal control paint which, based upon data supplied by McDonnell Douglas-West in supplemental information to the Skylab Design Certification Review, demonstrated an average surface density of 0.052 g/cm^2 for a 6 mil thick application. Based upon this assumption, the maximum allowable outgassing rate at 100°C per 50M02442 criteria 2) would be:

$$OGR_{MAX} = (0.052\ g/cm^2) \cdot (1\ cm^2) \cdot (0.04\%/cm^2/hr)$$

$$(hr/3600\ sec) = 5.77 \times 10^{-9}\ g/cm^2/s.$$

An equivalent OGR determined by utilizing a similar approach based upon the SP-R-0022A criteria normalized to 100°C would be:

$$OGR_{MAX} = (0.052\ g/cm^2) \cdot (1\%/24\ hr) \cdot (hr/3600\ sec) \cdot \left[e^{(100-T)/29} \right]$$

$$= 2.54 \times 10^{-9}\ g/cm^2/s \text{ for } T = 125°C.$$

The rates are normalized to 100°C to be compatible with model input format requirements. The model internally adjusts individual surface rates consistent with their specific temperatures and thermal profiles.

The implied early desorption rate (EDR) can also be determined using criteria 1) of 50M02442 assuming the same S13G surface density and that the maximum allowable EDR extrapolated to 100°C will occur when the material is set at 25°C. The maximum allowable EDR normalized to 100°C would, therefore be:

$$EDR_{MAX} = (0.052\ g/cm^2) \cdot (1\ cm^2) \cdot (0.2\%/cm^2/hr) \cdot$$

$$(hr/3600\ sec) \left[e^{(100-T)/29} \right]$$

$$= 4 \times 10^{-7}\ g/cm^2/s \text{ for } T = 25°C.$$

Assuming that the EDR decay curve as a function of vacuum exposure time is similar in shape to that of S13G test data, the EDR at 10 hours (which is that point in a mission when on orbit operations might be expected to commence) would be approximately

1.5×10^{-7} g/cm^2/s at 100°C. The ratio of the EDR at 10 hours to the steady-state OGR calculated from the materials screening criteria of 26:1 compares favorably to the ratio of outgassing and early desorption data (25:1) modeled during previous studies[5,6]. Therefore, based upon the analyses presented, an implied materials steady-state outgassing rate of 6×10^{-9} g/cm^2/s at 100°C and an early desorption rate at 10 hours of 1.5×10^{-7} g/cm^2/s at 100°C are used in the current contamination modeling for surfaces such as thermal control paints where actual test data is not available. The need to pursue such an empirical approach to determine necessary modeling parameters tends to further amplify the requirement for specific test data and materials identification and mapping for those nonmetallic materials displaying large surface areas (greater than 0.1 m^2) and those whose locations indicate potential contamination threats to sensitive instruments and systems.

2.2.2 Spacelab Temperature Profiles - As indicated in the parametric expressions depicted in Table I, the mass loss rates and ultimately the sticking coefficients of the Spacelab vacuum exposed nonmetallic materials are strongly dependent upon the surface temperatures and thermal profile histories of the materials in question. It follows then that the more accurate the model input thermal profile data, the higher will be the fidelity of the resulting induced environment predictions. The thermal profile input data has, therefore, been updated to be consistent with the results of the most recent Spacelab thermal modeling being conducted by Teledyne Brown Engineering in conjunction with MSFC[24]. Current data includes Spacelab LMOP and FIVP surface temperatures for the orbital attitudes presented in Figure 9. As indicated, these attitudes represent a) the maximum hot case thermal profile and b) the minimum cold case thermal profile for the Spacelab configurations. Thermal transient data between the extremes is not yet included in the current design and development model, although such a temperature profile history would be a definite requirement for specific detailed Spacelab mission evaluation. The attitudes presented encompass the Spacelab temperature extremes and correspondingly encompass the maximum and minimum outgassing and early desorption levels anticipated for Spacelab.

Computer printout of the updated temperature profiles in °C for the three modeled Spacelab configurations is presented in Table IV. Reference should be made to Figures 2 through 4 to determine the nodal location of each node number identified in Table IV. Selection of the nodal breakdown presented was dictated in part by the nodal descriptions utilized in the current thermal modeling, although in some cases average temperatures between

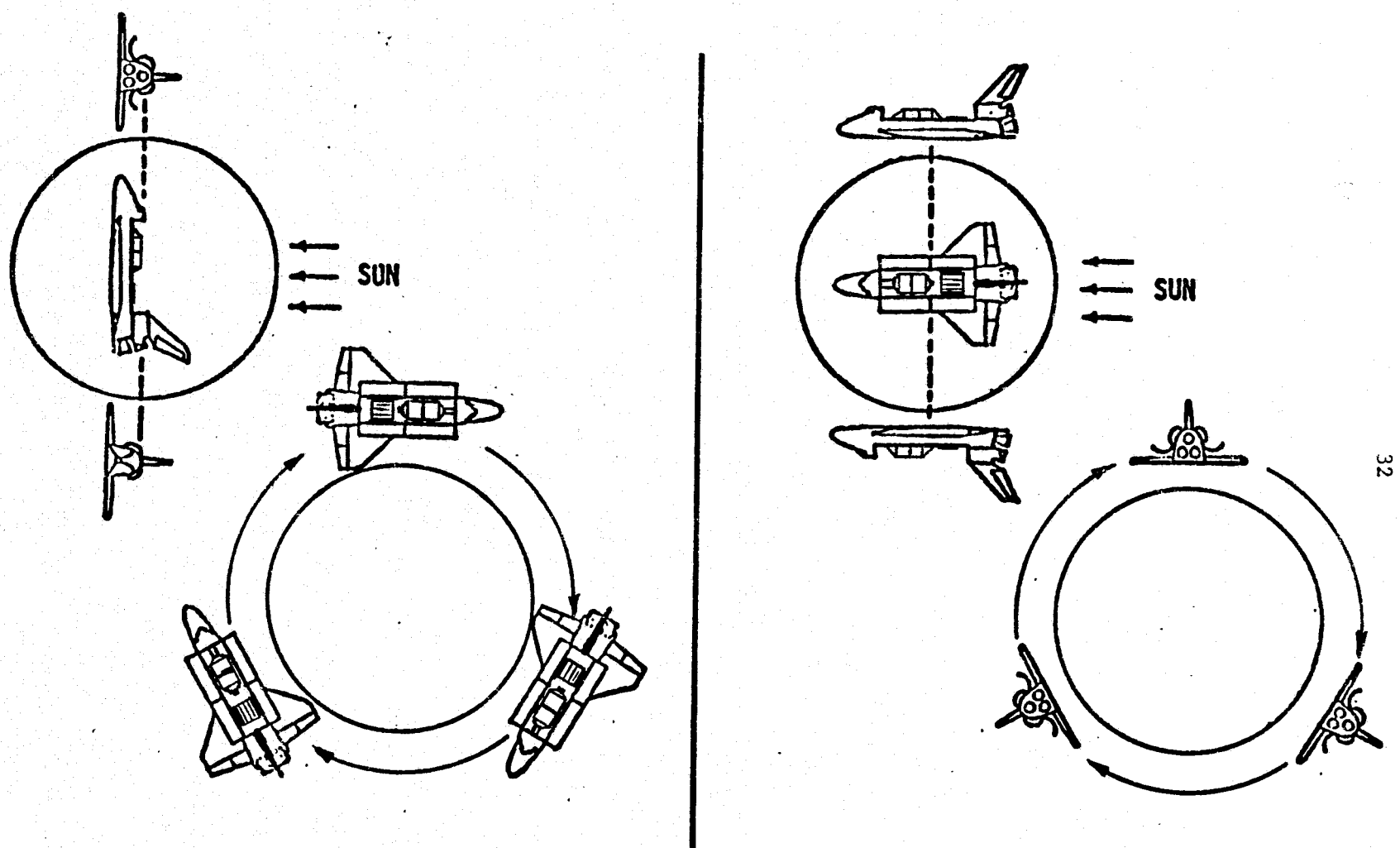

a) Maximum Hot Case Attitude

b) Minimum Cold Case Attitude

Figure 9. Spacelab Orbital Attitudes for Maximum/Minimum Thermal Profiles

Table IV. Modeled Maximum/Minimum Nodal Temperature Profiles for the Three Spacelab Configurations

LMOP Node Number	max °C	min °C
1000	83.9	-155.0
1001	83.9	-155.0
1002	77.2	-155.0
1003	77.2	-155.0
1005	168.9	-121.7
1010	68.9	-158.3
1011	68.9	-158.3
1012	60.0	-158.3
1013	60.0	-158.3
1015	155.6	-120.0
1023	77.2	-127.2
1022	57.2	-136.7
1021	52.2	-136.7
1020	71.7	-127.2
1025	154.4	-110.0
1200	-272.0	-272.0
1201	-272.0	-272.0
1030	51.1	-117.2
1031	46.7	-143.9
1032	32.8	-143.9
1033	35.0	-117.2
1035	101.7	-101.7
1040	43.3	-130.0
1041	46.1	-146.7
1042	31.7	-146.7
1043	27.2	-130.0
1045	96.1	-104.4
1050	35.0	-128.3
1051	28.9	-133.9
1052	26.7	-133.3
1053	32.2	-127.8
1055	84.4	-112.8
1060	84.4	-110.6
1061	27.8	-135.0
1065	52.2	-158.3
1070	87.8	-143.3
1081	67.2	-145.0
1080	62.8	-145.0
1083	34.4	-145.0
1082	34.4	-145.0
1085	53.9	-152.2
1084	46.7	-152.2
1087	66.1	-151.1
1086	66.1	-151.1
1088	67.8	-152.8
1110	45.6	-156.1
1111	45.6	-156.1
1120	45.6	-156.1
1121	45.6	-156.1
1130	27.8	-135.0
1131	27.8	-135.0

SMTP Node Number	max °C	min °C
1010	83.9	-155.0
1011	83.9	-155.0
1012	77.2	-155.0
1013	77.2	-155.0
1015	168.9	-121.7
1023	77.2	-127.2
1022	57.2	-136.7
1021	52.2	-136.7
1020	71.7	-127.2
1025	154.4	-110.0
1200	-272.0	-272.0
1201	-272.0	-272.0
1030	51.1	-117.2
1031	46.7	-143.9
1032	32.8	-143.9
1033	35.0	-117.2
1035	101.7	-101.7
1050	35.0	-128.3
1051	28.9	-133.9
1052	26.7	-133.3
1053	32.2	-127.8
1055	84.4	-112.8
1061	27.8	-135.0
1060	84.4	-110.6
1065	52.2	-158.3
1070	87.8	-143.3
1072	67.2	-145.0
1071	62.8	-145.0
1074	34.4	-145.0
1073	34.4	-145.0
1076	53.9	-152.2
1075	46.7	-152.2
1078	66.1	-151.1
1077	66.1	-151.1
1079	67.8	-152.8
1080	87.8	-143.3
1082	67.2	-145.0
1081	62.8	-145.0
1084	34.4	-145.0
1083	34.4	-145.0
1086	53.9	-152.2
1085	46.7	-152.2
1088	66.1	-151.1
1087	61.1	-151.1
1089	67.8	-152.8
1090	87.8	-143.3
1092	67.2	-145.0
1091	62.8	-145.0
1094	34.4	-145.0
1093	34.4	-145.0
1096	53.9	-152.2
1095	46.7	-152.2
1098	66.1	-151.1
1097	61.1	-151.1
1099	67.8	-152.8
1110	45.6	-156.1
1111	45.6	-156.1
1130	27.8	-135.0
1131	27.8	-135.0

FIVP Node Number	max °C	min °C
1090	63.9	-140.0
1092	56.1	-140.0
1091	51.1	-140.6
1094	34.4	-127.8
1093	33.3	-129.4
1096	45.6	-146.1
1095	38.3	-146.7
1098	55.6	-146.7
1097	50.0	-146.7
1099	57.2	-147.8
1080	70.6	-144.4
1082	56.1	-143.9
1081	50.6	-144.4
1084	31.7	-132.8
1083	29.4	-133.9
1086	44.4	-150.0
1085	36.7	-150.6
1088	56.1	-151.1
1087	49.4	-151.1
1089	57.2	-152.8
1070	77.2	-148.9
1072	56.1	-147.8
1071	49.1	-148.3
1074	28.3	-137.8
1073	25.6	-138.3
1076	43.9	-153.9
1075	34.4	-154.4
1078	56.1	-155.6
1077	48.9	-155.6
1079	56.7	-157.2
1060	81.7	-151.1
1062	60.0	-147.8
1061	54.4	-148.3
1064	30.6	-137.8
1063	29.4	-138.3
1066	49.4	-153.9
1065	40.6	-153.9
1068	60.6	-155.6
1067	53.9	-156.1
1069	60.6	-157.8
1050	85.6	-152.8
1052	63.3	-147.8
1051	58.9	-147.8
1054	32.8	-137.8
1053	33.3	-138.3
1056	54.4	-153.3
1055	46.7	-153.9
1058	65.0	-155.6
1057	58.9	-156.1
1059	64.4	-158.3

adjacent nodes were used in order to minimize the Spacelab Contamination Computer Model complexity while retaining resolution integrity. It is important to note that the Spacelab thermal analysis is not yet completed in that the combined use of pallet insulation, thermal shields, coatings and heaters is still under investigation. For example, a preliminary analysis of an insulated pallet showed significant changes in the predicted temperatures(25). Such changes will in turn modify the contamination predictions. Therefore, future required updates to the input temperature data are anticipated.

The Teledyne Brown/MSFC thermal model currently does not include the SMTP configuration, however, due to its similarity to the LMOP Spacelab, the assumption was made that the LMOP thermal profiles would be applicable for similar surfaces and more accurate than the previously used data supplied by ESRO(13). The SMTP module configuration was reconfigured to be compatible with the nodal structure of the LMOP thermal model which expanded the SMTP model to 55 nodes as compared to the previous 38 node configuration. New viewfactors were calculated for the SMTP lines-of-sight and corresponding outgassing and early desorption predictions were determined based upon the adjusted thermal data. The results of these model update activities will be reflected in a later section of this report.

2.2.3 Line-of-Sight Viewfactor Calculation Refinement and Expansion - The Spacelab contamination modeling approach to predict molecular column densities and return flux along a given line-of-sight in the past involved the input of a series of pseudo-surfaces as dimensioned spheres divided into quadrants along the line-of-sight of interest allowing each of them to act as individual contaminant receivers. This process was quite costly in terms of computer run time, and the accuracy of calculated sphere viewfactors was questionable under certain circumstances due to the fact that an erroneous cross-sectional dimension was being assigned to a line in space. To overcome this, a modeling approach was developed through modification of the TRASYS II configuration program to treat dimensionless points as contaminant receivers along a line-of-sight (requiring only one input node/point) which more closely approximates a geometric line in space. The result has been a significant reduction in viewfactor computer run times for the point lines-of-sight over those required for the quad sphere approach. In addition, the model fidelity has been increased. This refinement, which is reflected in the predictions presented later in this report, should represent considerable computer cost savings in the future.

Since this refinement was initially incorporated into the model and detailed in the interim report[26], troubleshooting and checkout of the methodology has led to an additional modification in the modeling approach. The required adjustment to the point receiver method resulted from the way the TRASYS II configuration viewfactor program defined the field-of-view of a dimensionless point. It was handled as though it were a 4π steradian emitter and viewfactors were then calculated. Since the points in the contamination program were used only as receivers, their fields-of-view must have been 2π steradians. This means that as a receiver, the points should have a pseudo-area equal to πr^2 (sphere projection to a circle) as opposed to an area of $4\pi r^2$ for the points as emitters. The result was that previously calculated viewfactors to points and corresponding column density and return flux predictions were too small by a factor of four[26]. This subtlety has been incorporated into the model and predictions contained herein also reflect this modification.

In maintaining consistency with the parametric format of the recognized contamination control criteria which is detailed in subsection 2.5, other modifications to the line-of-sight modeling technology were completed including:

a. baselining the PMP (X_o = 1107, Y_o = 0, Z_o = 507) as the point of origin for the modeled lines-of-sight;

b. adding an additional point located at the PMP to each line-of-sight to allow complete integration from the PMP to a distance of 300 meters along a line-of-sight for determining column densities and return flux; and

c. modeling seventeen lines-of-sight, as opposed to the nine lines-of-sight modeled under previous studies, for each Spacelab configuration to symmetrically encompass the 120 degree conical volume centered around the Spacelab +Z axis.

The additional point added to the lines-of-sight at the PMP allowed for the inclusion of mass along the line between the PMP and the point five meters out where the closest point had previously been modeled. This five meter gap was previously modeled assuming that the volume would be occupied by a "typical" optical telescope structure which would shadow that portion of the line-of-sight from the contaminant mass flux. In general, the incorporation of the additional point into the model increased the line-of-sight column densities and the return flux levels from 20 to 25 percent.

During previous modeling studies of the Spacelab carrier, nine lines-of-sight were chosen which essentially encompassed a 100 degree conical volume above the vehicle centered around the +Z axis. The rationale utilized in this selection was the fact that such a viewing volume would encompass the majority of viewing directions for Spacelab payloads. This fact is still true, however, the current criteria is based upon a 120 degree viewing volume which led to the noted change. Seventeen (17) lines-of-sight composed of sixteen (16) points each have currently been modeled for the three Spacelab configurations (see Figure 6) to establish a symmetrically spaced point viewfactor matrix within this volume. The viewfactor matrix has multiple uses in that it not only encompasses the required viewing volume, but it also establishes the basis for determining return flux to large field-of-view surfaces and column densities along lines-of-sight originating at points other than the PMP which are both discussed in subsection 2.3.1.1.

2.2.4 Orbital Maneuvering System (OMS) Engine Evaluation - Although the OMS engines are not explicitly a Spacelab contaminant source, their use is dictated by the particular Spacelab mission requirements levied upon them. At any time during a mission that the OMS engines are operated while the Orbiter payload bay doors are open, the potential of significant contamination of Spacelab and payload surfaces exists and requires evaluation. The modeling of this source has been refined during this period and the resulting posigrade predictions have diminished considerably from those previously reported while the retro thrust predictions have remainted essentially unchanged[6]. This change evolved from the integration of an expanded approach to molecular mean free path influence upon return flux as a function of orbital altitude at OMS burn initiation.

Figure 10 presents the updated deposition rate predictions for a 2π steradian surface oriented in the X-Y plane (representative of a +Z facing Spacelab thermal control surface for example) for posigrade and retro thrust maneuvers as a function of engine burn initiation altitude. Given any OMS engine burn time or fuel usage and the altitude of burn initiation, the resulting deposition can be determined. Sticking coefficient data used in the modeling was derived from MMH-N_2O_4 engine test data resulting from Lewis Research Center small engine testing conducted during the Skylab Program. This analysis would tend to indicate that closing of the payload bay doors during OMS posigrade maneuvers may no longer be necessary. However, until engine design and performance data becomes more firmly established, the potential

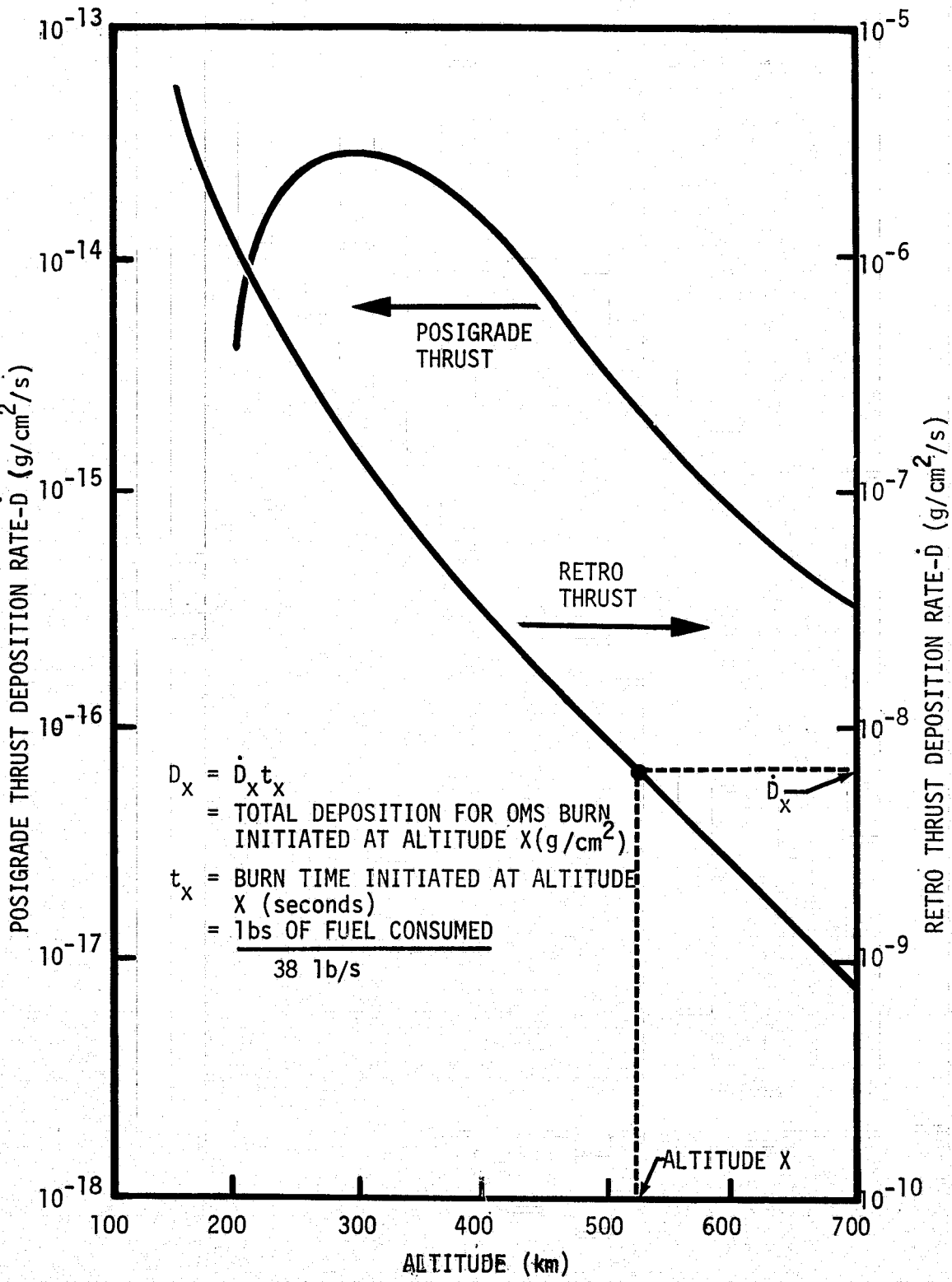

Figure 10. OMS Effluent Deposition Rate on a +Z Facing 2π Steradian Field-of-View Spacelab Surface as a Function of Orbital Altitude

of contamination during posigrade maneuvers should not be ignored. The analysis still substantiates the need to close the payload bay doors during retro thrust maneuvers.

2.3 Additional Studies - There were several additional studies conducted during the course of this contract. They include improvements on the Spacelab contamination analysis computer model, initiation of a Mission Profile Data Bank (MPDB), development of an early Spacelab mission preliminary mission support plan and the development of an interface document discussing the differences between the MMA CDC and MSFC UNIVAC computer systems. The latter two are covered in detail in separate reports (see References 27 and 28).

2.3.1 Model Improvement Studies - The Spacelab contamination model has proven to be an effective tool in contamination analysis and assessment although it is still in the development phase for certain contaminant phenomena. Although the model improvement studies were not a major effort under this contract, work was initiated in certain areas to improve both the physical and mathematical models used in the Spacelab contamination analysis computer program. As a result, refinements and improvements in the modeling technology and methodology have been evaluated to determine what increases in the fidelity of the model predictions may be required. The major areas which were investigated to improve the fidelity of the model predictions included: 1) return flux to large field-of-view surfaces; 2) contaminant self scattering; 3) return flux prediction capability of any altitude; 4) payload bay vicinity surface-to-surface disposition; 5) contaminant mean free path influences (see subsection 2.1.3.2); and 6) the contribution of reflected ambient molecules to the NCD. Of these, items 1), 2) and 4) have been configured and are workable as separate subroutines but have not been completely integrated into the model. Item 3) is completely functional in the model, and while items 5) and 6) are deemed important under certain circumstances, their influences are not explicitly in the model although they are considered in the contamination analysis where applicable.

In addition to improving the model's prediction accuracy and range of usefulness, effort was also spent integrating the various modules into a more user oriented analysis tool. Because a detailed analysis of on orbit contamination for a complete Spacelab mission becomes quite complicated, the analytical tool must have the capability to encompass all significant contamination phenomena but yet be simple for the user to exercise in a design and development mode.

In the past, individual trade studies could be conducted in a segmented fashion by exercising small modules or subroutines individually. It is now becoming necessary to systematically integrate these modules into a more complete analysis tool. Because of our self imposed requirement to produce a user oriented computer program, some time was spent in a definition phase deciding what was required of this tool.

This activity also evaluated the next phase which would be the actual design of the integrated computer program. It reviewed the functional aspects of the calculation procedure for Spacelab contamination analysis. This phase resulted in an overview of the entire computer program, the design standards used in constructing the code, a development of the four basic segments of the integrated model, description of the math and physics involved and flow diagrams of the major subroutines.

A third activity was initiated to compile the actual listings of the coded algorithms used in the contamination model. This latter activity is, of course, incomplete because the model improvement task was only a small portion of this past contractual effort.

The usefulness of the computer model has been strengthened through these activities and by the additional modules that were constructed during the course of this study. Several of these new modules introduce more accurate physical representations of contamination phenomena and allow the analyst to use the latest theoretical techniques and experimental data that is available in the industry.

For example, in the area of return flux, a new module was written and checked out that allows the user to access a basic network of precalculated "viewfactors" to the hemispherical cloud above the Spacelab/Orbiter and to draw from this network the information needed to define the mass column density (MCD) or number column density (NCD) along a generalized line-of-sight. No longer is the analyst confined to discrete lines-of-sight for which precalculated viewfactors exist. He now has the option of moving the origin of the line-of-sight anywhere on the Spacelab/Orbiter or out into the cloud itself. This new module gives the user a capability for performing the complex volume integrations required for return flux calculations. With the addition of this module to the basic contamination program, more accurate predictions of the return flux (both ambient and self scattered components) from the complicated three-dimensional cloud of contaminants above the Spacelab can be made.

Another module that has been added to the model is a more detailed algorithm of surface mass loss characteristics. Previously, basic types of contaminants (e.g.; outgassing, early desorption, engines, vents) were monitored. Now, if the user chooses, he can track individual chemical species (currently 10 species are being considered - H_2O, N_2, CO_2, O_2, CO, H_2 plus two outgassing large molecular weight species, and two additional species unique to RCS, VCS and OMS engines). The number of species can be extended at a later date if found necessary. The addition of this module allows more realistic physical models for return flux formulations (collision cross sections for each pair combination can be used for example), reflection/re-emission of second surface sources and for evaluation of electromagnetic attenuation along a line-of-sight which is yet to be added. In addition, this module provides more accurate surface mass loss characteristics. Each surface can now be assigned individual time dependent mass loss rates for H_2O, N_2, CO_2, O_2 (the predominant species during the early desorption period) and time dependent mass loss rates for two larger molecular weight species (to describe the long term outgassing period). This feature appears to be leading the available experimental data, however recent JSC data indicates such a model is required to correlate the mass loss rates of surfaces that have undergone different time/temperature cycling.

The following is a more detailed discussion of each of the above mentioned model improvements that were initiated during the course of this contract.

2.3.1.1 Return Flux to Large Field-of-View (FOV) Surfaces - To increase the Spacelab contamination computer model's capability to accurately describe the contaminant environment of the Spacelab carrier and its respective payload configurations, the prediction capability for return flux of emitted contaminant molecules through their collisions with the ambient atmosphere to surfaces having large fields-of-view (up to 2π steradians or hemispherical) was extended. Prior to the current contract, the computer model considered return flux only to surfaces having relatively small geometric acceptance angles (approximately 0.2 steradians) for the worse case situation where the ambient drag vector was perpendicular to the surface of interest. To determine the return flux to surfaces with acceptance angles differing from those modeled, the acceptance angles (in steradians) of the surface of interest and the modeled surface were simply ratioed and multiplied by the model derived return flux value.

Unfortunately, the simple ratio approach is not physically accurate for large geometric acceptance angles with varying NCDs.

To expand the capabilities of the current model, an innovative approach was developed which not only produces predictions for direct comparison with the existing contamination control criteria but can also be used effectively as a basic building block in a mission analysis computer program for complex vehicle geometries such as the Spacelab/Orbiter.

The approach divides the hemispherical space above the Spacelab/Orbiter into a matrix of volume elements that have midpoints strategically located along up to 25 significant lines-of-sight (see Figure 11). Seventeen of these lines-of-sight have currently been modeled.

Table V illustrates the network and coding used to encompass the hemispherical volume above the Spacelab/Orbiter configurations. A five digit code is used to relate each point to its spatial coordinates. The first digit describes the value of θ, the second the value of ϕ and the last 3 digits define the radial distance from the origin in meters. Thus, a point numbered 22100 would be found on a line-of sight 30^{o} off the Z-axis, leaning over the right wing, 100 meters from the origin.

Table V. Code for Volume Element Midpoints

θ(deg)	Code	(deg)	Code	R(meters)	Code
0	1	0	0(aft)	5	005
30	2	45	1	10	010
60	3	90	2(right)	15	015
82.5	4	135	3	20	020
		180	4(forward)	25	025
		225	5	30	030
		270	6(left)	40	040
		315	7	50	050
				75	075
				100	100
				150	150
				200	200
				300	300

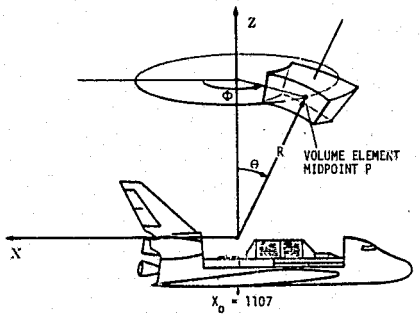

Nomenclature for Points in the Hemispherical Cloud

meters

• 300

FARFIELD ~ undisturbed cloud density varies as $1/r^2$ for constant θ and Φ

• 200

• 150

X-Z PLANE ONLY

• 100

NEARFIELD ~ cloud density complex function of r, θ, and Φ

• 50

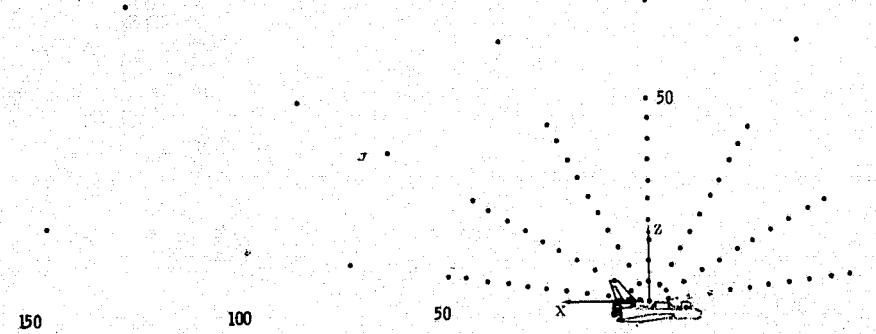

Figure 11. Location of Precalculated Viewfactors in Hemispherical Cloud

The origin of this matrix is located at the PMP, station X = 1107, Y = 0 and Z_o = 507, for ease in relating to current contamination control criteria. Note that the selection of this particular origin in no way limits the return flux or column density calculation capability to a surface located at X_o = 1107. A point selection subroutine has been developed that selects the proper points for interpolating along any line-of-sight originating at any desired location as shown in Figure 12. Typical output is shown in Table VI.

Another important feature of this matrix is that although there are some precalculated viewfactors to points out to 300 meter from the vehicle, our experience has shown that in many cases beyond 150 meters the viewfactors decrease simply as $1/r^2$ for a constant θ and Φ. The point selection routine contains an option to use a $1/r^2$ variation wherever the user desires prior to 300 meters.

The amount of mass leaving each Spacelab/Orbiter surface or point source that can enter the volume element centered around point P (Figure 11) is computed by accessing precalculated "form factors" (or mass fraction data) between point P and each source. As a result, the contaminant cloud density at any point above the vehicle can be defined knowing the particular source emission characteristics. It should be noted that there are no restrictions on the vehicle configuration such as assuming a spherical spacecraft.

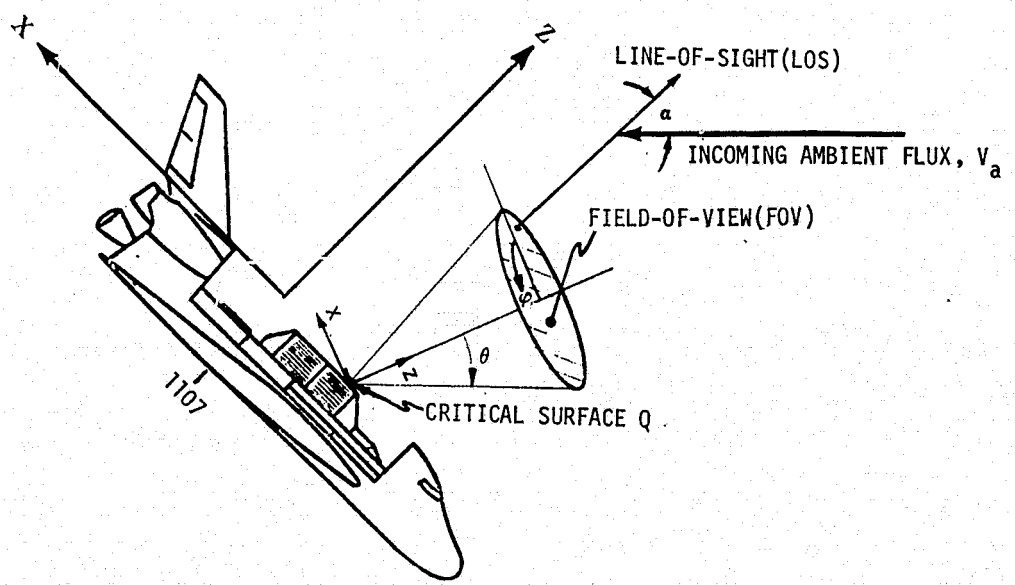

Figure 12. Example of a Critical Surface Location, Orientation and Field-of-View

Table VI. Sample Output from Point Select Routine Showing Line-of-Sight Segmentation

```
* * * * * *     LINE  OF  SIGHT  POINT  SELECTOR     * * * * * *


ORIGIN OF LINE OF SIGHT  7          (1107.0,   0.0, 507.0)

LOS ORIENTATION
    THETA(DEG)   =  30.0
    PHI  (DEG)   = 225.0
    DIRECTION COSINES
      S DOT XO   = -.354
      S DOT YO   = -.354
      S DOT ZO   =  .866

INCOMING AMBIENT CHARACTERISTICS
    SPEED(M/SEC)  = .765E+04
    DIRECTION COSINES
     VA DOT XO   = 0.000
     VA DOT YO   = 0.000
     VA DOT ZO   =-1.000
    DENSITY(#/CC) = .209E+09

ANGLE BETWEEN VA AND LOS
     ALPHA     =  30.0

WEIGHTING FACTORS FOR RETURN FLUX
     AMBIENT SCATTERING: NCD *       .671
     SELF SCATTERING:    NSS *    .30E-10

VOLUME CONSIDERATIONS
    HEMISPERICAL CLOUD (M**3)  = .718E+09
    VOL. ENCOMPASSED BY LOS    = .232E+08
    FRACTION OF TOTAL          =  .032


SEGMENT    1                                  LOS = (  7)
  MIDPOINT:    ORBITER COORDINATES( 1072.,  -35.,  592.)
  DISTANCE FROM LOS ORIGIN (M)  =    2.5
  LENGTH OF SEGMENT (M)         =    5.0
  VOLUME OF SEGMENT (M##3)      =   .88E+01
  NEAREST MATRIX POINTS
          ID            RELATIVE
          NUMBER        CONTRIBUTION
          15000         0.000 *   500.0
          25000          .500 *   500.0
          16000         0.000 *   500.0
          26000         0.000 *   500.0
          15005         0.000 *   500.0
          25005          .500 *   500.0
          16005         0.000 *   500.0
          26005         0.000 *   500.0

SEGMENT    2                                  LOS = (  7)
  MIDPOINT:    ORBITER COORDINATES( 1003., -104.,  763.)
  DISTANCE FROM LOS ORIGIN (M)  =    7.5
  LENGTH OF SEGMENT (M)         =    5.0
  VOLUME OF SEGMENT (M##3)      =   .59E+02
  NEAREST MATRIX POINTS
          ID            RELATIVE
          NUMBER        CONTRIBUTION
          15005         0.000 *   500.0
            .
            .
            .
            .
            .
            .
```

To calculate the return flux to a surface, the location and orientation of the critical surface Q and the direction of the incoming ambient flux vector, V_A, are defined with respect to Orbiter/Spacelab coordinates. In addition, the FOV for this surface is specified in terms of θ and φ. The return flux to the surface is then computed by performing a volume integration over the defined region of space within the surface field-of-view (see Figure 13). (Note: abnormal fields-of-view such as rectangles can also be considered through special model manipulation).

The return flux from the unit volume of space centered at the volume elemental midpoint P is a direct function of the collision rate of the contaminant molecules with ambient species and other contaminant species within that volume. The return flux due to ambient scattering is considered below. Self-scattering is discussed in subsection 2.3.1.2.

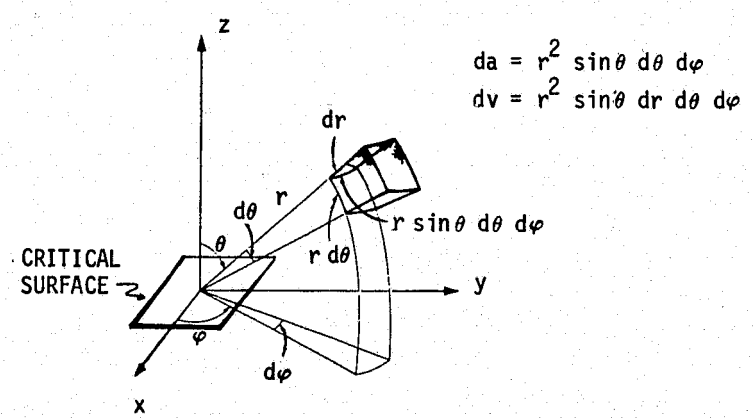

Figure 13. Nomenclature for Volume Integration Through Surface's Field-of-View

The collision rate between the ambient and contaminant molecules is defined by knowing the number density of both the contaminants ($N_o(P)$) and the ambient species (N_A) within that volume. This together with the relative velocity (approximately V_A) and the effective cross section of the collision process (σ_A) is used to determine the collision rate within the volume element

$$\dot{n}_{as}(P) = N_A N_o(P)\, V_A\, \sigma_A \qquad (1)$$

It is currently assumed that there is no attenuation in the ambient density due to the perturbation by the contaminant environment and that the impact of the ambient flux upon the contaminant density is negligible. It is also assumed that densities induced by surface sources can be defined knowing the mass loss characteristics and utilizing a Lambertian distribution from each surface.

A scattering model is then assumed which defines the number of collisions given in equation (1) that deflect molecules toward the critical surface. The scattering model currently used by most analysts reduces to a cosine or Lambertian distribution from the scattering center. When and if on orbit experimental data for this phenomena becomes available, the scattering model can be easily modified. By integrating over all space within the geometric acceptance angle or FOV of a critical surface the total return flux ($g/cm^2/s$) to the surface can be defined. Using the hard sphere scattering model,

$$RF_{as} = \int_{\theta}\int_{\varphi}\int_{0}^{r_{max}} \frac{r^2 \dot{n} \left[\cos \alpha\right] \cos\theta \, d\theta \, d\varphi \, dr}{r^2} \tag{2}$$

$$RF_{as} = N_A V_A \frac{\pi}{4} (\delta_o + \delta_A)^2 \int_{\theta}\int_{\varphi} \left[\frac{\cos\alpha}{\pi} \times \underbrace{\int_{0}^{r_{max}} N_C dr}_{NCD} \times \sin\theta \cos\theta \right] d\theta \, d\varphi. \tag{3}$$

In performing the volume integration, observe that for a given θ and $\emptyset$ that a line-of-sight (LOS) has been defined emanating from the critical surface (Figure 12). Since the scattering angle, α, is constant along each LOS, integration is first performed over the variable r (along the LOS) to obtain the number column density. The NCD is often a useful piece of information if the surface is a viewing optic and there is concern with not only the return flux deposition but also field-of-view interference through scattering, emission and/or absorption. The return flux is, therefore

$$RF = N_A V_A \frac{\pi}{4} (\delta_o + \delta_A)^2 \sum_{N} \frac{\cos \alpha_N}{\pi r^2} NCD_N \, r^2 \times \sin\theta_N \cos\theta_N \Delta\theta \Delta\varphi \tag{4}$$

and the volume integration has reduced to LOS integration followed by summation of a series of lines-of-sight that encompass the desired fields-of-view.

Note that if equation (4) is further modified

$$RF = N_A V_A \frac{\pi}{4} (\delta_o + \delta_A)^2 \sum_N \cos \alpha_N \, NCD_N \times \frac{\cos \theta_N}{\pi r^2} r^2 \sin \theta_N \qquad (5)$$

Now,

$$\frac{\cos \theta_N}{\pi r^2} \cdot r^2 \sin \theta_N \Delta\theta \Delta\varphi = \frac{\Delta A_N \cos \theta_N}{\pi r^2} = FF_{I-N}$$

there,

$$RF = N_A V_A \frac{\pi}{4} (\delta_o + \delta_A)^2 \sum_N \cos \alpha_N \, NCD_N \, FF_{I-N} \qquad (6)$$

where

NCD_N = molecular column density along line-of-sight N (molecules/cm^2)

α_N = angle drag vector makes with LOS N (degrees)

N_A = ambient density (molecules/cm^3)

V_A = ambient velocity (7.65×10^5 cm/s)

$\delta_o + \delta_A$ = effective scattering diameter 3.24×10^{-7} cm for outgassing/ambient and 1.98×10^{-7} cm for early desorption or leakage/ambient collisions)

FF_{I-N} = form factor from volume element coincident with line-of-sight N to surface of interest I.

This is the basic relationship currently used in modeling the contaminant return flux. Typical output for one line-of-sight with a critical surface's field-of-view is shown in Tables VI and VII.

Table VII. Sample Output from Point Select Routine that Summarizes the LOS Contributions

```
* * * * * *      LINE  OF  SIGHT  POINT  SELECTOR      * * * * * *
* * * * * *           SUMMARY  FOR  LOS( 7)            * * * * * *


ORIGIN OF LINE OF SIGHT  7          (1107.0,   0.0, 507.0)

LOS ORIENTATION
     THETA(DEG)   =  30.0
     PHI  (DEG)   = 225.0
     DIRECTION COSINES
       S DOT XO   = -.354
       S DOT YO   = -.354
       S DOT ZO   =  .866

INCOMING AMBIENT CHARACTERISTICS
     SPEED(M/SEC)   = .765E+04
     DIRECTION COSINES
      VA DOT XO   = 0.000
      VA DOT YO   = 0.000
      VA DOT ZO   =-1.000
     DENSITY(#/CC) = .209E+09

ANGLE BETWEEN VA AND LOS
      ALPHA     =  30.0

WEIGHTING FACTORS FOR RETURN FLUX
      AMBIENT SCATTERING: NCD *      .671
      SELF SCATTERING:    NSS *   .30E-10

VOLUME CONSIDERATIONS
     HEMISPERICAL CLOUD (M**3)  = .718E+09
     VOL. ENCOMPASSED BY LOS    = .232E+08
     FRACTION OF TOTAL          =  .032


CLOUD CONTIBUTORS
     AMBIENT SCATTERING              SELF SCATTERING
     RHO(25000)   *   .17E+03     RHO(25000)**2  *   .76E-08
     RHO(25005)   *   .34E+03     RHO(25005)**2  *   .15E-07
     RHO(25010)   *   .34E+03     RHO(25010)**2  *   .15E-07
     RHO(25015)   *   .34E+03     RHO(25015)**2  *   .15E-07
     RHO(25020)   *   .34E+03     RHO(25020)**2  *   .15E-07
     RHO(25025)   *   .34E+03     RHO(25025)**2  *   .15E-07
     RHO(25030)   *   .34E+03     RHO(25030)**2  *   .15E-07
     RHO(25035)   *   .34E+03     RHO(25035)**2  *   .15E-07
     RHO(25040)   *   .34E+03     RHO(25040)**2  *   .15E-07
     RHO(25045)   *   .34E+03     RHO(25045)**2  *   .15E-07
     RHO(25050)   *   .10E+04     RHO(25050)**2  *   .46E-07
     RHO(25075)   *   .17E+04     RHO(25075)**2  *   .76E-07
     RHO(25100)   *   .25E+04     RHO(25100)**2  *   .11E-06
     RHO(25150)   *   .99E+04     RHO(25150)**2  *   .45E-06
```

To demonstrate the flexibility of the current modeling approach, it can be compared with those developed by other investigators. An approach has been utilized by Robertson[10,11] in which a space vehicle is assumed to be equivalent to a sphere emitting mass uniformly in all directions. This approach results in constant molecular column density predictions for all lines-of-sight and viewing directions. Due to its spherical symmetry, this approach cannot account for variations in either the column density or return flux to large field-of-view surface predictions as a result of geometry and differing sources and source rates. Reference can be made to Figure 7 for an example of the variation in column density as a function of viewing direction for the uniform contaminant source of outgassing. These variations are the result of both geometry and temperature profiles for the various Spacelab configurations.

Plotting of similar predictions using the Robertson approach would result in a constant value for all viewing directions (i.e.; a straight line parallel to the bottom axis of Figure 7). Whether or not these predictions would even fall in the range of Figure 7 is a function of the parametric assumptions utilized in his approach.

What is important to point out is the fact that return flux to large field-of-view surfaces is directly proportional to the column densities in all directions within their fields-of-view. It should, therefore, be obvious that the simplified Robertson approach which results in constant column densities in all directions will establish return flux predictions which vary significantly (even for uniform sources such as outgassing) from those produced by the higher resolution modeling approach which considers such parameters as vehicle geometry, and different sources and source rates and surface/source temperature profiles.

Summary - As is indicated, these results demonstrate that the MMA model which is designed to handle return flux to large field-of-view surfaces for complex configurations such as the Spacelab/Orbiter will produce the necessary higher resolution to contamination predictions than these using a simple, uniform emitting sphere analytical approach -- in fact, the MMA approach would apply to any optical acceptance angle up to 2π steradians. The added benefits to using the approach through computer modeling as opposed to manual analysis are significant when considering what actually occurs physically for a complex space vehicle during a given mission. The modeling approach can easily handle the large number of calculations required to evaluate return

flux when the contaminant molecular column density varies spatially and temporally throughout the viewing volume encompassed by a large field-of-view surface. In addition, the direction of the incoming ambient species can be varied incrementally throughout an orbit simulating major attitude or viewing direction changes without significant effort. This entire approach appears to lend itself well to be used in a complete mission simulation/analysis contamination program and could be a major step in that possible direction of development and refinement.

2.3.1.2 Self Scattering of Contaminant Molecules - The return flux from self scattering is the result of collisions between a contaminant molecule and another contaminant molecule. Although this contribution to return flux appears to be 1 to 2 orders of magnitude less than the contribution due to scattering with ambient species (for altitudes between 200 and 700 km), the analytical approach proposed by Robertson[10] has been reconfigured for integration into the model.

Using the assumptions of Robertson, equation (1) is replaced by:

$$\dot{n}_{ss_i} = \sum \frac{N_i}{2} \cdot \frac{N_j}{2} (V_i + V_j) \cdot \frac{\pi}{4} (\delta_i + \delta_j)^2 \qquad (7)$$

where,

i denotes the scattered species, and
j denotes all other scattering species,

Using the assumption that the self scattered molecules emerge from the volume element with an equal probability in all directions and integrating over the hemispherical space above the vehicle, the return flux of the self scattering contaminants becomes:

$$RF_{ss_i} = \int_{\theta} \int_{\phi} \left[\int_{0}^{r_{max}} \frac{\dot{n}_{ss_i} r_2 \, dr}{4 \pi r^2} \right] \cos\theta \sin\theta \, d\theta \, d\phi \qquad (8)$$

Although the volume integration is performed over the variable r first (in brackets), the result is not the NCD as found for return flux. This term can be easily integrated in the model

with the final relationship determined using the same procedure as was used in equation (6) determination.

Therefore,

$$RF_{ss_i} = (V_i + V_j) \frac{\pi}{64} (\delta_i + \delta_j)^2 \sum_N N_{ss_N} \cdot FF_{I-N} \qquad (9)$$

Summary - The self scattering technique devised by Robertson[10] has been expanded and coded into a module for future incorporation into the MMA integrated computer model. A preliminary test case for a surface with a 0.1 steradian field-of-view at a 700 km altitude indicates the return flux from self scattering of outgassing molecules was insignifcant relative to the return flux due to ambient collisions. Additional effort in this area is recommended since under certain conditions there is some applicability.

2.3.1.3 Second Surface Sources - One phenomena that was evaluated during the model improvement phase was the reflection/re-emission of contaminants from surfaces other than their original sources. For example, the bottom portion of the LMOP pallet (surface 1088 shown in Figure 2) can receive contaminant material from other LMOP surfaces (1050, 1051, 1052, 1053, 1055, 1060, 1061, 1065, 1084, 1085, 1086 and 1087), the Orbiter payload bay liner, the OMS pods and the rear payload bay bulkhead. These contaminants could in turn be re-emitted from 1088 onto an experiment attached to the pallet or into an instrument line-of-sight.

A certain amount of engineering judgement must be used when evaluating second surface sources. For example, any surface that has a direct line-of-sight to an Orbiter engine should be considered a potential second surface source because of the high mass flux that could be incident on the surface during engine firing and the fact that exhaust from bi-propellant engines can deposit upon the surface and later desorb or sublimate.

To illustrate the magnitude of the second surface source phenomenon, the bottom portion of the LMOP pallet (1088) was examined using the maximum surface temperatures defined in Table IV. At 10 hours into a mission, the mass loss rate of surface 1088 is expected to be increased by 25% with the addition of material from other surfaces.

Once significant problem areas are defined, those surfaces that could be potential second surface sources can be considered in the contamination analysis using the following logic.

Given a critical surface (I) in terms of deposition, a search is made of all surfaces (J) that see the critical surface. If surface J was flagged as a potential second surface source then another search is made for all surfaces and point sources (K) that can see surface J.

Depending on the temperature of the reflecting/re-emitting surface, certain species may or may not condense. The total incident flux of a species is compared to the evaporation or sublimation rate of the surface. If the loss rate exceeds the incident rate it is assumed all the material is instantaneously reflected or re-emitted. The accommodation of energy at the surface is assumed complete and the material emerges diffusely with a velocity dictated by the temperature of the surface. Either a specular or diffuse re-emission could be assigned, but until experimental data is available to warrant a change, only the diffuse emission is generally considered.

For material that can condense and leave a deposit that later evaporates or sublimates, an additional feature can be evaluated - namely its susceptibility to UV. Consider, for example, the unsymmetrical dimethyl hydrazine (UDMH) from the engine deposits which has a certain sublimation rate. This would normally be added to the mass loss rate of the original surface. However, the UV incident on the surface can chemically alter the physical properties of the deposit and decrease its mass loss characteristics.

Summary - The bottom of the LMOP pallet (surface 1088) is an example of a surface where contaminants from second surfaces can significantly alter the effective mass loss rate of the original surface. Our experience has shown that if a surface has viewfactors to other emitting surfaces that sum to more than 0.2, second surface sources should be examined. Also, if a surface is exposed to the exhaust from an Orbiter engine, it should be considered a potential second surface source.

2.3.1.4 Ambient Atmosphere Density Data File - In order to make the contamination model flexible enough to determine return flux at any altitude or at any combination of variable altitudes, tabular data contained in the Satellite Environment Handbook(29) has been coded into a data file that can be accessed by the computer model. These data define the ambient temperature, density and molecular weight as a function of altitude. Data are available between 105 km and 2500 km for three levels of sunspot activity (low/medium/high).

Current model predictions contained herein utilize the medium density profile as a function of altitude. It should be noted that if the high density profile were used (which represents maximum solar activity on the solar side of an orbit) the resulting return flux predictions would be higher by a factor of up to 7 depending upon altitude.

Subsequent to the development of this data file, it was learned through conversations with MSFC personnel that similar data could be obtained from the Marshall Interactive Planning System (MIPS) data files. Provisions are now being made to modify the MMA computer program to accept atmospheric density and other input data from the MSFC data bank.

Summary - An atmospheric density data file is now available at MMA for use by the contamination analysis program. Table VIII is a listing of the data that will be used until the interface with the MIPS data files has been completed.

2.3.1.5 Payload Bay Vicinity Surface-to-Surface Deposition - The direct line-of-sight deposition on an experiment located on the LMOP pallet was evaluated using maximum surface temperatures to determine the magnitude of the various sources in the payload bay vicinity. The method used to evaluate deposition levels was first devised during the Skylab program and later refined and applied to other configurations the most recent being the Department of Defense DMSP and DSP satellites (Reference 30).

Geometrical relationships are first defined using a modified version of the Martin Marietta Thermal Radiation Analysis System (TRASYS II) computer program[9]. As indicated in Table IX, there are 26 surfaces that can see the bottom of the pallet directly. Temperatures computed in Reference 24 were assigned to the Spacelab and Orbiter payload bay surfaces from which mass loss rates for each surface are defined (see Table X).

The viewfactors between surfaces shown in Table IX are then used to compute the amount of contaminants that can be transported to a critical surface. The fraction of incident flux that deposits on a surface is defined using an empirical condensation coefficient (or sticking coefficient) as described in subsection 2.1.3.3.

Summary - Using the above described line-of-sight transport methodology which proved successful for Skylab, the deposition on a 22°C surface located on the bottom of the LMOP pallet could

Table VIII. Ambient Atmospheric Density Data File

FILE AADDF AMB. ATMOS. DENSITY DATA FILE ** LOW ***

ALT (KM)	TEMP (K)	TOTDEN (P/CM3)	DEN (G/CM3)	M	DEN O (P/CM3)	DEN O2 (P/CM3)	DEN N2 (P/CM3)
105	224	4.59E+12	2.14E-10	28.07	2.80E+11	7.93E+11	3.48E+12
110	243	2.14E+12	9.86E-11	27.73	1.74E+11	3.34E+11	1.62E+12
120	290	5.51E+11	2.47E-11	26.96	7.33E+10	7.04E+10	4.05E+11
130	350	1.76E+11	7.64E-12	26.12	3.42E+10	1.85E+10	1.23E+11
140	425	6.83E+10	2.87E-12	25.27	1.76E+10	5.98E+09	4.46E+10
150	490	3.21E+10	1.30E-12	24.45	1.03E+10	2.36E+09	1.94E+10
160	548	1.71E+10	6.70E-13	23.66	6.52E+09	1.05E+09	9.46E+09
180	625	6.25E+09	2.30E-13	22.19	3.11E+09	2.74E+08	2.86E+09
200	664	2.80E+09	9.71E-14	20.87	1.69E+09	8.55E+07	1.03E+09
220	688	1.40E+09	4.57E-14	19.72	9.66E+08	2.90E+07	3.97E+08
240	699	7.47E+08	2.33E-14	18.77	5.73E+08	1.04E+07	1.61E+08
260	700	4.21E+08	1.26E-14	17.99	3.47E+08	3.82E+06	6.72E+07
280	700	2.43E+08	7.02E-15	17.38	2.12E+08	1.42E+06	2.82E+07
300	700	1.44E+08	4.02E-15	16.89	1.29E+08	5.29E+05	1.19E+07
350	700	4.11E+07	1.09E-15	15.97	3.82E+07	4.61E+04	1.41E+06
400	700	1.28E+07	3.19E-16	14.99	1.15E+07	4.17E+03	1.72E+05
450	700	4.46E+06	9.88E-17	13.33	3.51E+06	3.91E+02	2.16E+04
500	700	1.85E+06	3.26E-17	10.61	1.09E+06	3.79E+01	2.81E+03
600	700	6.34E+05	5.07E-18	4.82	1.11E+05	3.93E-01	5.16E+01
700	700	3.93E+05	1.67E-18	2.55	1.21E+04	4.65E-03	1.06E+00
800	700	2.93E+05	9.37E-19	1.93	1.40E+03	6.22E-05	2.44E-02
900	700	2.32E+05	6.36E-19	1.65	1.72E+02	9.36E-07	6.20E-04
1000	700	1.90E+05	4.64E-19	1.47	2.23E+01	1.58E-08	1.74E-05
1500	700	9.20E+04	1.67E-19	1.09	1.80E-03	1.02E-16	1.19E-12
2000	700	5.34E+04	9.04E-20	1.02	4.45E-07	6.27E-24	5.83E-19
2500	700	3.35E+04	5.60E-20	1.00	2.81E-10	2.50E-30	1.46E-24

NOTE: P = Particles (Molecules)
M = Molecular Weight

Table VIII. Ambient Atmospheric Density Data File (continued)

FILE AADDF AMB. ATMOS. DENSITY DATA FILE ** MEDIUM ***

ALT (KM)	TEMP (K)	TOTDEN (P/CM3)	DEN (G/CM3)	M	DEN O (P/CM3)	DEN O2 (P/CM3)	DEN N2 (P/CM3)
105	224	4.59E+12	2.14E-10	28.07	2.80E+11	7.93E+11	3.48E+12
110	245	2.13E+12	9.80E-11	27.73	1.73E+11	3.33E+11	1.61E+12
120	295	5.47E+11	2.45E-11	26.97	7.25E+10	7.01E+10	4.02E+11
130	466	1.51E+11	6.58E-12	26.25	2.79E+10	1.64E+10	1.06E+11
140	693	6.09E+10	2.60E-12	25.71	1.37E+10	5.86E+09	4.12E+10
150	880	3.33E+10	1.40E-12	25.28	8.57E+09	2.92E+09	2.18E+10
160	997	2.18E+10	9.00E-13	24.89	6.25E+09	1.76E+09	1.37E+10
180	1140	1.14E+10	4.58E-13	24.17	3.91E+09	7.90E+08	6.70E+09
200	1213	6.85E+09	2.67E-13	23.47	2.72E+09	4.06E+08	3.72E+09
220	1251	4.39E+09	1.66E-13	22.78	1.98E+09	2.22E+08	2.18E+09
240	1275	2.91E+09	1.07E-13	22.11	1.47E+09	1.25E+08	1.32E+09
260	1286	1.99E+09	7.10E-14	21.44	1.11E+09	7.17E+07	8.09E+08
280	1294	1.39E+09	4.80E-14	20.81	8.43E+08	4.16E+07	5.02E+08
300	1299	9.83E+08	3.30E-14	20.21	6.43E+08	2.43E+07	3.14E+08
350	1300	4.41E+08	1.38E-14	18.91	3.33E+08	6.54E+06	9.94E+07
400	1300	2.09E+08	6.23E-15	17.92	1.75E+08	1.79E+06	3.20E+07
450	1300	1.04E+08	2.97E-15	17.19	9.23E+07	5.01E+05	1.05E+07
500	1300	5.36E+07	1.48E-15	16.66	4.92E+07	1.42E+05	3.50E+06
600	1300	1.54E+07	4.05E-16	15.90	1.44E+07	1.22E+04	4.06E+05
700	1300	4.82E+06	1.21E-16	15.09	4.36E+06	1.12E+03	5.02E+04
800	1300	1.68E+06	3.85E-17	13.80	1.36E+06	1.09E+03	6.58E+03
900	1300	6.79E+05	1.32E-17	11.74	4.41E+05	1.14E+01	9.11E+02
1000	1300	3.30E+05	5.05E-18	9.20	1.47E+05	1.23E+00	1.33E+02
1500	1300	5.95E+04	3.57E-19	3.61	9.16E+02	4.94E-05	1.84E-02
2000	1300	2.40E+04	1.17E-19	2.93	1.05E+01	6.46E-09	7.38E-06
2500	1300	1.24E+04	4.91E-20	2.38	1.98E+01	2.31E-12	7.13E-09

NOTE: P = Particles (Molecules)
M = Molecular Weight

Table VIII. Ambient Atmospheric Density Data File (concluded)

FILE AADDF AMB. ATMOS. DENSITY DATA FILE ** HIGH ***

ALT (KM)	TEMP (K)	TOTDEN (P/CM3)	DEN (G/CM3)	M	DEN O (P/CM3)	DEN O2 (P/CM3)	DEN N2 (P/CM3)
105	224	4.59E+12	2.14E-10	28.07	2.80E+11	7.93E+11	3.48E+12
110	246	2.12E+12	9.78E-11	27.73	1.73E+11	3.32E+11	1.60E+12
120	435	4.41E+11	1.98E-11	27.10	5.44E+10	5.83E+10	3.26E+11
130	705	1.58E+11	7.00E-12	26.67	2.43E+10	1.88E+10	1.14E+11
140	985	7.90E+10	3.46E-12	26.35	1.40E+10	8.76E+09	5.61E+10
150	1190	5.00E+10	2.16E-12	26.08	9.84E+09	5.22E+09	3.48E+10
160	1324	3.56E+10	1.53E-12	25.84	7.67E+09	3.52E+09	2.44E+10
180	1455	2.15E+10	9.05E-13	25.36	5.40E+09	1.92E+09	1.41E+10
200	1545	1.39E+10	5.76E-13	24.88	4.01E+09	1.12E+09	8.79E+09
220	1605	9.50E+09	3.85E-13	24.40	3.08E+09	6.91E+08	5.72E+09
240	1656	6.65E+09	2.64E-13	23.92	2.41E+09	4.35E+08	3.80E+09
260	1690	4.79E+09	1.86E-13	23.43	1.92E+09	2.81E+08	2.58E+09
280	1721	3.50E+09	1.33E-13	22.94	1.54E+09	1.84E+08	1.78E+09
300	1745	2.60E+09	9.70E-14	22.46	1.24E+09	1.22E+08	1.24E+09
350	1785	1.31E+09	4.64E-14	21.29	7.48E+08	4.52E+07	5.19E+08
400	1799	7.09E+08	2.38E-14	20.21	4.64E+08	1.75E+07	2.26E+08
450	1800	4.02E+08	1.29E-14	19.07	2.93E+08	6.98E+06	1.01E+08
500	1800	2.35E+08	7.22E-15	18.48	1.86E+08	2.82E+06	4.57E+07
600	1800	8.73E+07	2.51E-15	17.33	7.65E+07	4.77E+05	9.66E+06
700	1800	3.50E+07	9.65E-16	16.59	3.23E+07	8.49E+04	2.13E+06
800	1800	1.49E+07	3.97E-16	16.08	1.40E+07	1.59E+04	4.91E+05
900	1800	6.63E+06	1.72E-16	15.61	6.17E+06	3.10E+03	1.18E+05
1000	1800	3.10E+06	7.73E-17	15.04	2.79E+06	6.34E+02	2.94E+04
1500	1800	1.84E+05	2.63E-18	8.61	7.13E+04	4.14E-01	4.80E+01
2000	1800	5.41E+04	4.04E-19	4.50	2.82E+03	6.50E-04	1.69E-01
2500	1800	2.60E+04	1.66E-19	3.86	1.61E+02	2.11E-06	1.12E-03

NOTE: P = Particles (Molecules)
M = Molecular Weight

Table IX. List of Surfaces That Have Direct Line-of-Sight to Bottom of LMOP Pallet

REPORT NO. 08 *** SAMPLE CASE NO. 1 LMOP SPACELAB CONFIGURATION ***
7/20/76
CONTENTS: LIST OF MASS FLUX (VIEW FACTOR) DATA READ IN

NODEI	NODEJ	MFIJ	MFJI	AREAJ	THETAI	THETAJ	RADIUS
CARDS ARE BEING LOADED ONTO TAPE20 INDIVIDUALLY							
1050	1088	.169E-01	.565E-02	.787E+04	.671E+02	.584E+02	.145E+03
1051	1088	.221E-02	.740E-03	.787E+04	.750E+02	.477E+02	.156E+03
1052	1088	.221E-02	.740E-03	.787E+04	.750E+02	.477E+02	.156E+03
1053	1088	.169E-01	.565E-02	.787E+04	.671E+02	.584E+02	.145E+03
1055	1088	.201E-01	.268E-01	.787E+04	.309E+02	.888E+02	.114E+03
1060	1088	.257E-01	.776E-02	.787E+04	.104E+03	.577E+02	.104E+03
1061	1088	.257E-01	.776E-02	.787E+04	.104E+03	.577E+02	.104E+03
1065	1088	.143E+00	.374E-01	.787E+04	.388E+02	.513E+02	.890E+02
1084	1088	.888E-01	.583E-01	.787E+04	.547E+02	.537E+02	.814E+02
1085	1088	.888E-01	.583E-01	.787E+04	.547E+02	.537E+02	.814E+02
1086	1088	.933E-01	.485E-01	.787E+04	.580E+02	.740E+02	.484E+02
1087	1088	.933E-01	.485E-01	.787E+04	.580E+02	.740E+02	.484E+02
1088	1	.832E-02	.246E-02	.266E+05	.967E+02	.524E+02	.887E+02
1088	2	.531E-02	.157E-02	.266E+05	.943E+02	.673E+02	.140E+03
1088	5	.832E-02	.246E-02	.266E+05	.967E+02	.524E+02	.887E+02
1088	6	.531E-02	.157E-02	.266E+05	.943E+02	.673E+02	.140E+03
1088	442	.439E-02	.100E-01	.344E+04	.671E+02	.561E+02	.168E+03
1088	443	.464E-02	.106E-01	.344E+04	.594E+02	.431E+02	.128E+03
1088	447	.439E-02	.100E-01	.344E+04	.671E+02	.561E+02	.168E+03
1088	448	.464E-02	.106E-01	.344E+04	.594E+02	.431E+02	.128E+03
1088	11	.845E-01	.203E-01	.327E+05	.695E+02	.205E+02	.159E+03
1088	399	.278E-04	.572E-04	.382E+04	.417E+02	.917E+02	.438E+03
1088	60	.329E-02	.226E-01	.115E+04	.535E+02	.457E+02	.213E+03
1088	62	.280E-02	.281E-02	.785E+04	.528E+02	.938E+02	.251E+03
1088	80	.329E-02	.226E-01	.115E+04	.535E+02	.457E+02	.213E+03
1088	82	.275E-02	.277E-02	.781E+04	.530E+02	.936E+02	.251E+03

Table X. List of Surface Sources in Payload Bay Vicinity

REPORT NO. 10 *** SAMPLE CASE NO. 1 LMOP SPACELAB CONFIGURATION ***
7/20/76
CONTENTS: PHYSICAL CHARACTERISTICS OF SURFACE SOURCES

SURFACE NUMBER	AREA (IN**2) (CM**2)	SECTION MATERIAL	MASS LOSS (GM/SEC) TEMP (DEG C)	SPECIES MASS LOSS RATES (GM/CM**2/SEC) H2O OUT2	N2 CO	CO2 H2	O2 H	OUT1 NO	EARLY DESORPTION	OUT GASSING
1	.27E+05	BAY	.178E-04	.16E-10	.10E-10	.83E-11	.39E-11	.65E-10		
	.17E+06	LINER	94.	0.	0.	0.	0.	0.	.388E-10	.649E-10
2	.27E+05	BAY	.114E-04	.10E-10	.65E-11	.53E-11	.25E-11	.41E-10		
	.17E+06	LINER	81.	0.	0.	0.	0.	0.	.248E-10	.414E-10
5	.27E+05	BAY	.178E-04	.16E-10	.10E-10	.83E-11	.39E-11	.65E-10		
	.17E+06	LINER	94.	0.	0.	0.	0.	0.	.388E-10	.649E-10
6	.27E+05	BAY	.114E-04	.10E-10	.65E-11	.53E-11	.25E-11	.41E-10		
	.17E+06	LINER	81.	0.	0.	0.	0.	0.	.248E-10	.414E-10
442	.34E+04	BAY	.488E-06	.35E-11	.22E-11	.18E-11	.83E-12	.14E-10		
	.22E+05	LINER	49.	0.	0.	0.	0.	0.	.821E-11	.137E-10
443	.34E+04	BAY	.713E-06	.51E-11	.32E-11	.26E-11	.12E-11	.20E-10		
	.22E+05	LINER	60.	0.	0.	0.	0.	0.	.120E-10	.201E-10
447	.34E+04	BAY	.488E-06	.35E-11	.22E-11	.18E-11	.83E-12	.14E-10		
	.22E+05	LINER	49.	0.	0.	0.	0.	0.	.821E-11	.137E-10
448	.34E+04	BAY	.713E-06	.51E-11	.32E-11	.26E-11	.12E-11	.20E-10		
	.22E+05	LINER	60.	0.	0.	0.	0.	0.	.120E-10	.201E-10
11	.33E+05	BAY	.375E-04	.64E-10	.40E-10	.33E-10	.15E-10	.25E-10		
	.21E+06	BLKHED	-7.	0.	0.	0.	0.	0.	.153E-09	.252E-10
60	.11E+04	OMS	.455E-06	.98E-11	.61E-11	.49E-11	.23E-11	.38E-10		
	.74E+04	LRSI	25.	0.	0.	0.	0.	0.	.232E-10	.383E-10
62	.79E+04	OMS	.312E-05	.98E-11	.61E-11	.49E-11	.23E-11	.38E-10		
	.51E+05	LRSI	25.	0.	0.	0.	0.	0.	.232E-10	.383E-10
80	.11E+04	OMS	.455E-06	.98E-11	.61E-11	.49E-11	.23E-11	.38E-10		
	.74E+04	LRSI	25.	0.	0.	0.	0.	0.	.232E-10	.383E-10
82	.78E+04	OMS	.310E-05	.98E-11	.61E-11	.49E-11	.23E-11	.38E-10		
	.50E+05	LRSI	25.	0.	0.	0.	0.	0.	.232E-10	.383E-10
1050	.26E+04	LMOP	.287E-03	.69E-08	.43E-08	.35E-08	.16E-08	.64E-09		
	.17E+05	MTCS	35.	0.	0.	0.	0.	0.	.163E-07	.636E-09
1051	.26E+04	LMOP	.233E-03	.56E-08	.35E-08	.28E-08	.13E-08	.52E-09		
	.17E+05	MTCS	29.	0.	0.	0.	0.	0.	.132E-07	.516E-09
1052	.26E+04	LMOP	.216E-03	.52E-08	.32E-08	.26E-08	.12E-08	.48E-09		
	.17E+05	MTCS	27.	0.	0.	0.	0.	0.	.123E-07	.478E-09
1053	.26E+04	LMOP	.261E-03	.63E-08	.39E-08	.32E-08	.15E-08	.58E-09		
	.17E+05	MTCS	32.	0.	0.	0.	0.	0.	.148E-07	.578E-09
1055	.11E+05	LMOP	.631E-02	.38E-07	.24E-07	.19E-07	.90E-08	.35E-08		
	.68E+05	MTCS	84.	0.	0.	0.	0.	0.	.896E-07	.350E-08

Table X. List of Surface Sources in Payload Bay Vicinity (concluded)

SURFACE NUMBER	AREA (IN**2) (CM**2)	SECTION MATERIAL	MASS LOSS (GM/SEC) TEMP (DEG. C)	SPECIES MASS LOSS RATES (GM/CM**2/SEC) H2O OUT2	N2 CO	CO2 H2	O2 H	OUT1 NO	EARLY DESORPTION	OUT GASSING
1060	.24E+04	LMOP	.143E-02	.38E-07	.24E-07	.19E-07	.90E-08	.35E-08	.896E-07	.350E-08
	.15E+05	MTCS	84.	0.	0.	0.	0.	0.		
1061	.24E+04	LMOP	.2[illegible]E-03	.54E-08	.33E-08	.27E-08	.13E-08	.50E-09	.127E-07	.496E-09
	.15E+05	MTCS	28.	0.	0.	0.	0.	0.		
1065	.21E+04	LMOP	.419E-03	.13E-07	.80E-08	.65E-08	.31E-08	.12E-08	.303E-07	.118E-08
	.13E+05	MTCS	53.	0.	0.	0.	0.	0.		
1084	.52E+04	LMOPP	.846E-03	.10E-07	.64E-08	.52E-08	.25E-08	.95E-09	.244E-07	.954E-09
	.33E+05	PTCS	47.	0.	0.	0.	0.	0.		
1085	.52E+04	LMOPP	.108E-02	.13E-07	.82E-08	.67E-08	.31E-08	.12E-08	.313E-07	.122E-08
	.33E+05	PTCS	54.	0.	0.	0.	0.	0.		
1086	.41E+04	LMOPP	.131E-02	.20E-07	.13E-07	.10E-07	.48E-08	.19E-08	.477E-07	.186E-08
	.26E+05	PTCS	66.	0.	0.	0.	0.	0.		
1087	.41E+04	LMOPP	.131E-02	.20E-07	.13E-07	.10E-07	.48E-08	.19E-08	.477E-07	.186E-08
	.26E+05	PTCS	66.	0.	0.	0.	0.	0.		
1088	.79E+04	LMOPP	.267E-02	.21E-07	.13E-07	.11E-07	.51E-08	.20E-08	.505E-07	.198E-08
	.51E+05	PTCS	68.	0.	0.	0.	0.	0.		
TOTALS	.23E+06		.167E-01	.20E-06	.13E-06	.10E-06	.48E-07	.19E-07	.481E-06	.192E-07
				0.	0.	0.	0.	0.		

approach 5500Å for a 7 day continuous exposure to the payload bay vicinity sources. This large amount of deposition would only occur if the mission maintained an attitude where surface temperatures were at their maximum values for the full 7 days and if the critical surface had an acceptance angle equivalent to the pallet bottom surface (approximately 2π steradians) and were located on the bottom of the pallet.

2.3.1.6 Contribution of Reflected Ambient Molecules to Column Density - An additional contribution to the column density that was evaluated during this period was that resulting from reflected ambient molecules off of the spacecraft. Two cases were evaluated using the computer model of the Shuttle Orbiter, one with the velocity vector perpendicular to the XY plane (in a -Z direction) and the other parallel to this plane (-X direction). The flux was calculated for each component (O, O_2 and N_2) of the ambient at an altitude of 400 km and an effective temperature of 1300°K. For the perpendicular case, the reflected molecules were assumed to come off with a speed one-third that of the orbital velocity with no accommodation on the surface. Thus, the NCD is independent of the surface temperature. For the parallel case, the impingement flux is calculated by using one-fourth the average thermal velocity which is the velocity component for a random gas in the -Z direction. These slower molecules are allowed to accommodate to the surface and thus are reemitted at the temperature of the surface.

Table XI shows the molecular column density (NCD) for each case for maximum surface temperature and minimum surface temperature along line-of-sight number 1. Note that the maximum NCD (2.65×10^{11} molecules/cm^2) occurs for the coldest temperature. This is because the NCD is inversely proportional to the molecular velocity and thus the colder surface reemits the accommodated molecules at much slower velocities. As can be seen in Table XI, the contribution of reflected ambient to the NCD is comparable to that of the vehicle surface outgassing.

Table XI. Contribution to NCD by Reflected Ambient Molecules from the Shuttle Orbiter Along Line-of-Sight 1

Temperature Profile	Ambient Moving -Z Direction	Ambient Moving +X Direction	Orbiter Outgassing
	NCD (molecules/cm^2)	NCD (molecules/cm^2)	NCD (molecules/cm^2)
Min.	1.27×10^{12}	2.65×10^{11}	8.8×10^{9}
Max.	1.27×10^{12}	2.28×10^{11}	2.0×10^{11}

The basic conclusion that can be drawn from this evaluation is that the reflection of ambient molecules from spacecraft surfaces will impact the total column density along a given line-of-sight. This impact will be a direct function of orbital altitude and ambient density. It should be noted, however, that the ambient contains no H_2O molecules, and that much higher NCDs than those predicted in Table XI would be required to produce undesirable background brightness levels for most payloads. For those payloads sensitive to the O and N_2 molecules in the ambient, this phenomena should be considered.

2.3.3 Mission Profile Data Bank (MPDB) - As a result of the Spacelab/Orbiter mission compatibility assessment (previously termed IMAP) studies conducted during this period, the MPDB has been updated and expanded wherever possible to establish a strong, yet flexible data base system of contamination oriented Spacelab/Orbiter mission and payload information formatted for direct input into the contamination computer model. Included in the data bank is such data as mission duration, orbital attitudes and altitudes, pointing requirements, payload definitions, thermal profiles and usage requirements. The limitations of the primary source of information (i.e., the Payload Description Documents of SSPD[31]) still exist and have been discussed in Reference 6 and will not be reiterated here. Consequently, the MPDB is far from a complete or finished product, although information obtained in conducting the mission compatibility assessment task tends to fill many of the information voids for a given mission being evaluated. The data base is currently adequate for checkout of the computer model and past mission compatibility assessment activities.

No further effort is planned for expanding the Mission Profile Data Bank. In the future to avoid duplication of effort, the Marshall Interactive Planning System (MIPS) data bank will be the source of all Spacelab mission data. Plans have been devised to modify the MMA contamination analysis program to develop an interface preprocessor program to accept input from the MIPS data bank in the future.

2.4 Spacelab Molecular Induced Environment Predictions - Through the use of the Spacelab Contamination Computer Model subelements of the VOLCAN Program, molecular induced environment predictions were established for the contaminant sources and Spacelab configurations/lines-of-sight described in subsection 2.1. These predictions reflect the major model updates and modifications that have been discussed previously in subsection 2.2 and the state of the technology refinements presented in subsection 2.3. The contaminant sources evaluated in detail in this section include nonmetallic materials outgassing, early desorption at 10 hours of vacuum exposure and cabin atmosphere leakage.

Although the Spacelab Condensate Vent (SCV) has been identified as an additional major contaminant source for LMOP and SMTP, sufficient supplemental design data is not yet available from ESA, and consequently, the evaluation of this source has not changed significantly from that reported in Reference 5. It is, therefore, not repeated herein.

To summarize, however, in its current assumed design; the column density, return flux, background brightness and particle sighting criteria limits are exceeded during SCV operation. A clearing time of up to 17 minutes may be required after vent termination for the particle cloud to dissipate to an acceptable level. An additional concern is the SCV plume impingement upon structural surfaces in the Orbiter payload bay which will significantly alter the plume geometry and increase the clearing time of particles as well as allow potential accumulation of ice within the payload bay volume. It is recommended that this situation be eliminated through vent nozzle relocation or vent plume centerline redirection. Interference with the operation of sensitive Spacelab payloads should easily be avoided through vent expulsion timelining since current plans are to operate the vent only once for each 7 days on orbit. If this frequency increases, proper timelining will become more critical.

For convenience and to eliminate potential errors in transferring output data from computer printout to tabular form, the model output routine was refined to present the final predictions in a format such that it could be directly inserted into a report. The prediction tables presented later in this subsection are the result of this refinement. Before discussing the final induced environment predictions, it is first necessary to explain the printout format in general to facilitate the understanding of the data presented. Reference should be made to Table XII for an example of the printout format. Initially, each data sheet establishes the contaminant source under investigation and pertinent information concerning the modeled emission rate. In this case, the source is outgassing modeled with all nodes designated as outgassing sources having an initial outgassing rate of 6.0×10^{-9} g/cm^2/s at 100°C. The modeled configuration (LMOP) and the specific line-of-sight modeled are then presented. Line-of-sight 1 is denoted in Table XII for which reference can be made to Figure 6 for a pictorial description of the viewing directions of each designated line-of-sight. In the case of a source which is temperature dependent such as outgassing, separate sets of predictions are presented for the maximum and minimum temperature profiles discussed in subsection 2.2.2. For

Table XII. Spacelab LMOP Outgassing Induced Environment Predictions

MARTIN MARIETTA AEROSPACE

SPACELAB CONTAMINATION MODEL

SOURCE = OUTGASSING
(INITIAL RATE = 6.0E-9 G/CM2/S AT 100 C)
CONFIGURATION = LONG MODULE/ONE PALLET
LINE-OF-SIGHT = 1,(0 DEGREES OFF +Z TOWARDS THE X-Y PLANE AT 0 DEGREES)

+++ MAXIMUM TEMPERATURE PROFILE +++

SECTION	TOTAL MCD G/CM2	TOTAL NCD MOL/CM2	RETURN FLUX FOR 0.1 SR SURFACE 250 KM MOL/CM2/S	400 KM MOL/CM2/S	700 KM MOL/CM2/S	% OF LMOP
MODULE	8.89E-12	5.36E+10	2.61E+11	2.20E+10	5.02E+08	47.9
PALLET	9.04E-12	5.45E+10	2.65E+11	2.23E+10	5.11E+08	48.7
WINDOW	6.23E-13	3.76E+09	1.83E+10	1.54E+09	3.52E+07	3.4
+ LMOP +						
+ TOTAL +	1.86E-11	1.12E+11	5.43E+11	4.58E+10	1.05E+09	100.0

+++ MINIMUN TEMPERATURE PROFILE +++

MODULE	2.65E-14	1.60E+08	7.77E+08	6.55E+07	1.50E+06	70.5
PALLET	9.90E-15	5.97E+07	2.90E+08	2.45E+07	5.59E+05	26.3
WINDOW	1.18E-15	7.13E+06	3.47E+07	2.92E+06	6.68E+04	3.1
+ LMOP +						
+ TOTAL +	3.76E-14	2.26E+08	1.10E+09	9.28E+07	2.12E+06	100.0

leakage only, one set of predictions is necessary. The data sheets then present the induced environment contributions for the major Spacelab structures/surfaces as well as the totals for the entire vehicle. The level of detail in this segment is left to the discretion of the program user (i.e..; each unique Spacelab nodal or surface material contribution can be individually broken out). The predicted values depicted in the data sheets include: 1) total mass column density (MCD) in g/cm^2 along the modeled line-of-sight; 2) total number column density (NCD) in molecules/cm^2 along the modeled line-of-sight; 3) maximum return flux in molecules/cm^2/s of contaminant molecules resulting from collisions with the ambient flux at three altitudes to a surface having a 0.1 steradian acceptance angle situated perpendicular to the modeled line-of-sight and the ambient drag vector; and 4) the percent of the total values predicted that is contributed by the designated major surfaces or sections. For presentation purposes, the data sheets included herein indicate the contributions from only the major Spacelab components including the module segments (includes tunnel, module, end caps, etc.), pallet segments (denoted PLT) and the windows which are assumed to be covered.

An additional model output refinement developed for visual display and checkout purposes was the capability to graphically present the variation of contaminant density in g/cm^3 with distance from the Spacelab X axis (Z_o = 400) along the modeled lines-of-sight. An example of this computer output is presented in Figure 14. In this case, the variation of LMOP outgassing density along line-of-sight 1 for the maximum Spacelab temperature profile is depicted. Integration under this curve will result in the total mass column density along line-of-sight 1 which is presented in Table XII for the identical conditions. A series of such curves for the modeled lines-of-sight can be used as a basis for completely mapping the induced contaminant environment around the Spacelab vehicle for each source and parametric variation evaluated.

In order to maintain a level of continuity in the text of this report; the induced environment predictions for all analyzed Spacelab sources, configurations and lines-of-sight have been calculated while only line-of-sight 1 predictions have been included in this subsection for discussion purposes. The information for all seventeen lines-of-sight is used as the basis for the Spacelab contamination control criteria evaluation which is discussed further in subsection 2.5 and for the Spacelab design

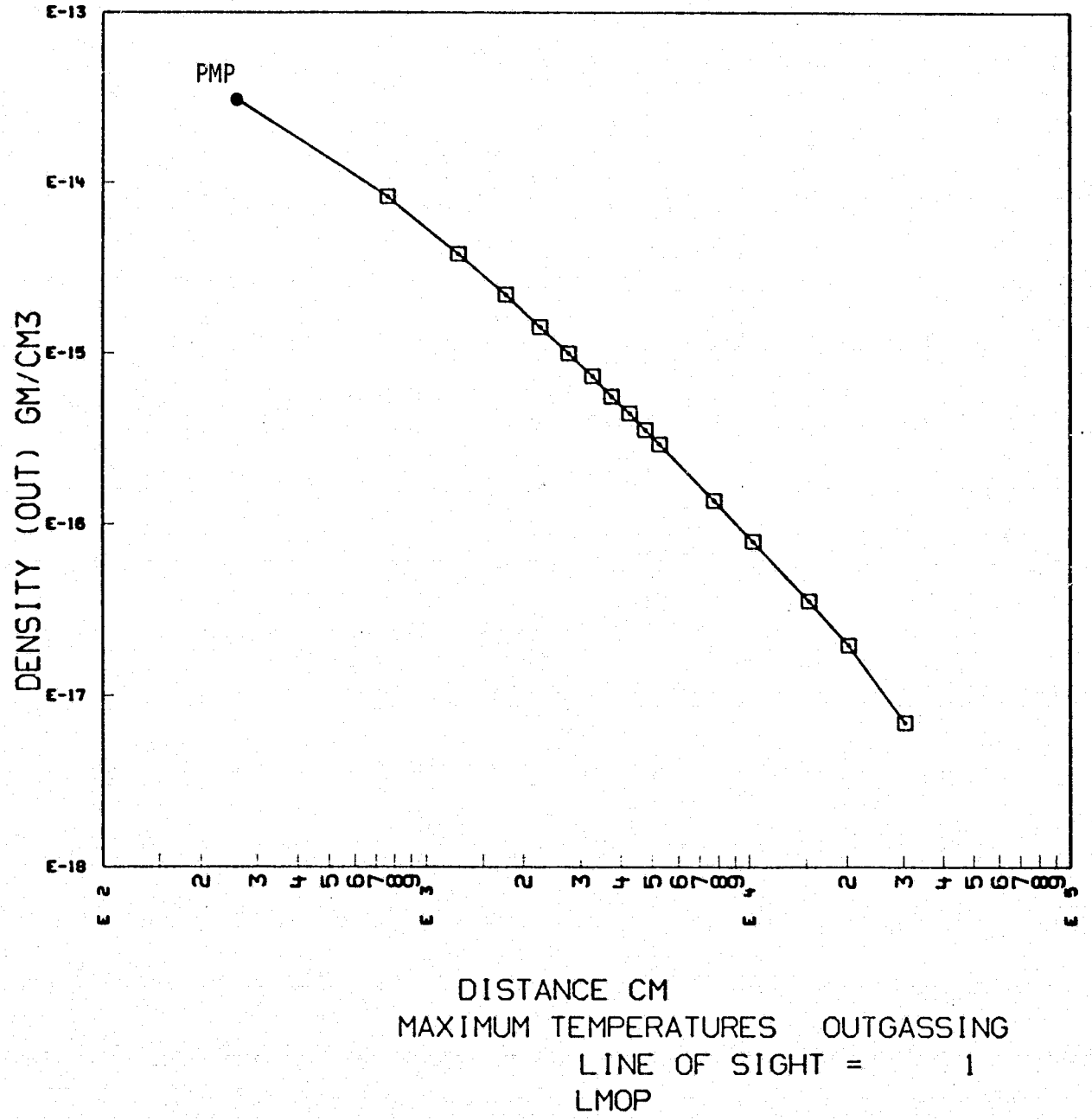

Figure 14. Outgassing Density Variation Along Line-of-Sight 1 for LMOP at Maximum Temperatures

and development recommendations included therein.

2.4.1 Outgassing Induced Environment Predictions - Tables XII through XIV present a comparative summary of the outgassing induced environment predictions for the three modeled Spacelab configurations for line-of-sight 1. The predictions are based upon an initial outgassing rate for all externally exposed Spacelab surfaces of 6×10^{-9} g/cm^2/s at 100°C adjusted to meet individual nodal temperatures. Subsection 2.1.2 presents the rationale behind using this outgassing rate in the current modeling. As adequate materials mapping and test data are supplied by ESA, the model nodal structure as well as source input rates can easily be modified accordingly.

For line-of-sight 1, the predicted number column densities (NCD) vary from a maximum of 1.60×10^{11} molecules/cm^2 for the SMTP maximum temperature profile to a minimum of 1.96×10^{8} molecules/cm^2 for the FIVP minimum temperature profile. Within the 120 degree modeled viewing volume, the worst case lines-of-sight for the three configurations are: 1) LMOP line-of-sight 13 where NCD = 1.93×10^{11} molecules/cm^2; 2) SMTP line-of-sight 11 where NCD = 2.51×10^{11} molecules/cm^2; and 3) FIVP line-of-sight 11 where NCD = 1.75×10^{11} molecules/cm^2. As can be established through analysis of the segment contributions shown in Tables XII to XIV, the influencing parameter for the maximum temperature profile predictions seems to be the location of outgassing surfaces with respect to the line-of-sight, while for the minimum temperature profile predictions, the individual surface temperatures appear to be the major influencing parameter. Such knowledge might be useful during mission evaluations if, for example, selective protection or partial elimination of selected nonmetallic materials might be adequate to meet specific contamination requirements of a particular payload as opposed to more costly Spacelab design modifications.

For most Spacelab payloads the primary transport mechanism of this source will be the return flux through collisions of the NCD with the ambient atmosphere. Direct line-of-sight and self scattering transport were evaluated and deemed negligible under most conditions (see subsection 2.3.1.5 and 2.3.1.2 respectively). These were all influencing factors in development of the tabular printout. The outgassing return flux levels that appear in the tables have been calculated at selective orbital altitudes of 250 km, 400 km and 700 km. Previous studies extended the lower altitude down to 200 km which resulted in some rather confusing predictions. At 200 km, the return flux of outgassing molecules is attenuated to approximately zero for the modeled drag vector

Table XIII. Spacelab SMTP Outgassing Induced Environment Predictions

MARTIN MARIETTA AEROSPACE

SPACELAB CONTAMINATION MODEL

SOURCE = OUTGASSING
(INITIAL RATE = 6.0E-9 G/CM2/S AT 100 C)
CONFIGURATION = SHORT MODULE/THREE PALLETS
LINE-OF-SIGHT = 1,(0 DEGREES OFF +Z TOWARDS THE X-Y PLANE AT 0 DEGREES)

+++ MAXIMUM TEMPERATURE PROFILE +++

SECTION	TOTAL MCD G/CM2	TOTAL NCD MOL/CM2	RETURN FLUX FOR 0.1 SR SURFACE 250 KM MOL/CM2/S	400 KM MOL/CM2/S	700 KM MOL/CM2/S	% OF SMTP
MODULE	3.94E-12	2.38E+10	1.16E+11	9.75E+09	2.23E+08	14.9
PLT1	5.16E-12	3.11E+10	1.51E+11	1.28E+10	2.91E+08	19.5
PLT2	8.46E-12	5.10E+10	2.48E+11	2.09E+10	4.78E+08	32.0
PLT3	8.80E-12	5.31E+10	2.58E+11	2.18E+10	4.97E+08	33.2
WINDOW	1.14E-13	6.89E+08	3.35E+09	2.82E+08	6.45E+06	.4
+ SMTP +						
+ TOTAL +	2.65E-11	1.60E+11	7.75E+11	6.54E+10	1.49E+09	100.0

+++ MINIMUN TEMPERATURE PROFILE +++

MODULE	1.04E-14	6.29E+07	3.05E+08	2.58E+07	5.89E+05	29.4
PLT1	5.47E-15	3.30E+07	1.60E+08	1.35E+07	3.09E+05	15.4
PLT2	9.48E-15	5.72E+07	2.78E+08	2.34E+07	5.36E+05	26.7
PLT3	9.89E-15	5.96E+07	2.90E+08	2.44E+07	5.59E+05	27.9
WINDOW	2.20E-16	1.32E+06	6.43E+06	5.43E+05	1.24E+04	.6
+ SMTP +						
+ TOTAL +	3.55E-14	2.14E+08	1.04E+09	8.77E+07	2.00E+06	100.0

Table XIV. Spacelab FIVP Outgassing Induced Environment Predictions

MARTIN MARIETTA AEROSPACE

SPACELAB CONTAMINATION MODEL

SOURCE = OUTGASSING
(INITIAL RATE = 6.0E-9 G/CM2/S AT 100 C)
CONFIGURATION = FIVE PALLETS
LINE-OF-SIGHT = 1,(0 DEGREES OFF +Z TOWARDS THE X-Y PLANE AT 0 DEGREES)

+++ MAXIMUM TEMPERATURE PROFILE +++

SECTION	TOTAL MCD G/CM2	TOTAL NCD MOL/CM2	RETURN FLUX FOR 0.1 SR SURFACE 250 KM MOL/CM2/S	400 KM MOL/CM2/S	700 KM MOL/CM2/S	% OF FIVP
PLT1	2.26E-12	1.36E+10	6.61E+10	5.58E+09	1.27E+08	10.8
PLT2	2.67E-12	1.61E+10	7.81E+10	6.59E+09	1.51E+08	12.8
PLT3	3.50E-12	2.11E+10	1.03E+11	8.66E+09	1.98E+08	16.8
PLT4	6.04E-12	3.64E+10	1.77E+11	1.49E+10	3.41E+08	29.0
PLT5	6.38E-12	3.85E+10	1.87E+11	1.58E+10	3.61E+08	30.6
+ FIVP + TOTAL +	2.09E-11	1.26E+11	6.11E+11	5.15E+10	1.18E+09	100.0

+++ MINIMUN TEMPERATURE PROFILE +++

PLT1	2.36E-15	1.42E+07	6.91E+07	5.83E+06	1.33E+05	7.2
PLT2	3.24E-15	1.95E+07	9.50E+07	8.01E+06	1.83E+05	9.9
PLT3	5.04E-15	3.04E+07	1.48E+08	1.25E+07	2.85E+05	15.5
PLT4	1.00E-14	6.03E+07	2.93E+08	2.47E+07	5.65E+05	30.7
PLT5	1.20E-14	7.21E+07	3.50E+08	2.96E+07	6.76E+05	36.7
+ FIVP + TOTAL +	3.26E-14	1.96E+08	9.55E+08	8.05E+07	1.84E+06	100.0

orientation due to the small mean free paths of outgassing molecules traveling into the ambient "wind" (less than one meter). This prevents the outgassing molecules from traveling far enough into the ambient drag vector to be reflected back to a surface at the PMP. Therefore, for outgassing only, the return flux predictions are made at 250 km where the mean free path influence becomes less of a factor. This establishes a more realistic presentation of outgassing contaminant levels at lower altitudes.

Figures 14 through 16 graphically display the variation of outgassing density from the PMP to 300 meters along line-of-sight 1 for the LMOP, SMTP and FIVP maximum temperature profiles, respectively. Density plots for each source, configuration, temperature profile and line-of-sight modeled are available, but have not been included herein due to their similarities of shape and magnitude. As can be seen in Figures 14, 15 and 16; the density levels at the PMP all fall in the mid 10^{-14} g/cm^3 range (which is equivalent to the ambient density at approximately 300 km altitude) and decay more than three orders of magnitude at the 300 meter distance. The smoothness of the curves is dictated by the uniformity of the outgassing emission pattern and due to the minimal influence of surface shadowing between the Spacelab configurations and line-of-sight 1. For point sources such as engines and vents or for lines-of-sight not parallel to the Z axis, undulations in the density plots can be observed which are the result of geometry and engine exhaust plume considerations.

The primary threat of an outgassing source is its ability to accommodate or stick to surfaces upon which it impinges thus absorbing the radiant energy which scientific instruments are attempting to detect. Therefore, the optimum approach to decreasing the impacts of outgassing upon sensitive surfaces is to minimize the impingement or reduce its ability to stick. Impingement can be minimized through proper selection of low outgassing materials, flying in attitudes where major contributing surfaces are cool, flying in attitudes where return flux is minimized or by the payloads supplying their own operable protective covers. Sticking can be reduced by providing heater systems for the sensitive surfaces or in some cases by providing an enert gas purge system which "sweeps" contaminant molecules away.

2.4.2 Early Desorption Induced Environment Predictions - Tables XV through XVII present the induced contaminant environment predictions for early desorption at 10 hours into a mission for line-of-sight 1 of the three modeled Spacelab configurations. The early desorption rate used in the modeling was 1.5×10^{-7} $g/cm^2/s$ at $100^{\circ}C$ as based upon the materials screening criteria

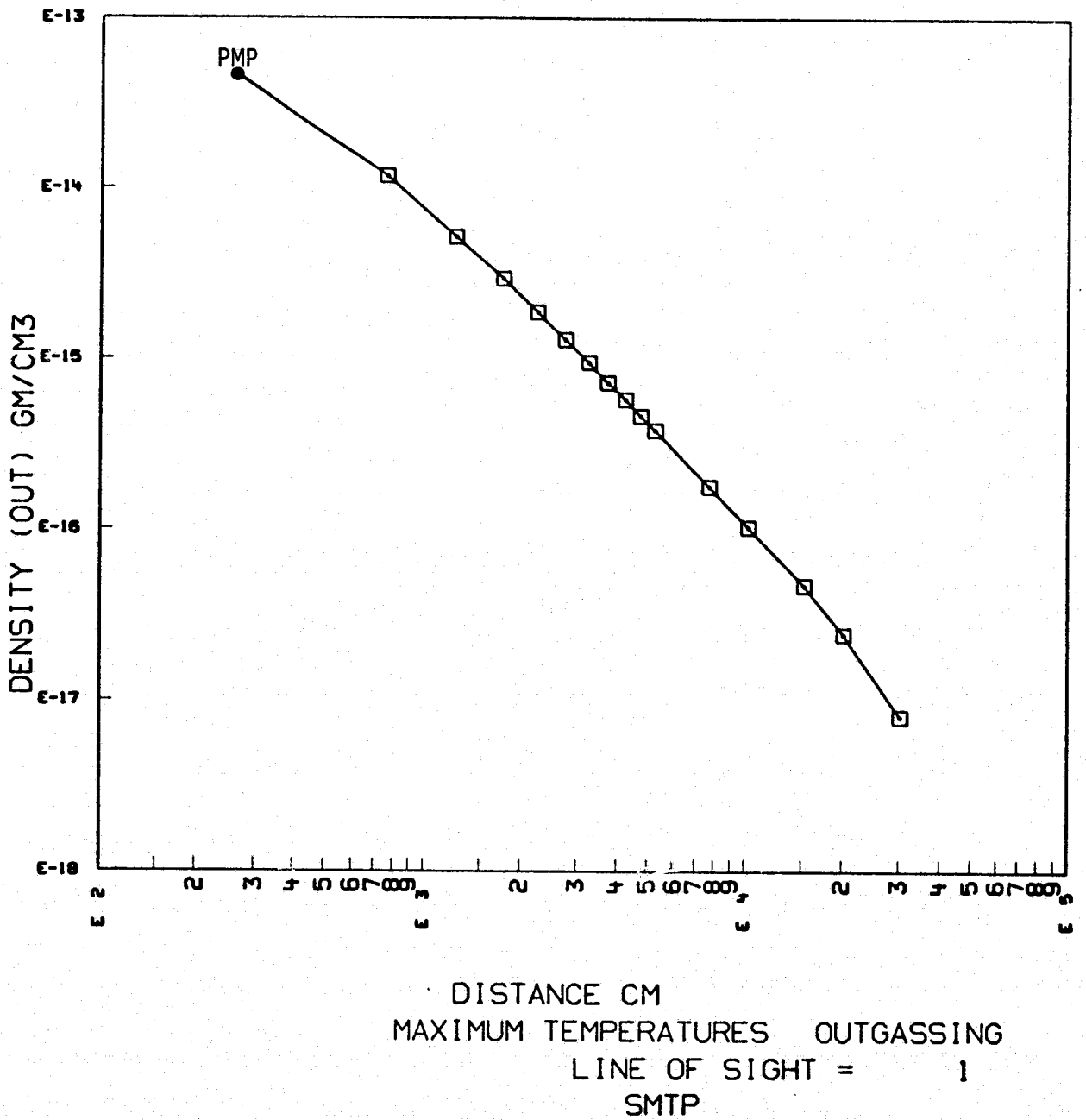

Figure 15. Outgassing Density Variation Along Line-of-Sight 1 for SMTP at Maximum Temperatures

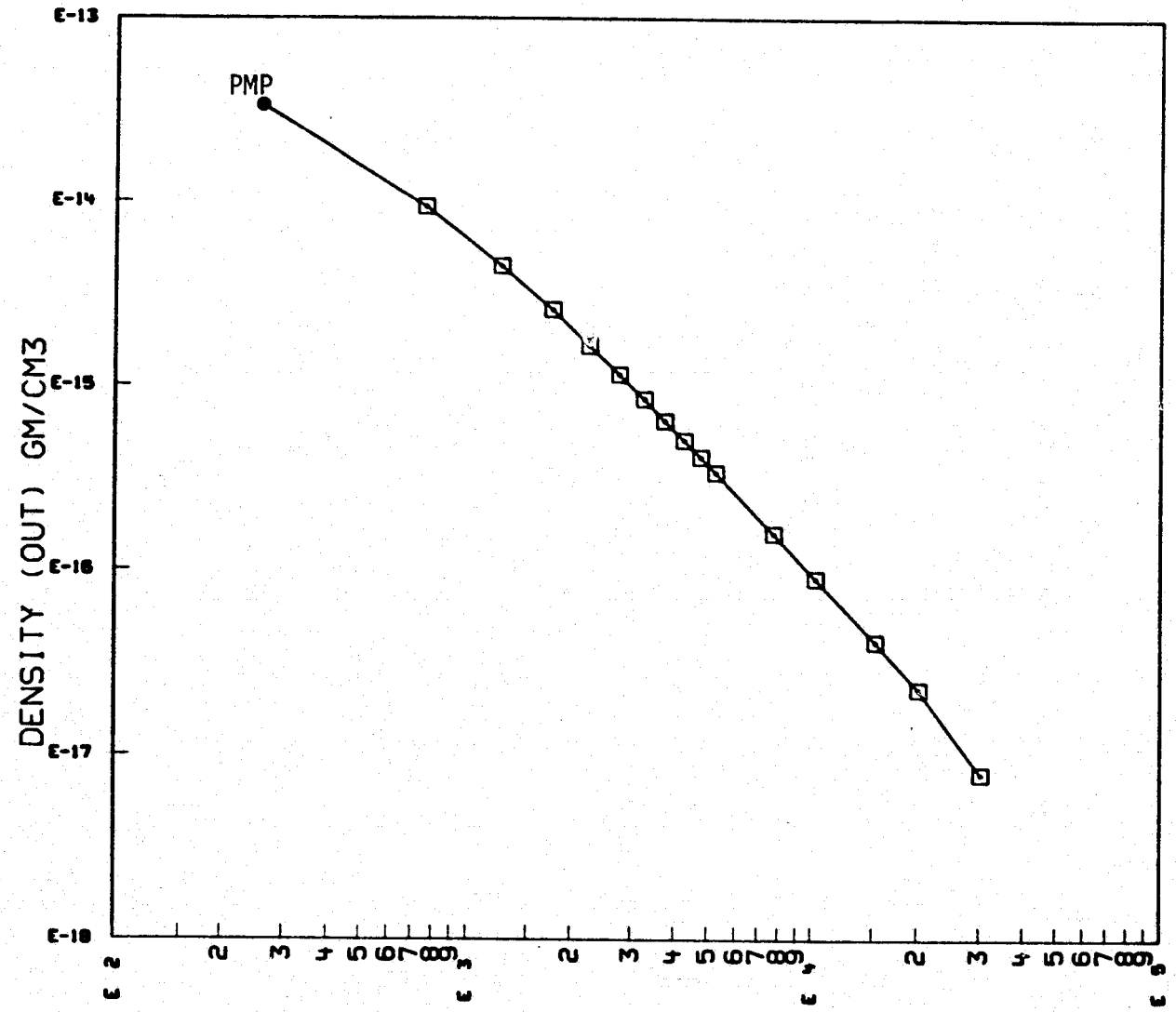

Figure 16. Outgassing Density Variation Along Line-of-Sight 1 for FIVP at Maximum Temperatures

Table XV. Spacelab LMOP Early Desorption Induced Environment Predictions

MARTIN MARIETTA AEROSPACE

SPACELAB CONTAMINATION MODEL

SOURCE = EARLY DESORPTION
(AT 10 HOURS INTO MISSION RATE = 1.5E-7 G/CM2/S AT 100 C)
CONFIGURATION = LONG MODULE/ONE PALLET
LINE-OF-SIGHT = 1,(0 DEGREES OFF +Z TOWARDS THE X-Y PLANE AT 0 DEGREES)

+++ MAXIMUM TEMPERATURE PROFILE +++

SECTION	TOTAL MCD G/CM2	TOTAL NCD MOL/CM2	RETURN FLUX FOR 0.1 SR SURFACE 200 KM MOL/CM2/S	400 KM MOL/CM2/S	700 KM MOL/CM2/S	% OF LMOP
MODULE	9.43E-11	3.16E+12	1.65E+13	5.04E+11	1.15E+10	47.9
PALLET	9.59E-11	3.21E+12	1.68E+13	5.12E+11	1.17E+10	48.7
WINDOW	6.61E-12	2.21E+11	1.16E+12	3.53E+10	8.09E+08	3.4
+ LMOP + TOTAL +	1.97E-10	6.59E+12	3.44E+13	1.05E+12	2.41E+10	100.0

+++ MINIMUM TEMPERATURE PROFILE +++

MODULE	2.61E-13	9.42E+09	4.92E+10	1.50E+09	3.44E+07	70.5
PALLET	1.05E-13	3.52E+09	1.84E+10	5.61E+08	1.28E+07	26.3
WINDOW	1.26E-14	4.20E+08	2.19E+09	6.70E+07	1.54E+06	3.1
+ LMOP + TOTAL +	3.99E-13	1.34E+10	6.97E+10	2.13E+09	4.88E+07	100.0

Table XVI. Spacelab SMTP Early Desorption Induced Environment Predictions

MARTIN MARIETTA AEROSPACE

SPACELAB CONTAMINATION MODEL

SOURCE = EARLY DESORPTION
(AT 10 HOURS INTO MISSION RATE = 1.5E-7 G/CM2/S AT 100 C)
CONFIGURATION = SHORT MODULE/THREE PALLETS
LINE-OF-SIGHT = 1,(0 DEGREES OFF +Z TOWARDS THE X-Y PLANE AT 0 DEGREES)

+++ MAXIMUM TEMPERATURE PROFILE +++

SECTION	TOTAL MCD G/CM2	TOTAL NCD MOL/CM2	RETURN FLUX FOR 0.1 SR SURFACE 200 KM MOL/CM2/S	400 KM MOL/CM2/S	700 KM MOL/CM2/S	% OF SMTP
MODULE	4.18E-11	1.40E+12	7.31E+12	2.23E+11	5.12E+09	14.9
PLT1	5.47E-11	1.83E+12	9.57E+12	2.92E+11	6.70E+09	19.5
PLT2	8.98E-11	3.01E+12	1.57E+13	4.79E+11	1.10E+10	32.0
PLT3	9.34E-11	3.13E+12	1.63E+13	4.99E+11	1.14E+10	33.2
WINDOW	1.21E-12	4.06E+10	2.12E+11	6.47E+09	1.48E+08	.4
+ SMTP + TOTAL +	2.81E-10	9.41E+12	4.91E+13	1.50E+12	3.44E+10	100.0

+++ MINIMUM TEMPERATURE PROFILE +++

MODULE	1.11E-13	3.70E+09	1.93E+10	5.91E+08	1.35E+07	29.4
PLT1	5.80E-14	1.94E+09	1.01E+10	3.10E+08	7.10E+06	15.4
PLT2	1.01E-13	3.37E+09	1.76E+10	5.37E+08	1.23E+07	26.7
PLT3	1.05E-13	3.51E+09	1.83E+10	5.60E+08	1.28E+07	27.9
WINDOW	2.33E-15	7.80E+07	4.07E+08	1.24E+07	2.85E+05	.6
+ SMTP + TOTAL +	3.76E-13	1.26E+10	6.58E+10	2.01E+09	4.61E+07	100.0

Table XVII. Spacelab FIVP Early Desorption Induced Environment Predictions

MARTIN MARIETTA AEROSPACE

SPACELAB CONTAMINATION MODEL

SOURCE = EARLY DESORPTION
(AT 10 HOURS INTO MISSION RATE = 1.5E-7 G/CM2/S AT 100 C)
CONFIGURATION = FIVE PALLETS
LINE-OF-SIGHT = 1,(0 DEGREES OFF +Z TOWARDS THE X-Y PLANE AT 0 DEGREES)

+++ MAXIMUM TEMPERATURE PROFILE +++

SECTION	TOTAL MCD G/CM2	TOTAL NCD MOL/CM2	RETURN FLUX FOR 0.1 SR SURFACE 200 KM MOL/CM2/S	400 KM MOL/CM2/S	700 KM MOL/CM2/S	% OF FIVP
PLT1	2.39E-11	8.01E+11	4.18E+12	1.28E+11	2.93E+09	10.8
PLT2	2.83E-11	9.47E+11	4.94E+12	1.51E+11	3.46E+09	12.8
PLT3	3.72E-11	1.25E+12	6.50E+12	1.99E+11	4.55E+09	16.8
PLT4	6.41E-11	2.15E+12	1.12E+13	3.42E+11	7.84E+09	29.0
PLT5	6.77E-11	2.27E+12	1.18E+13	3.62E+11	8.29E+09	30.6
+ FIVP +						
+ TOTAL +	2.21E-10	7.41E+12	3.87E+13	1.18E+12	2.71E+10	100.0

+++ MINIMUM TEMPERATURE PROFILE +++

PLT1	2.50E-14	8.37E+08	4.37E+09	1.33E+08	3.06E+06	7.2
PLT2	3.44E-14	1.15E+09	6.01E+09	1.84E+08	4.21E+06	9.9
PLT3	5.35E-14	1.79E+09	9.36E+09	2.86E+08	6.55E+06	15.5
PLT4	1.06E-13	3.56E+09	1.86E+10	5.67E+08	1.30E+07	30.7
PLT5	1.27E-13	4.25E+09	2.22E+10	6.78E+08	1.55E+07	36.7
+ FIVP +						
+ TOTAL +	3.46E-13	1.16E+10	6.05E+10	1.85E+09	4.23E+07	100.0

evaluated in subsection 2.1.2. Here, as with outgassing, the need for accurate materials mapping and test data forthcoming from ESA is necessary to increase the resolution of the model predictions.

The predicted early desorption NCD levels in Tables XV through XVII vary between 9.41 x 10^{12} molecules/cm^2 for the SMTP maximum temperature profile to 1.16 x 10^{10} molecules/cm^2 for the FIVP minimum temperature profile. Within the 120 degree modeled viewing volume, the worst case lines-of-sight for the three Spacelab configurations are identical to those determined for outgassing. These are: 1) LMOP line-of-sight 13 where NCD = 1.4 x 10^{13} molecules/cm^2; 2) SMTP line-of-sight 11 where NCD = 1.27 x 10^{13} molecules/cm^2; and 3) FIVP line-of-sight 11 where NCD = 1.04 x 10^{13} molecules/cm^2. Unlike outgassing, these levels should decrease rapidly as the early desorption rate decays with time of vacuum exposure. The primary contamination threats from early desorption will, therefore, be limited to the early on orbit phases of a given Spacelab mission when pressure induced high voltage system corona arc-over damage and optical payload data degradation such as field-of-view interference perturbation or skewing of the ambient atmosphere composition and deposition upon cryogenic surfaces will be of concern.

Note that the early desorption return flux levels presented in Tables XV through XVII have been extended down to an altitude of 200 km. Due to the smaller scattering cross sections of early desorption molecules, their mean free paths are sufficiently large enough at 200 km to allow ambient backscattering or return flux to a surface at the PMP. Since the Spacelab carrier may orbit in the region of this lower altitude, it is necessary to include it in the predictions to encompass the actual parametric extremes that will be experienced.

Figures 17 through 19 present the computer generated early desorption density plots for the LMOP, SMTP and FIVP maximum temperature profiles, respectively, along line-of-sight 1. Early desorption density levels at the PMP fall in the mid 10^{-13} g/cm^3 range for all three Spacelab configurations. This density is equivalent to the density of the medium ambient atmosphere density at approximately 180 km altitude and implies a pressure in the 10^{-6} Torr range. Although points below the PMP within the payload bay volume have not been modeled ($Z_o < 507$), the shape of curves suggests even higher pressures at locations nearer the pallet hardware where high voltage corona susceptible power systems may be mounted. This could dictate the need to avoid early

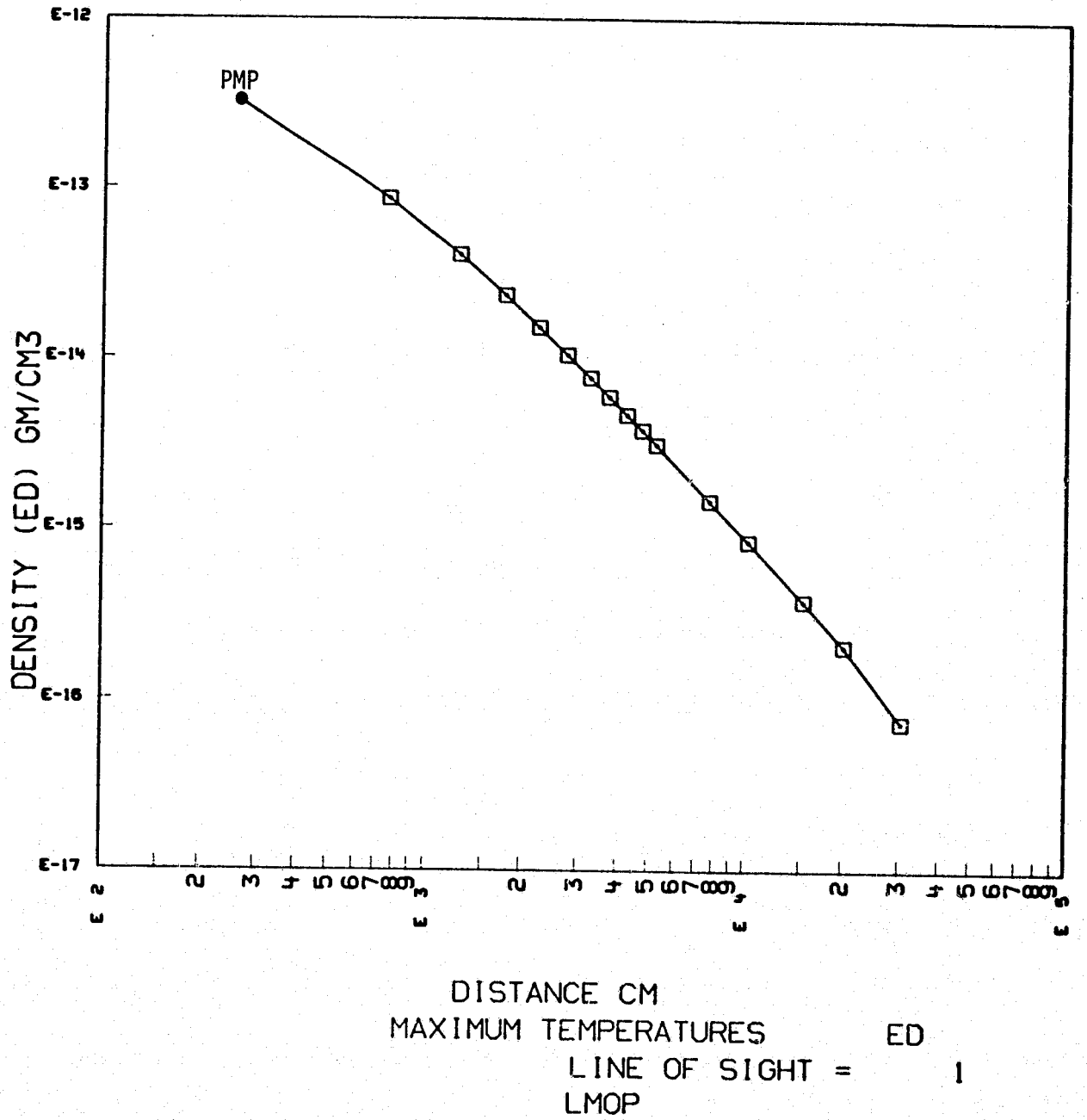

Figure 17. Early Desorption Density Variation Along Line-of-Sight 1 for LMOP at Maximum Temperatures

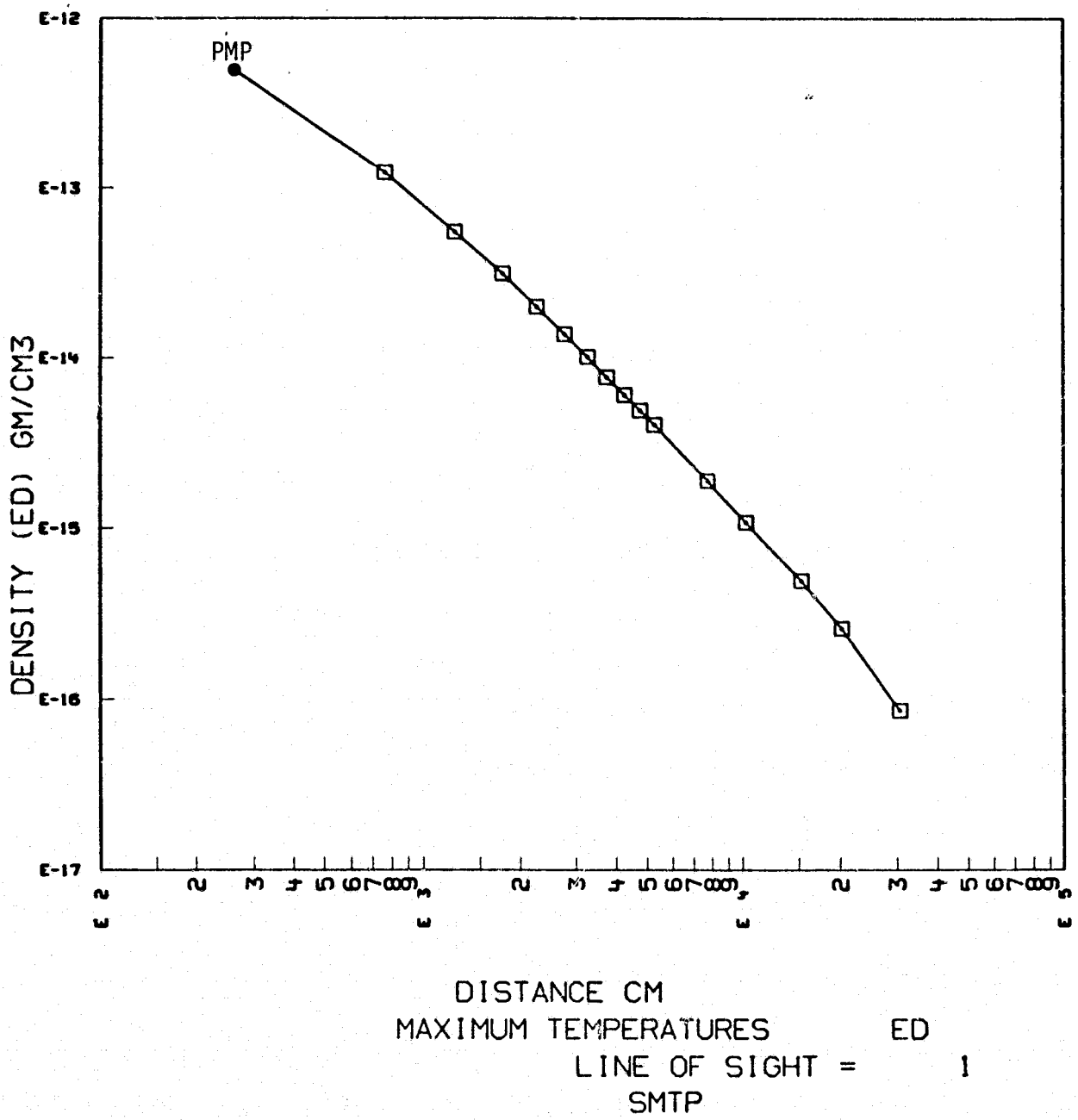

Figure 18. Early Desorption Density Variation Along Line-of-Sight 1 for SMTP at Maximum Temperatures

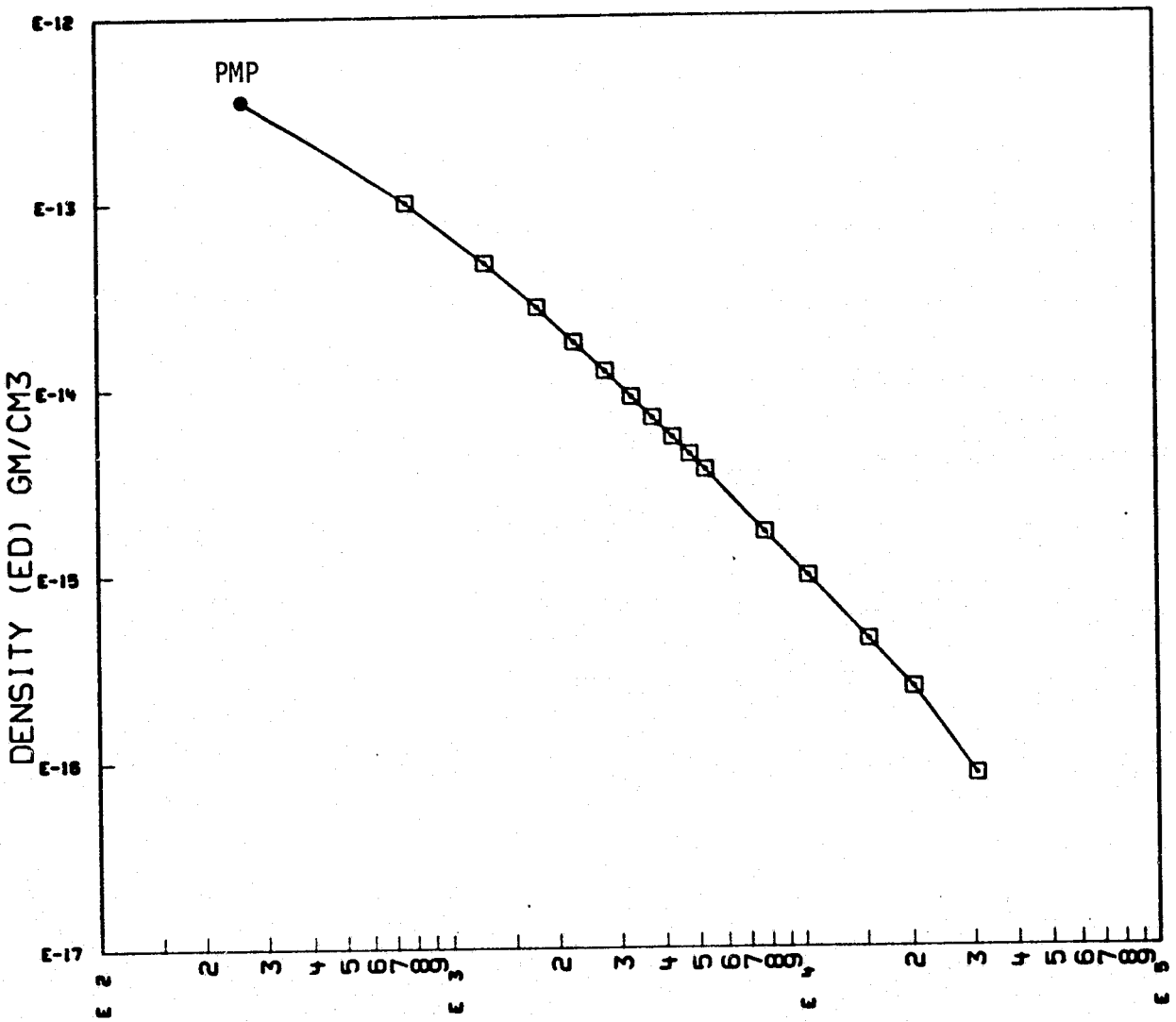

Figure 19. Early Desorption Density Variation Along Line-of-Sight 1 for FIVP at Maximum Temperatures

activation of these systems until early desorption has decayed to an acceptable level. Twenty-four hours is currently estimated as a safe delay time for most corona susceptible systems.

2.4.3 Cabin Atmosphere Leakage Induced Environment Predictions - The model output summaries of the cabin atmosphere leakage induced environment predictions for LMOP and SMTP line-of-sight 1 are presented in Tables XVIII and XIX, respectively. Since the FIVP configuration contains no pressurized module components, cabin leakage is not a FIVP contaminant source concern and no predictions are necessary. The modeled cabin atmsophere leak rate for both the LMOP and SMTP was 1.35 kg/24 hours as based upon the maximum allowable design specification leakage rates published in the "Spacelab Payload Accommodations Handbook".[8] The header sections of Tables XVIII and XIX indicate the conversion factors necessary to determine individual leakage constituent NCDs along a given line-of-sight. For example, Table XVIII indicates that the total NCD for LMOP leakage is 2.59×10^{12} molecules/cm^2 for line-of-sight 1. To determine the NCD for H_2O molecules, simply take this total NCD times 0.016 (from the header) which results in an NCD for H_2O of 4.14×10^{10} molecules/cm^2. Such information is useful for detailed contamination effects analysis and the contamination control criteria evaluation conducted in the next subsection.

The predicted leakage NCD levels will fall near the 10^{12} total molecules/cm^2 range within the 120 degree modeled viewing volume, varying from a maximum of 4.46×10^{12} molecules for the LMOP line-of-sight 11 to a minimum of 9.88×10^{11} molecules for the SMTP line-of-sight 3. The major contamination concern for leakage is the fact that it is a continuous uncontrollable source which: 1) can perturb the ambient environment composition interferring with scientific instrument measurements of the ambient atmosphere; and 2) which results in relatively high return flux levels that can condense upon exposed cryogenic surfaces. The return flux can be minimized through the methods previously recommended to minimize the impact of outgassing return flux. On the other hand, the problem of ambient atmosphere perturbation will require analysis by individual scientific instrument Principal Investigators (PI) to determine their sensitivities to the leakage induced environment predictions and to establish methods to subtract if necessary the leakage impact from acquired flight data.

Figures 20 and 21 present graphical illustrations of the predicted variation of leakage density along line-of-sight 1 for the LMOP and SMTP configurations respectively. Leakage

Table XVIII. Spacelab LMOP Leakage Induced Environment Predictions

MARTIN MARIETTA AEROSPACE

SPACELAB CONTAMINATION MODEL

SOURCE = LEAKAGE
(STEADY STATE RATE = 1.35 KG/24 HRS)
LEAKAGE
CONSTITUENTS = O2(.218 X NCD), N2(.759 X NCD),
H2O(.016 X NCD),CO2(.007 X NCD)
CONFIGURATION = LONG MODULE/ONE PALLET
LINE-OF-SIGHT = 1,(0 DEGREES OFF +Z TOWARDS THE X-Y PLANE AT 0 DEGREES)

SECTION	TOTAL MCD G/CM2	TOTAL NCD MOL/CM2	RETURN FLUX FOR 0.1 SR SURFACE 200 KM MOL/CM2/S	400 KM MOL/CM2/S	700 KM MOL/CM2/S	% OF LMOP
MODULE	1.10E-10	2.28E+12	1.19E+13	3.63E+11	8.31E+09	93.3
PALLET	0.	0.	0.	0.	0.	0.
WINDOW	7.91E-12	1.64E+11	8.55E+11	2.61E+10	5.98E+08	6.7
+ LMOP + TOTAL +	1.18E-10	2.44E+12	1.27E+13	3.89E+11	8.91E+09	100.0

Table XIX. Spacelab SMTP Leakage Induced Environment Predictions

MARTIN MARIETTA AEROSPACE

SPACELAB CONTAMINATION MODEL

SOURCE = LEAKAGE
(STEADY STATE RATE = 1.35 KG/24 HRS)

LEAKAGE
CONSTITUENTS = O2(.218 X NCD), N2(.759 X NCD),
H2O(.016 X NCD), CO2(.007 X NCD),

CONFIGURATION = SHORT MODULE/THREE PALLETS

LINE-OF-SIGHT = 1,(0 DEGREES OFF +Z TOWARDS THE X-Y PLANE AT 0 DEGREES)

SECTION	TOTAL MCD G/CM2	TOTAL NCD MOL/CM2	RETURN FLUX FOR 0.1 SR SURFACE 200 KM MOL/CM2/S	400 KM MOL/CM2/S	700 KM MOL/CM2/S	% OF SMTP
MODULE	6.08E-11	1.26E+12	6.57E+12	2.01E+11	4.60E+09	96.3
PLT1	0.	0.	0.	0.	0.	0.
PLT2	0.	0.	0.	0.	0.	0.
PLT3	0.	0.	0.	0.	0.	0.
WINDOW	2.33E-12	4.81E+10	2.51E+11	7.67E+09	1.76E+08	3.7
+ SMTP + TOTAL +	6.31E-11	1.31E+12	6.82E+11	2.08E+11	4.77E+09	100.0

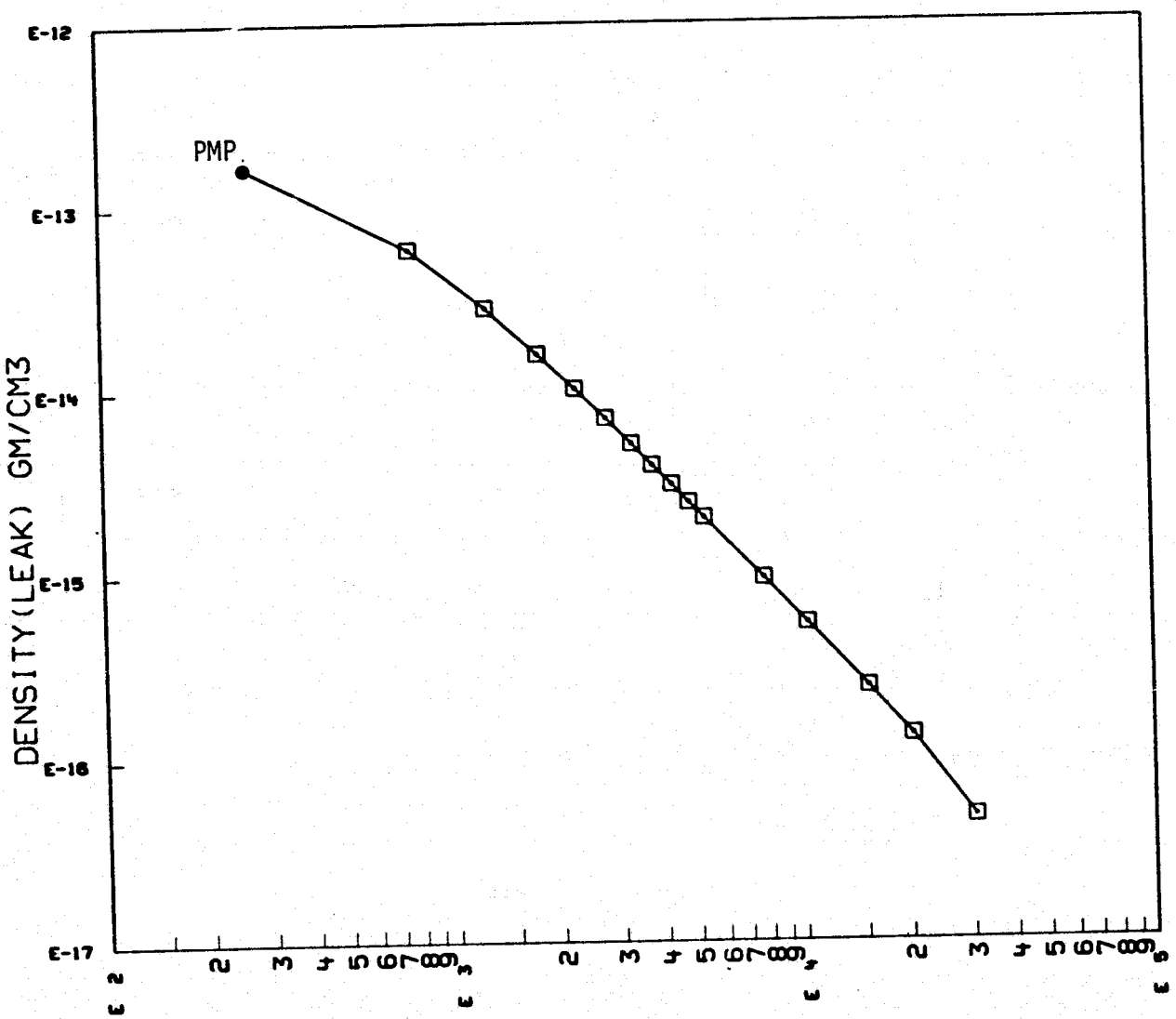

Figure 20. Leakage Density Variation Along Line-of-Sight 1 for LMOP

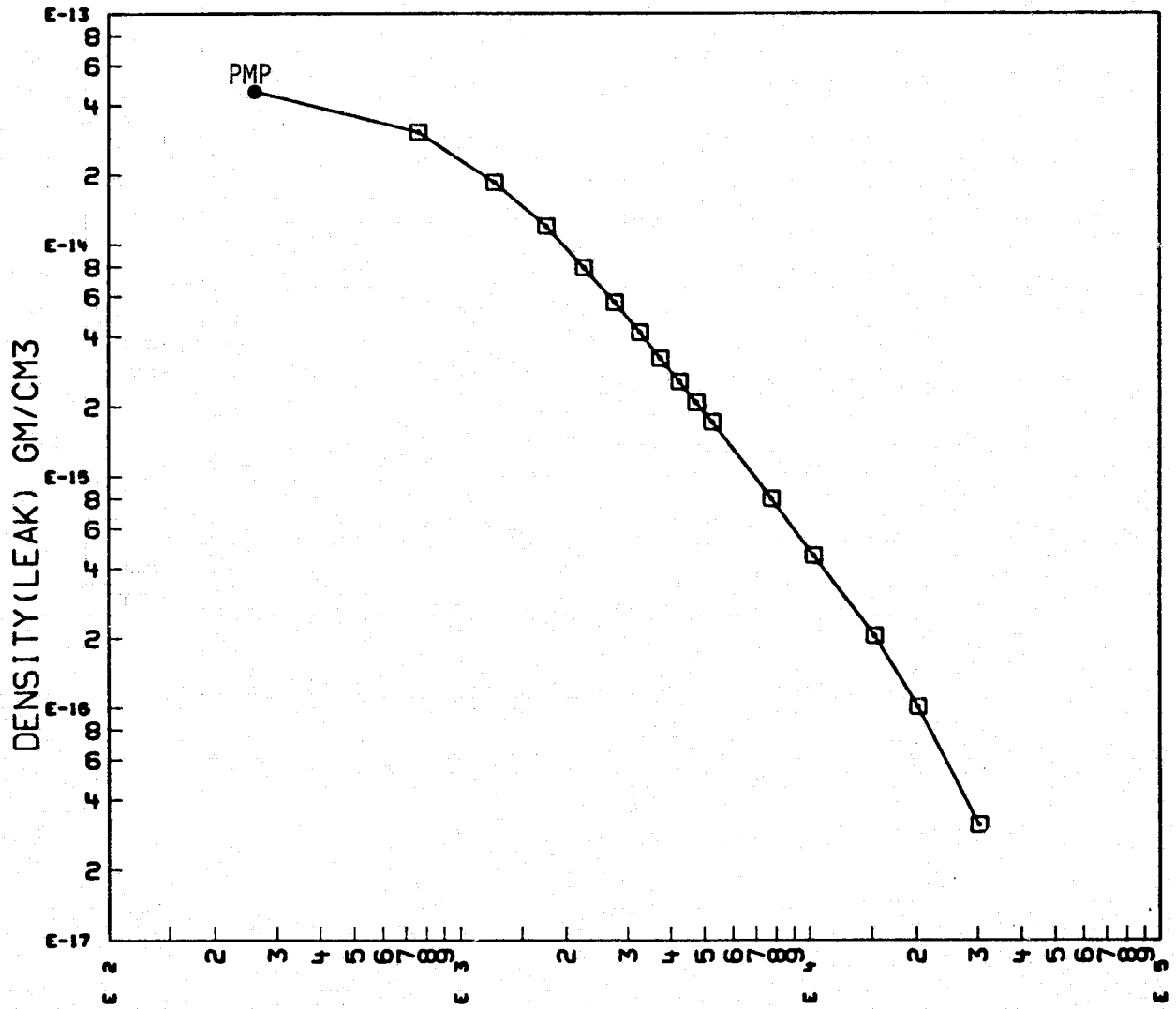

Figure 21 Leakage Density Variation Along Line-of-Sight 1 for SMTP

density levels at the PMP fall between 2 x 10^{-13} g/cm^3 for the LMOP and 4 x 10^{-14} g/cm^3 for the SMTP configuration which is equivalent to the ambient atmosphere density between approximately 220 km and 280 km where the implied pressure is in the mid 10^{-7} Torr range.

Gaseous nitrogen leakage from the Spacelab Igloo system is an an additional identified leakage contaminant source not currently included in the presented predictions pending the receipt of required flowrate and source location data from ESA. In general, the impact from this source to the overall predictions is expected to be small, however, due to its proximity to many pallet mounted payloads, detailed evaluation of its localized impacts is necessary.

2.4.4 Induced Environment Prediction Summary - It is apparent that the accuracy and fidelity of the Spacelab induced environment model predictions are strongly dependent upon the level of detail and accuracy of the input data to the computer model and the required assumptions employed when all such necessary data is not available. In conducting the preceding modeling activities, several areas were identified where additional design and/or test data is necessary to minimize the need for engineering assumptions in the modeling methodology. These included:

a. Spacelab external nonmetallic materials outgassing and early desorption test data as identified in Reference 6, pages 6-7;

b. Spacelab external nonmetallic materials mapping of all surfaces having an exposed surface area greater than 0.1 m^2 including location, area of coverage and material identification;

c. Spacelab Igloo leak rates and leakage point locations;

d. current design, location, vent direction, flowrates, exit orifice design and operational timelines of the SCV as well as any system test data that might be available; and

e. the maximum allowable degradation of Spacelab thermal control surfaces.

All of this data has been previously requested from ESA and when received, can be quite easily integrated into the Spacelab Contamination Computer Model for assessment.

As stated, several assumptions such as the nonmetallic materials outgassing rates (see subsection 2.2.1) were required to establish the enclosed induced environment predictions, but this fact should in no way detract from the final conclusions derived from this study. The predictions demonstrate that a sound modeling methodology has been established which is workable for Spacelab design and development analysis. Taking the next step of utilizing the methods developed to determine Spacelab design requirements actually bypasses the lack of some of the mentioned desired input data by taking the allowed contaminant levels and essentially running the model in reverse to fix the design levels of the Spacelab systems and hardware to meet the allowable contaminant levels. This is the approach used in subsection 2.5.

This is not meant to suggest that the data requested from ESA is not necessary. The design and development activities conducted up to this point have been completed quite effectively without some of the desired data. However, when conducting detailed Spacelab mission contamination analysis for specific payload configurations and mixes which might have contamination requirements more restrictive than the existing criteria[1,2], all of the requested data is necessary for an accurate assessment.

It should also be mentioned that for any given mission, the Spacelab predictions contained herein will be additive to those of the Shuttle Orbiter sources which in some instances are orders of magnitude more severe than those of Spacelab.

Indications are that the Spacelab design will be close to meeting the intent of the established contamination control criteria if the design and operational recommendations discussed in subsections 2.5 and 2.6 are instituted, but there is no evidence that the same is true for the Orbiter. This leads to the conclusion that the combined STS-SL configurations should be evaluated in detail utilizing model input data as depicted above for both vehicles to establish criteria compliance and induced environment predictions for actual mission conditions.

2.5 Contamination Control Criteria Evaluation - The induced environment predictions presented in the previous subsection in conjunction with supplemental analysis can now be utilized to determine the ability of the various Spacelab configurations to meet the existing contamination control criteria imposed upon Spacelab[2] and to establish Spacelab design and development requirements to insure that the criteria is satisfied. To accomplish this, each major Spacelab contaminant source was evaluated against the five criteria statements based upon the interpretations

and assumption sanctioned by the CRDG in Reference 3. In the ensuing paragraphs, each main criteria statement is presented as depicted in Reference 2. Each is then followed in parenthesis by the applicable CRDG interpreatations and finally a detailed analysis of the Spacelab contaminant sources.

2.5.1 Induced Particulate Environment - "It is a design and operational goal for Spacelab to control in an instrument field-of-view particles of 5 microns in size to one event per orbit." (This assumes a field-of-view of 1.5×10^{-5} steradian and is restricted to particles within 5 km of the spacecraft.)

A general review of the entire problem of particle contamination was conducted during this study but is not included herein. This subsection dwells primarily upon the phenomena of random particle emission, available flight data and its applicability to the assessment of the Spacelab vehicle and its ability to comply with the existing criteria.

In determining the induced particulate environment of a manned spacecraft such as the Spacelab carrier, known defined particulate sources like the Spacelab condensate vent (SCV) can be parametrically analyzed in a closed mathematical form by knowing the primary vent system characteristics (based upon existing system test data or detailed stream tube vent plume and freezing analysis) and integrating these into an appropriate particle trajectory analysis program. This was conducted for the SCV under a previous contract[5] and is briefly summarized in subsection 2.1.2. The acquired results indicate that this criteria statement can be exceeded during and for up to a minimum time increment as much as 17 minutes after SCV operation. Under this condition, the intent of the criteria can be met through timelining of the SCV overboard dump around operations of payloads that have been determined susceptible to particles in their fields-of-view. Current planning is for the SCV to be operated only once per each seven days on orbit, therefore, noninterference timelining should create minimal problems.

In constrast to well defined controllable particulate sources such as the SCV, intermittent particulate sources (i.e.; random particle emission) present a more difficult analytical problem. Actual flight observations of past orbiting systems are currently used in most instances as the primary data base for random particle evaluation. The applicability of such flight data to a different space vehicle such as Spacelab is questionable. Previous analysis of this phenomena has been based

primarily upon particle tracks observed on the Skylab ATM S052 White Light Coronagraph film frames which were analyzed by J. McGuire, MSFC.[32] His data presented the number of detectable random events (particles) per time period (approximately 4.8 particles/sr/s) as well as information about their velocity and size ranges for the field-of-view and sensitivity of the S052 instrument. This excluded such known particulate producing events as overboard liquid vents. Early information from McGuire indicated the sizes to be greater than 10 to 25 microns in diameter which is near the size level of 5 microns quoted in existing contamination control criteria.[1,2] Later analysis by F. Witteborn, Ames Research Center[33] for the Sensitive Infrared Telescope Facility (SIRTF) indicated that only much larger particles could be detected by the S052. The fact that such variations existed in the data interpretation prompted a further investigation into the sensitivity of the S052 instrument and its detectivity of particulate matter within its field-of-view.

Data supplied by R. M. MacQueen[34], PI for S052, stated that the Coronagraph had an 8 arc second resolution (3.88×10^{-5} radians) and that the faintest particle track on the S052 film had a brightness, $B = 7 \times 10^{-10} B_{\odot}$ ergs/cm^2/s/sr where $B_{\odot}$ = radiance of mean solar disc. The power radiated into the 3.2 cm aperture of the S052 camera from a particle of this angular size and brightness is found by:

$$P = B \cdot \Omega \cdot A$$

where,

P = power radiated from source, erg/s

B = brightness of source = $7 \times 10^{-10} B_{\odot}$ erg/cm^2/s/sr

$B_{\odot}$ = radiance of mean solar disk = $1,989 \times 10^{10}$ erg/cm^2/s/sr

$\Omega = \pi \sin^2 \frac{(2.2 \times 10^{-3})}{(2)} = 1.2 \times 10^{-9}$ sr

A = area of aperture = 8 cm^2

therefore,

$$P = (13.9)(1.2 \times 10^{-9})\ (8) = 1.33 \times 10^{-7} \text{ erg/s.}$$

The best contrasted data frames were exposed for 9 seconds. Therefore, the minimum amount of energy required to expose the film was 1.2×10^{-6} ergs which is the smallest amount of energy

detectable on a 3.88×10^{-5} radian square piece of film. The intensity of light scattered from a particle in the S052 field-of-view would be[35]:

$$I = I_o \left(\frac{(-a^2)^2}{\lambda^2 r^2} \right) \left(\frac{2 J_1 \quad (\sin \theta)}{\sin \theta} \right)^2$$

where,

a = particle radius, cm

r = distance from particle, cm

λ = wavelength of incident radiation, cm

I_o = incident intensity, $erg/cm^2/s$

θ = scattering angle

J_1 = Bessel function of order 1

Consider the case where $\lambda = 5 \times 10^{-5}$ cm, $r = 6 \times 10^4$ cm (distance where particle image size equals S052 resolution element), $4R_\odot \leq \theta \leq 6R_\odot$, and $I = 1.36 \times 10^6$ erg/cm/s ($R_\odot$ = one solar radii); the power at $5R_\odot$ (1.25° from the center of the S052 photographs) is approximated by $1/4 \left[I_{max} (1.0^o) + I_{max} (1.5^o) \right] \cdot A$, where I_{max} (1.0°) and I_{max} (1.5°) are the nearest maximum of I, and A is the area of the camera lens. The energy deposited per unit length of particle track is dependent on the velocity parallel to the plane of the film. McGuire found that the most probable velocity for focused particles was 4.6×10^{-4} radians/s so that a particle track resolution element (3.88×10^{-5} radians) was exposed for 0.084 seconds.

Using the above parameters for 400 and 510 micron diameter particles yields:

Diameter Microns	Average Power ergs/s	Energy Deposited in 0.084 seconds, ergs
400	1.2×10^{-5}	1×10^{-6}
510	2.3×10^{-5}	1.9×10^{-6}

From this calculation, it is seen that to deposit the minimum energy (1.2×10^{-6} ergs) to leave a particle track on the film, the particle must have been approximately 450 microns in diameter at 600 meters away. This is, therefore, the minimum detectable particle size for the S052 instrument.

It is difficult to compare the S052 particle observation data for detected particles greater than 450 microns to the current contamination control criteria[1,2] since this criteria is for 5 micron diameter particles which is 90 times smaller than what the S052 coronagraph could detect. A possible comparison can be made by assuming a log-normal particle size distribution (representative of a given clean room environment which could be a source of such particles) as identified in MIL-STD 1246A which would give a factor of 1×10^6 more particles greater than 5 microns in diameter for every particle 450 microns in diameter. This would equate to approximately 3.9×10^5 particles greater than 5 microns per orbit in a 1.5×10^{-5} steradian field-of-view at 600 meters based on McGuire's data which far surpasses the criteria. Using such a method has some logical basis, but is questionable at best. Qualitative assessments utilizing the S052 data can still be made, but when quoting or referencing the data, all assumptions and limitations should be clearly stated to insure proper interpretation of the results. One important implication that might be drawn from the S052 analysis is that the current contamination control criteria for particles may be very difficult for the Spacelab carrier as well as the Shuttle Orbiter to meet.

The particle sighting study conducted by Hughes Aircraft on the Infrared Sensor Celestial Mapping Program[36] orbited by the United States Air Force (USAF) Space Test Program 71-2 Agena vehicle attempted to correlate (with limited quick-look IR sensor flight data) the particles detected on orbit with the prelaunch ground handling procedures utilized. These varied from class 10K clean room and level 200-300 surface cleanliness for the sensor system to lesser control for the Agena. Although the report states that the quick-look data indicated minimal particle sightings for the spacecraft, the quantity of presented data does not appear adequate to draw any final conclusions. Three to five particles were detected in 6220 seconds of observation or 2.9 to 4.8 particles/orbit for the sensor's 1.2 degree field-of-view. This equates to 0.127 to 0.208 particles in a 1.5×10^{-5} steradian field-of-view per orbit for a vehicle that has approximately 1/30 the surface area of the Shuttle Orbiter. Since the sensitivity of the sensor is classified, additional correlation with contamination control criteria cannot be firmly established. It is therefore, felt that this data is far too inconclusive as presented to use as a data base for random particulate emission assessment of Spacelab.

2.5.2 Molecular Column Density - "It is a design and operational goal for Spacelab to control induced water vapor column

density to 10^{12} molecules/cm^2 or less." (This is measured along any vector within 60 degrees of the +Z axis originating at the Prime Measurement Point (PMP) (X_o = 1107, Y_o = 0, Z_o = 507). It is further assumed that this represents the worst case situation.)

Three of the four major Spacelab contaminant sources must be evaluated for compliance within this criteria statement. The modeled sources which are of concern include the SCV, early desorption of externally exposed Spacelab surfaces and the leakage of cabin atmosphere from the pressurized Spacelab module/tunnel segments. No control is required for outgassing materials as stated by this criteria since this source is considered to contain no water constituents (i.e.; the outgassing contaminant sources meets the NCD criteria statement).

The SCV exceeds the NCD criteria during its operation and must be timelined around the operation of those payloads deemed susceptible to water column densities greater than 10^{12} molecules/cm^2 in order that the intent of the criteria be met.

Since this overboard dump is currently planned to occur only once each seven days on orbit, interference with payload operations should be minimal if properly timelined and if structural impingement by the vent plume is avoided.

In the evaluation of the leakage contaminant source, the worst case line-of-sight prediction within 60 degrees of the +Z axis is for the LMOP line-of-sight 11 where the total NCD = 4.46 x 10^{12} molecules/cm^2 and the water vapor NCD = 7.14 x 10^{10} molecules/cm^2. This value is well within the criteria limits and, therefore, leakage is in compliance.

The final contaminant source, early desorption, demonstrates a maximum total NCD of 1.27 x 10^{13} molecules/cm^2 for the SMTP line-of-sight 11 at 10 hours into a mission assuming all externally exposed Spacelab surfaces are contributing to the early desorption induced environment. Approximately 57% of this material is emitted in the form of water vapor which equates to a 7.24 x 10^{12} molecules/cm^2 NCD for water thus exceeding the criteria limit. In order to meet the intent of the NCD criteria for early desorption, it will be necessary for the external Spacelab surfaces to demonstrate an early desorption rate (EDR) of less than 2.1 x 10^{-8} g/cm^2/s at 100°C. This can be accomplished through selection of external materials having an EDR less than this value, through decreasing the total area of coverage of high early desorbing

materials or by delaying data acquisition by susceptible instruments until the NCD levels for water vapor have decayed to less than 10^{12} molecules/cm^2. Based upon the developed decay curve currently in the model for early desorption, this delay time could be as high as 40 hours. This is highly dependent upon the thermal history of surfaces during that period and the specific Spacelab materials characteristics which are to be tested by ESA. Until such data is made available, it is assumed that an average delay time of 24 hours will bring the early desorption NCD levels into compliance with the criteria.

2.5.3 Molecular Return Flux - "It is a design and operational goal for Spacelab to control return flux to 10^{12} molecules/cm^2/s." (This refers to the total flux on an unshielded surface (2π steradian acceptance) oriented in the +Z direction at the PMP under worst case situation.)

Analysis of the phenomena of return flux to large field-of-view surfaces (2π steradian acceptance angle) at the PMP requires the use of the NCD predictions for all seventeen modeled lines-of-sight for a particular Spacelab configuration to account for the spatial variations of the NCDs in the hemispherical viewing volume above the Spacelab and their resulting contributions to the return flux at the PMP. The analytical approach utilized for this evaluation is described in detail in subsection 2.3.1.1. At this stage in the development of the Spacelab modeling, it is currently necessary to make the assumption that the various contaminant source NCDs do not vary appreciably between angles 60° and 90° off of the +Z axis since this viewing volume has not been modeled. For the worst case drag vector orientation evaluated here, this assumption for the far off axis locations has minimal impact upon the accuracy of the predictions.

The stated criteria applies to the summation of return flux from all contaminant sources with no specific stipulations on the separate constituent levels allowable. However, the ensuing evaluation accounts for the acceptable source levels to meet the criteria on an individual basis. It is realized that from a practical viewpoint that each source should be allowed only a budgeted percentage of the total. This same consideration should also be applied to the Orbiter sources (which are not accounted for herein) to budget between Spacelab and Orbiter source levels. However, for the basic Spacelab design and development analytical approach which has been previously acceptable, it is assumed that each source may have an allowable return flux level of 10^{12} molecules/cm^2/s or less. It should be noted that if the design and operational recommendations in the ensuing paragraphs are

followed, that the 10^{12} molecules/cm^2/s total return flux criteria will inherently be met,

The molecular return flux levels experienced during SCV operation significantly exceed the stated criteria limits. Sensitive surfaces should be protected from return flux possibly by utilizing operable covers, if practical, while SCV dumps are in progress. Return flux could also be minimized through vehicle attitude selection which is not conducive to return flux during SCV operation. Ideally, such an attitude would place the ambient drag vector continually in the Spacelab +Z direction, thus reducing return flux to the PMP to almost zero.

The worst case Spacelab configuration for both outgassing and early desorption return flux to a 2π steradian surface at the PMP is the SMTP during the maximum temperature profile attitude. The outgassing return flux prediction for the Spacelab SMTP under maximum ambient drag vector orientation is 1.84×10^{13} molecules/cm^2/s at 250 km altitude assuming 100% of its surface area is covered with a nonmetallic material that just meets the existing materials screening criteria[14,15] implied outgassing rate (OGR) of 6×10^{-9} g/cm^2/s at 100°C. The SMTP return flux prediction exceeds the return flux criteria by more than a factor of 18. To meet this criteria, materials selected for use on the external Spacelab surfaces must demonstrate an effective OGR of less than 3.3×10^{-10} g/cm^2/s at 100°C. This can be accomplished through selection of low outgassing materials or by limiting the area of coverage and/or locations of external coatings. In addition, the intent of the criteria can be met by selecting orbital altitudes above 435 km for missions that are susceptible to 10^{12} molecules/cm^2/s return flux, by selecting orbital attitudes during which the major outgassing surfaces are held at low temperatures and by avoiding worst case drag vector orientations with respect to sensitive surfaces. Operable covers for sensitive payloads should also be considered.

Utilizing a similar approach for early desorption, it was determined that the maximum SMTP return flux rate would be 1.1×10^{15} molecules/cm^2/s based upon the 200 km altitude predictions. To meet the return flux criteria for early desorption, the EDR would have to be less than 9.22×10^{-11} g/cm^2/s at 100°C assuming that all external Spacelab surfaces contribute. As in the case of early desorption compliance with the NCD criteria statement, the intent of the return flux criteria can be met for susceptible payloads if the exposure of their sensitive surfaces is delayed until such time that the early desorption return flux rate has decayed through vacuum exposure to an acceptable level.

Although this specific delay time will remain unknown until adequate materials test data is supplied by ESA, the estimated average delay time for early desorption to meet the criteria intent is currently assumed to be approximately 24 hours. If practical, susceptible surfaces should provide their own protective devices such as operable covers and the maximum ram vehicle attitudes should be avoided during the Spacelab early mass loss period. Selecting orbital altitudes above approximately 680 km would also reduce the return flux to an acceptable level.

Meeting the intent of the return flux criteria for cabin atmosphere leakage may be more difficult to achieve due to its continuous, uncontrollable characteristics. Predictions for the worst case Spacelab leakage configuration, LMOP, indicate a return flux to a 2π steradian surface at the PMP of 3.09×10^{14} molecules/cm^2/s at 200 km altitude which exceeds the criteria. Decreasing the allowable design leak rate of the Spacelab vehicles could be extremely costly to the program and such an approach is somewhat impractical in that only 4.37 g/day could be allowed to leak to insure criteria compliance. Realistically, leakage return flux should not impact any exposed surfaces other than possibly such cryogenic systems as the LHe Infrared Telescope which will have an acceptance angle much less than 2π steradian (closer to 0.1 steradian). However, as stated, the return flux criteria is exceeded. The levels for leakage return flux can be decreased by utilizing previously suggested methods of surface protection, attitude and orbital altitude selection (above 575 km).

2.5.4 Background Brightness - "It is a design and operational goal for Spacelab to control continuous emissions or scattering to not exceed 20th magnitude/s^2 in the UV range." (This is equivalent to 10^{-12} $B_\odot$ at a wavelength of 360 nanometers.)

Background brightness induced by the scattering or emission of radiant energy can result from the presence of either contaminant particles or molecules within the field-of-view of a sensitive optical instrument. For the major modeled Spacelab molecular contaminant sources, the primary phenomena of concern in this regard is the scattering of solar energy from the irradiated contaminant molecules. Since this criteria statement actually involves a contaminant effect rather than a specific contaminant level such as NCD, it is first necessary to express the criteria statement in terms that are compatible with the Spacelab Contamination Computer Model predictions to determine compliance with the criteria. This can be accomplished for molecular sources utilizing the expression having the general form.

$$H = \frac{H_o}{r^2} \left(\frac{\partial \sigma}{\partial \Omega}\right)$$

where,

$$\frac{\partial \sigma}{\partial \Omega} = \frac{8\pi^4 \rho^6}{\lambda^4} \left(\frac{n^2-1}{n^2+2}\right)^2 (1 + \cos^2 \theta) \text{ for one molecule.}$$

therefore,

$$H = \frac{H_o}{r^2} \frac{8\pi^4 \rho^6}{\lambda^4} \left(\frac{n^2-1}{n^2+2}\right)^2 (1 + \cos^2 \theta)$$

At some distance r along a line-of-sight, the number of contaminant molecules in an elemental volume is given by $N(r)\ r^2\ d\emptyset dr$ where $N(r)$ = number density and $d\emptyset$ = solid angle of the element. Then, the incremental irradiance can be expressed as

$$dH_{total} = N(r)\ r^2\ d\emptyset dr\ \frac{H_o}{r^2} \frac{8\pi^4 \rho^6}{\lambda^4} \left(\frac{n^2-1}{n^2+2}\right)^2 (1 + \cos^2 \theta)$$

$$H_{total} = \emptyset \cdot H_o \frac{8\pi^4 \rho^6}{\lambda^4} \left(\frac{n^2-1}{n^2+2}\right)^2 \int_{R_o}^{\infty} N(r)\ dr$$

$$= \emptyset \cdot H_o \frac{8\pi^4 \rho^6}{\lambda^4} \left(\frac{n^2-1}{n^2+2}\right)^2 (1 + \cos^2 \theta) \cdot NCD$$

where,

$\emptyset$ = solid angle of surface of interest, steradians

H_o = source irradiance, $w/cm^2/\mu$

ρ = molecular radius, cm

n = complex index of refraction

θ = scattering angle, degrees

NCD = contaminant number column density, $molecules/cm^2$

This expression in conjunction with the proper parametric input data establishes the maximum allowable NCD to just meet the background brightness criteria statement. For the Spacelab contaminant source of outgassing where ρ is assumed to be 3.75Å (3.75×10^{-8} cm), the resulting maximum allowable NCD for a 90 degree scattering angle would be 1.1×10^{16} molecules/cm^2. This is over 5×10^4 times higher than the maximum predicted outgassing NCD levels for the Spacelab configurations and equates to an allowable Spacelab outgassing rate of approximately 3.4×10^{-4} g/cm^2/s at 100°C. Even if the background brightness criteria were two orders of magnitude more restrictive as recommended by R. Naumann[3] for Spacelab astronomy payloads (i.e.; scattering or emission less than 10^{-14} $B_\odot$), the Spacelab vehicle as modeled would comply with the criteria from an outgassing viewpoint.

Utilizing a similar approach for the Spacelab contaminant sources of early desorption and cabin atmosphere leakage (both having a molecular radius of 1.65Å yields a maximum allowable NCD of 2.6×10^{18} molecules/cm^2. This value compared to the maximum predicted NCDs of 1.27×10^{13} molecules/cm^2 for early desorption and 4.46×10^{12} molecules/cm^2 for leakage indicates complete compliance of these sources with the background brightness criteria even if it were two orders of magnitude more restrictive as previously discussed.

Although approximately 15% of the vent effluents from the SCV will be emitted in the form of water molecules, the greater concern of this source with regard to the background brightness criteria will be the scattering and emission from the generated ice particles. Due to its potential production of many particles in the submicron region where the scattering level can be significant, exceeding this criteria during vent operations is highly probable. For this reason, the SCV overboard dumps should be timelined to avoid interference with sensitive Spacelab payload data acquisition.

2.5.5 Absorption Due to Condensible Deposition - "It is a design and operational goal for Spacelab to control to 1% the absorption of UV, visible and IR radiation by condensibles on optical surfaces." (This refers to the objective of an optical system that would typically have a dielectric surface at ambient temperature (approximately 300°K) that is located at the PMP, is oriented along the +Z axis and has an acceptance of 0.1 steradian. It is also assumed that this is for a 7 day mission with random orientation of the ambient drag vector.)

Evaluation of this criteria statement indicates that the only major modeled Spacelab contaminant source presenting a concern for absorption by condensibles under the above stated assumptions is the outgassing of Spacelab external nonmetallic materials. This is due to the fact that negligible amounts of the other evaluated source constituents will stick to a surface at 300°K for any measureable time period. To analyze the phenomena of outgassing deposition, a systematic approach was taken utilizing the stated assumptions in conjunction with the predictions contained in Tables III through V for line-of-sight 1. Since this criteria statement is also based upon the contaminant effect rather than a specific contaminant level as in subsection 2.5.4, a more comprehensive evaluation is necessary to determine the compliance of the model predictions with the criteria limits. The following listing establishes the step-by-step analytical assumptions and methodology utilized to evaluate this criteria for the contaminant source of outgassing:

a. All three modeled Spacelab configurations were assumed to be completely coated with a nonmetallic thermal control coating.

b. This nonmetallic thermal control coating was assumed to just meet the maximum allowable outgassing rate (OGR) implied by program materials screening criteria 50M02442[14] and SP-R-0022A[15]. This OGR equates to 6×10^{-9} g/cm^2/s for the material at 100°C.

c. Surface OGR was modeled as a function of temperature by the relationship $OGR_T = OGR_{100} \{\exp [(T-100)/29]\}$ where T = surface temperature in °C and OGR_{100} = outgassing rate at 100°C.

d. Individual Spacelab surface temperatures were modeled assuming a continuous maximum hot case orbital attitude (i.e. $\beta = 90°$, +Z solar inertial, and +Y local vertical) from MSFC supplied thermal data.[24]

e. Outgassing was modeled assuming a Lambertian mass distribution transport mechanism.

f. Return flux of outgassing molecules was modeled assuming a hard sphere collision between the outgassing molecules and the ambient atmosphere molecules. The velocity of the outgassing molecules (V_o) was determined as the "most probable" velocity based upon the explicit temperatures of each emitting surface and a molecular weight of 100, and the ambient velocity (V_A) was assumed to be equal to Spacelab's orbital velocity (7.65 km/s). The return flux mass distribution was assumed to be a random or Lambertian function from the plane of impact reaching a maximum when parallel to the ambient flux. The general expression for determining return flux is:

$$RF = \int_1^N \frac{flux_N}{V_o} \cdot VF_N \cdot \frac{\pi (\delta_o + \delta_A)^2 N_A V_A \, dx}{4}$$

where,

$flux_N$ = flux of outgassed molecules to node N along a line-of-sight, $g/cm^2/s$

VF_N = viewfactor or percent of mass reflected from node N (Lambertian) able to impinge upon a surface of interest

$\frac{\pi}{4} (\delta_o + \delta_A)^2$ = scattering cross section (8.3×10^{-14} cm^2)

N_A = medium ambient atmosphere density[29] calculated at 250, 400 and 700 km altitude, molecules/cm^3

g. The sensitive surface for which return flux was calculated was located at the Prime Measurement Point for each Spacelab parallel to the (X,Y) plane and had a geometric acceptance angle of 0.1 steradians.

h. The sensitive surface was assumed to be positioned such that the ambient drag vector was randomly oriented with respect to the surface (this equates to approximately 25% of the continuous maximum return flux).

i. The sensitive surface temperature was assumed to be 300°K and the sticking coefficient was based upon the expression $S = \Delta T/200$ where, S = sticking coefficient and ΔT = temperature difference between each source and the sensitive surface in °C.

j. Deposition thickness was assumed to equate to: 1×10^{-6} g/cm^2 = 100Å thickness based on unit density.

k. Spectral extinction coefficient data (α) used to establish absorption of incident radiation as a function of wavelength and deposition thickness was obtained from Gemini XII flight data[37] for "typical" spacecraft on orbit contamination. Absorption at a specific wavelength equals $1-e^{-\alpha x}$, where x = deposition thickness.

l. The sensitive surface was assumed to be a reflective optic detecting at 1500Å wavelength. (Using these parameters, one monolayer (3Å) equates to approximately 1% absorption.)

m. The final predictions were made assuming a 7 day mission and 100% surface exposure to the random return flux.

Based upon these assumptions, outgassing deposition levels were predicted for the three Spacelab configurations as a function of various orbital altitudes. Figure 22 presents the results of this parametric evaluation along with an indication of the required levels to meet the 1% absorption criteria limits. The maximum predicted deposition level in Figure 22 is 2.55×10^{-6} g/cm^2 for the S[illegible]P Spacelab configuration at 250 km altitude which equates to to 36% reflectance loss for the 0.1 steradian surface detecting at 1500Å wavelength. In order that the Spacelab design meet the absorption criteria, nonmetallic materials selected for use on the external Spacelab surfaces must demonstrate an effective outgassing rate of less than 5.6×10^{-11} $g/cm^2/s$ at 100°C which is by far the most restrictive outgassing limit established in the criteria evaluation. This might be attainable through rigorous materials selection or by limiting or eliminating the use of external nonmetallic materials. The intent of the criteria can be met by limiting sensitive payload missions to altitudes above approximately 580 km, but care must be taken with this approach due to the large variations in the density of the ambient atmosphere with time around the medium atmosphere density levels utilized in the modeling. Other possible methods which may be employed to decrease the impact of outgassing deposition include raising the sensitive surface temperature, providing sensitive surfaces with operable covers, selecting orbital attitudes conducive to low outgassing surface temperature profiles and avoiding impingement of the ambient drag vector upon the sensitive surface.

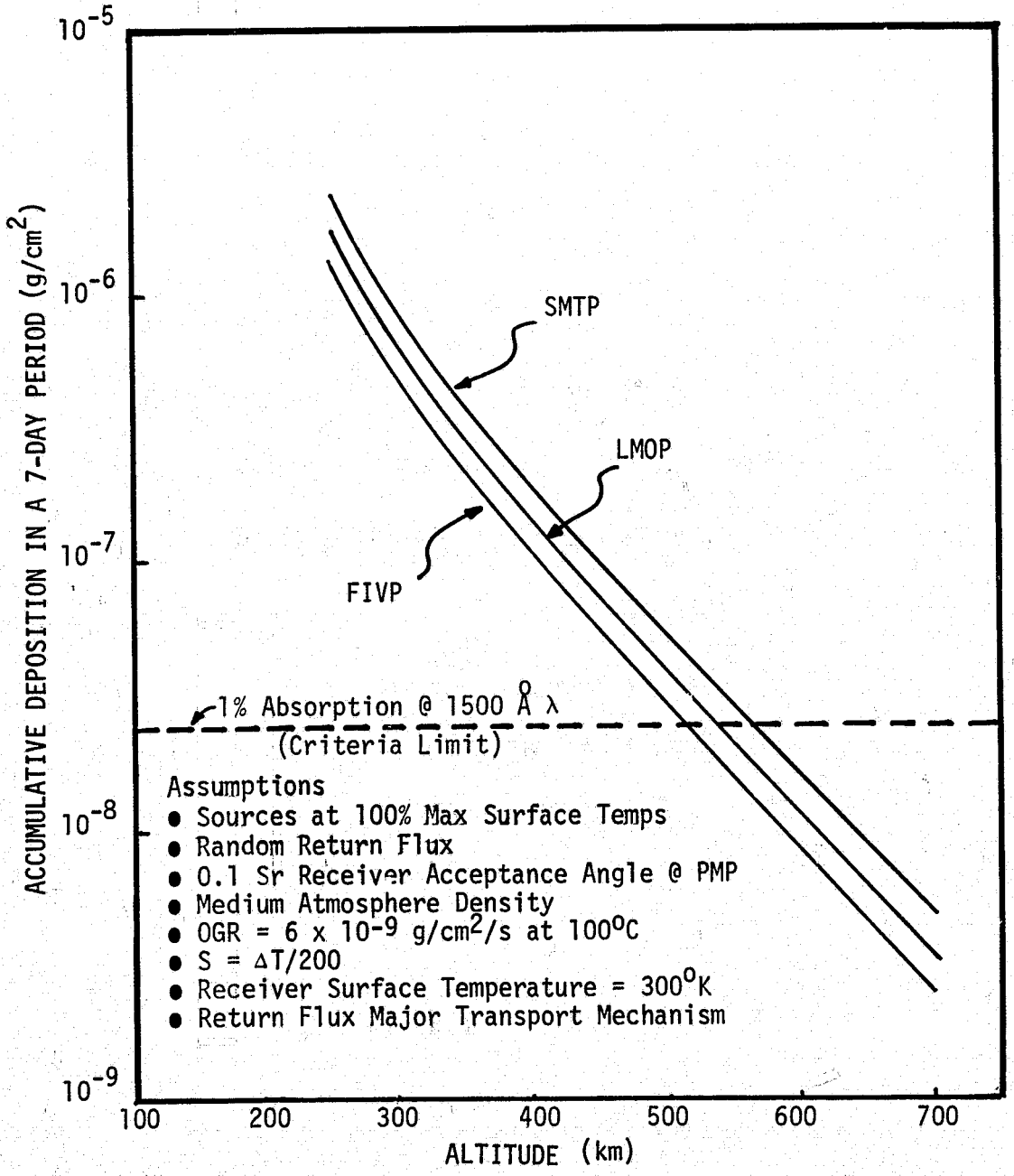

Figure 22. Spacelab Outgassing Deposition as a Function of Orbital Altitude for a 0.1 Steradian Receiver Surface at the PMP

2.6 Evaluation Summary - To facilitate the interpretation of the preceding criteria evaluation, with respect to Spacelab design/development control, the major results and conclusions are summarized in Table XX. From this table, certain program overview design and development directions can be made concerning the major modeled Spacelab contaminant sources and preliminary design/operational requirements. These include:

a. Selection of the Spacelab external nonmetallic materials which demonstrate an effective outgassing rate of less than 5.6×10^{-11} g/cm^2/s at 100°C will satisfy all of the stated contamination control criteria for the contaminant source of outgassing.

b. The most restrictive criteria statement for Spacelab early desorption is that for return flux. An early desorption rate of less than 9.2×10^{-11} g/cm^2/s at 100°C will result in compliance with the criteria. If materials control to this level proves impractical from a design viewpoint, activation and/or exposure of payloads sensitive to the early desorption induced environment should be delayed up to 24 hours until early desorption has decayed to an acceptable level.

c. Cabin atmosphere leakage cannot from a practical point of view be controlled to a satisfactory level of compliance with the return flux criteria through Spacelab design alone. For Spacelab missions on which instruments that are sensitive to this phenomena are to be flown, the impact of leakage can be minimized through proper selection of orbital altitude, attitude and sensitive surface protective devices such as operable covers. For a vast majority of proposed Spacelab payloads, the impact of the predicted levels of return flux of cabin atmosphere leakage will be negligible.

d. During its operation the SCV will exceed all of the criteria statements with the exception of the 1% absorption due to condensibles. This source cannot be controlled through design without major system modifications such as storing the condensate rather than expelling it overboard. The logical approach to complying with the intent of the criteria statements by the SCV would be to timeline venting to avoid interference with sensitive payload data acquisition and protect sensitive surfaces during vent operations.

Table XX. Spacelab Contamination Control Criteria Evaluation Summary

Requirement	Conclusions	Recommendations
• Particulate Background	• Condensate vent exceeds criteria during operation	• Timeline operation around operation of sensitive payloads
	• Random emission impacts unknown, but indications are that criteria will be exceeded	• Ground control equivalent to Skylab
• Molecular Column Density	• Condensate vent exceeds criteria during operation	• Timeline operation around operation of sensitive payloads
	• Early desorption exceeds criteria	• Delay operation of susceptible payloads until early desorption rate (EDR) = 2.1×10^{-8} g/cm^2/s at 100°C
	• Leakage is acceptable	• None
• Return Flux	• Outgassing exceeds criteria at 250 to 435 km altitude	• Control outgassing rate (OGR) to 3.3×10^{-10} g/cm^2/s at 100°C or fly sensitive instruments above 435 km or below 250 km altitude
	• Early desorption exceeds criteria at 200 to 680 km altitude	• Delay operation of susceptible payloads until EDR = 9.2×10^{-11} g/cm^2/s at 100°C or fly above 680 km altitude
	• Leakage exceeds criteria at 200 to 575 km altitude	• Control leakage to 4.37 g/day or fly susceptible payloads above 575 km alt.
	• Condensate vent exceeds criteria during operation	• Timeline operation around operation of sensitive payloads

Table XI. Spacelab Contamination Control Criteria Evaluation Summary (continued)

Requirement	Conclusions	Recommendations
• Background Brightness	• Outgassing, early desorption, and leakage present no problems	• None
	• Condensate vent exceeds criteria during operation	• Timeline operation around operation of sensitive payloads
• 1% Absorption by Condensibles	• Early desorption, leakage, and condensate vent present no problems	• None
	• Outgassing exceeds criteria at 250 to 580 km altitude	• Control OGR to 5.6×10^{-11} g/cm^2/s at 100°C or fly sensitive payloads at altitudes above 580 km or below 250 km

Note: Other contamination phenomena not explicitly covered by the Contamination Control Criteria include pressure induced corona arc-over damage to high voltage power supplies, perturbation or skewing of the composition of the ambient atmosphere, and deposition upon cryogenic surfaces.

One additional concern which should be addressed is whether or not a vehicle such as the Spacelab or Spacelab/Orbiter that complies with the five CRDG approved contamination control criteria statements will be acceptable to all potential scientific instruments from a contamination viewpoint. For example, if the 1% absorption due to condensibles on an optical surface statement is met based upon the assumptions and interpretations as set forth by the CRDG, will payload unique constraints or requirements (such as a one monolayer maximum allowable deposition level for a payload like the Open Envelope Traveling Wave Tube Experiment, CN-08) be met under actual flight conditions.

To further investigate this, consider the CN-08 payload being considered for the seventh Spacelab mission (SL-7). The SSPD[31] data sheets for this payload state that its amplitron and traveling wave tube components can tolerate no more than one monolayer of outgassing deposition. If it is assumed that the Orbiter and Spacelab designs both meet the 1% absorption due to condensibles criteria previously evaluated and assuming that the following mission/payload parameters are representative of the actual SL-7 mission, it is found that up to 1.6×10^{-6} g/cm^2 or approximately 54 monolayers will deposit on the CN-08 traveling wave tube and/or amplitron.

Assumed CN-08/SL-7 Mission Parameters

- CN-08 has 2π steradian acceptance angle.
- CN-08 is mounted on 30 meter boom along +Z axis.
- Ambient drag vector continually perpendicular to boom and CN-08 wake shield.
- CN-08 data take for 112 hours total exposure time.
- Mission at 325 km altitude.
- SMTP Spacelab configuration.
- CN-08 average temperature 243^{o}K.
- Orbit - 60 percent sunside; 40 percent dark.

It should be pointed out that a large percentage of the predicted impact is the result of Orbiter sources which must be included in any Spacelab mission analysis.

This preliminary evaluation demonstrates for a vehicle whose design meets the contamination control criteria statements that individual payload contamination requirements may still be exceeded. Similar situations arise for payloads attempting to study the physics and composition of the ambient atmosphere in the vicinity of the Spacelab/Orbiter due to the fact that the contaminant environment actually modifies the molecular specie composition of the ambient atmosphere. Therefore, individual payload/mission evaluation will still be necessary to determine specific impacts to scientific data and design/operational requirements to insure mission success.

To place the contamination control criteria evaluation in perspective, it is apparent from the analysis in the preceding subsections that many of the criteria are exceeded under the conditions evaluated. Spacelab design recommendations have been made, where feasible, to meet the criteria, but design alone does not necessarily satisfy all of the requirements. In certain cases; mission dependent recommendations such as orbital altitude, attitude, covers, etc. were necessary in order that Spacelab meet the intent of the criteria. It should be apparent that the logical approach to contamination control for Spacelab or in fact the entire STS-SL is not uniquely through design but instead through optimizing the design as much as is practical from a contamination viewpoint and then through the use of a total mission contamination simulation program to evaluate each individual Spacelab mission based upon its specific payload mix and mission profile. With this approach; required payload protection (covers, heaters, etc.) can be identified early in the program, mission operational requirements and constraints necessary to insure the success of the evaluated mission can be determined and the proper controls between Orbiter, Spacelab and payload contaminant sources can be established.

This approach is substantiated by the example deposition calculations for the CN-08 payload mission which indicated that even if the contamination control criteria were met by the STS-SL, contamination could still be a significant problem for particular susceptible payloads and certain mission profiles. The basic conclusion that can be drawn from the preceding evaluation is that the CRDG contamination control criteria sets a practical design goal and base from which to work which establishes a relatively clean Spacelab environment. The next logical step is a detailed mission analysis which provides the necessary operation control.

3. CONCLUSIONS AND RECOMMENDATIONS

3.1 Conclusions - The following conclusions are presented as a result of the activities and studies conducted during this contract period. These conclusions are in part a function of the fidelity of the available Spacelab design and test data and the status of development of the Spacelab Contamination Computer Model.

a. Even if the design and recommended operational procedures of the Spacelab vehicle meet the intent of the contamination control criteria, contamination limits for specific sensitive payloads can be exceeded under certain mission situations (see subsection 2.6 for a typical example of this for payload CN-08). For this reason, detailed mission contamination modeling evaluation and subsequent planning will be required.

b. The applicability of the existing random particulate emission data base to Spacelab evaluation is questionable, although implications are that the contamination criteria for particles may be difficult for Spacelab to meet. This may not be determined until data is received from Orbital Flight Tests and early Spacelab missions.

c. Nonmetallic material outgassing for the anticipated thermal control material on Spacelab and qualified under current materials screening criteria exceeds return flux and signal loss criteria in certain situations assuming 100% Spacelab coverage. In addition, early desorption from the same materials exceeds the column density and return flux criteria. Materials test data as specified in Reference 6 is required for more exact analysis.

d. Cabin atmosphere leakage satisfies all criteria statements with the exception of return flux. This contaminant source may present some problems for cryogenic systems exposed to the worst case ambient drag vector situation for extended periods of time and pointing requirements and attitude/altitude constraints may be necessary.

e. The Spacelab condensate vent exceeds every contamination control criteria statement with the exception of absorption due to condensibles during vent operations. Current plans are to operate this system only once for each 7 days on orbit, therefore, noninterference timelining with payload operations should be no problem provided that the vent plume does not impinge upon Orbiter/Spacelab structural surfaces so that vent cleaning times can be accurately determined.

f. Updated NASA Spacelab thermal profile data which is generally much more cold-biased than the previously used ESA data has decreased outgassing and early desorption predictions by up to a factor of 20 for some configurations. It is indicated that anticipated updates of pallet temperature profiles (with insulation, thermal shields, coatings, and heaters considered) will result in an increase in the contamination predictions (based on preliminary insulated configuration analysis). In addition, SMTP profile data which is currently based on LMOP profiles is required for more accurate SMTP predictions.

g. The modeling approach of using point receivers to calculate line-of-sight viewfactors appears to offer a substantial computer cost savings as well as increasing model resolution. This method will be used in all future analyses.

h. Updated OMS engine effluent deposition predictions would tend to negate the need to close the payload bay doors during posigrade maneuvers for Spacelab/payload protection, although the doors should be closed during retro thrust periods. Until OMS engine design and test parameters are more firmly established, consideration should be given to closing the doors during all OMS firings due to the enormous amount of material that is expelled by these engines when operated.

i. Under the conditions evaluated for Spacelab sources, backscatter of contaminant molecules to sensitive surfaces resulting from self scattering from other contaminant molecules is several orders of magnitude lower than ambient atmosphere induced backscatter levels.

j. For purposes of determining return flux, an effective molecular scattering cross section of 8.3×10^{-14} cm^2 is deemed representative of outgassed molecules in general and will be utilized in the computer modeling until applicable test data is obtained.

k. The elemental volume approach developed to determine return flux to large field-of-view surfaces appears to be a feasible and accurate technique when compared to techniques and results obtained by other investigators on this phenomena.

l. The contamination phenomena of second surface source characteristics and payload bay vicinity surface-to-surface deposition both appear to be significant under certain conditions. Refinements to the Spacelab Contamination Computer Model should reflect these results.

m. Molecular collisions within the cloud are considered important. The industry does not yet have the ultimate model for predicting the density of contaminants above the Spacelab/Orbiter. We have utilized a Spacelab design approach herein which tends to worst case the conditions evaluated. For example, under certain drag vector and altitude conditions the cloud density is not attenuated due to molecular collisions. For other conditions such as differing altitudes and drag vector orientations the predicted levels may be lower. The work performed by Robertson[38] has an important limitation because it fails to conserve mass. Molecules scattered from a line-of-sight do not "disappear"; they simply are scattered into another line-of-sight. The molecule cannot be suddenly ignored after it has undergone its first collision with either the ambient or an engine exhaust plume as Robertson assumes. The recent results of the work by Robertson[38] are therefore unrealistically low.

When conducting design and development activities, the conservative approach is generally the acceptable approach and it is consistent to all the contamination activities conducted to date. To further treat the molecular collisions within the cloud would increase the complexity of the current model and at this time

the value to improving the design and development studies is questionable. However, when performing mission evaluations for Spacelab, these types of improvements should be considered because specific payload/instrument geometries and the continually varying drag vector orientation will have to be considered as well as the sensitivities of certain specific instruments to components of the contaminant environment.

3.2 Recommendations - The following recommendations are presented as a result of the activities conducted during this reporting period which are felt necessary to insure Spacelab compliance with the current criteria or required to continue the modeling and analysis activities.

a. The following design configuration data should be supplied by ESA with periodic updates on at least a yearly basis so that continued analysis and updates can be conducted consistent with program milestones: 1) nonmetallic materials map of surfaces in excess of 0.1 m^2; 2) corresponding materials mass loss/contamination data; 3) current baseline configuration drawings; 4) allowable systems degradation (passive thermal surfaces, windows, etc); 5) overboard vent system designs, flowrates, constituents, locations, vent directions, etc. for condensate, airlock and experiment vents; and 6) Igloo purge gas leakage flowrates and locations. The lack of such data has not significantly limited the ability to conduct Spacelab design and development analyses, but is highly desirable when performing detailed Spacelab/payload mission evaluations.

b. Required nonmetallic materials test data not furnished by ESA should be supplied by NASA through inhouse testing on materials treated as to be flown.

c. To meet the intent of the 1% signal loss criteria, consideration should be given to either eliminating or restricting the use of nonmetallic external materials, selecting materials demonstrating effective outgassing rates at 100°C less than the mid 10^{-11} $g/cm^2/s$ range, or requiring sensitive payloads to provide their own protective devices and procedures.

d. To meet the intent of the column density criteria, activation of sensitive instruments should be delayed up to 24 hours until the early desorption rate has decayed sufficiently (to less than 3×10^{-8} g/cm^2/s at 100°C) and the SCV should be timelined to avoid interference with sensitive payloads.

e. To meet the intent of the particle sighting and background brightness criteria, the SCV should be timelined to avoid interference with sensitive payload data acquision.

f. To meet the intent of the return flux criteria, orbital altitudes above 575 km should be selected for sensitive missions (e.g. those containing cryogenic payloads) to minimize cabin atmosphere leakage impacts. Activation or exposure of sensitive surfaces should be delayed approximately 24 hours until early desorption has decayed sufficiently, and orbital attitudes should be selected to avoid maximum return flux orientation and to avoid the maximum vehicle surface temperature profiles.

g. To avoid being overly restrictive or overly optimistic of Spacelab contamination control, a detailed criteria evaluation of the entire STS (i.e., Orbiter, external tanks, and solid rocket boosters) in conjunction with Spacelab should be conducted to establish necessary contaminant environment "budgeting" between the STS-SL components. Spacelab payload contaminant sources should also be considered.

h. A laboratory test should be conducted to determine the effective molecular diameter or scattering cross-section of typical outgassed molecules for use in the return flux modeling analysis and radiant scattering evaluations.

i. The SCV should be located such that its effluent plume does not impinge upon any Orbiter or Spacelab surfaces. Venting along the +Z axis is considered the optimum condition.

j. Since it has been shown that design alone cannot insure a contaminant free environment for the STS-SL, complete Spacelab/Orbiter mission modeling and analysis

for each proposed payload mix and mission profile should be conducted to determine the necessary operational timelines, constraints, design modifications, etc. to insure the success of each mission from a contamination viewpoint. This activity would involve the continued development of a dynamic mission contamination model such as VOLCAN. This is deemed necessary when considering that while attempting to utilize the static predictions for one point in time to extrapolate predictions for an entire mission, variances over the mission model predictions are as great as 300%.

k. In order to expedite the continual required updating of model input data in order to maintain the mission Profile Data Bank the Spacelab Contamination Computer Model should be capable of accessing the Marshall Interactive Planning System for such data. This may require the development of a preprocessor program to establish the proper interfaces.

l. Activities which should be continued or expanded include:

   1) Spacelab model improvement and update studies including further evaluation of the influences of contaminant interactions with the ambient and other contaminants upon column density and return flux; further investigation into the "sphere of influence" or scattering cross sections for the above interactions; establishment of sticking coefficient relationships for Spacelab outgassing based upon test data on Spacelab materials; and evaluation of the ultimate impact of the contribution of reflected ambient molecules to the NCD.

   2) Combined Spacelab/Orbiter mission compatibility assessment;

   3) Integration of ESA supplied Spacelab design and test data in such areas as space nonmetallic materials and overboard vent systems; and

   4) Analysis of the Spacelab model interface requirements with MSFC for computer model transfer.

m. An activity should be conducted to establish a computer model similar in approach to the molecular Spacelab Contamination Computer Model to geometrically synthesize the induced particulate environment of a space vehicle such as Spacelab. The model should contain the major elements of source functions, transport phenomena (both aerodynamic drag and orbital mechanics) and effects upon sensitive scientific instrumentation.

n. An additional phenomena relating to the influence of mean free paths upon column density and return flux involving the molecular interactions within engine and vent plumes requires further evaluation. One major consideration that relates to this overall phenomena is that evaluation of the pulse mode operation of the flash evaporator and the RCS vernier engines indicates that films deposited on surfaces will re-evaporate during the down or off portion of each cycle. This is an additional source of mass not affected by the molecular collisions and was not considered in the predictions of Robertson[38]. This phenomena in turn increases the cloud density which is contrary to the conclusions presented in Reference 38.

o. The governing equations for most physical phenomena such as those utilized in the contamination modeling are rather simple and can be calculated rather easily, however, as one applies these relationships to an actual case; repetitive calculations are required. For this reason, MMA recommends and has chosen to put the task to the computer and use a computer model for all current and future activities in contamination assessment and evaluation. Within seconds, a tedious computation of the integrated density along an arbitrary line-of-sight can be performed consistently, a task that can consume at least a half man day of hand calculations. In addition, as stated in recommendation j, the accuracy of a single point in time calculation extrapolated to an entire mission may be questionable. The modeling approach can handle the numerous mission parametric variables with a minimal time requirement.

This should be evident with the extensive use of computer programs to evaluate other system design activities such as thermal profiles, solar cell performance,

trajectory problems, etc. For any of these evaluations, an accurate static evaluation can be performed for a point in time. However, it is the dynamic range and rates of variations which actually dictate the design and/or operational usage of a system. This requires many calculations to adequately simulate a condition. Therefore, a computer solution is a timely and cost effective approach to treat a technology that has as many variables as contamination.

4. REFERENCES

The following references are presented to support the technical and programmatic material referenced in the text of this report.

1) JSC 07700, Vol. X and XIV, Revision C, "Space Shuttle Program Space Shuttle System Payload Accommodations," July 3, 1974, Lyndon B. Johnson Space Center.

2) ECR 00049, European Space Agency, "Goals for Spacelab External Contamination Requirements."

3) Memo: ES31 from R. Naumann to NA01/Manager Spacelab Program Office, Subject: Withdrawal of ECR EL 52-0032R1, May 24, 1976.

4) "Payload/Orbiter Contamination Control Requirement Study," MSFC NAS8-30452, MCR-74-93, May 1974, Martin Marietta Aerospace, Denver Division.

5) "Payload/Orbiter Contamination Control Requirement Study," MSFC NAS8-30755 Exhibit A, MCR 74-474, December 1974, Martin Marietta Aerospace, Denver Division.

6) "Payload/Orbiter Contamination Control Requirement Study," MSFC NAS8-30755 Exhibit B, MCR-75-202, June 1975, Martin Marietta Aerospace, Denver Division.

7) "Payload/Orbiter Contamination Control Assessment Support," JSC NAS9-14212, MCR 75-13, June 1975, Martin Marietta Aerospace, Denver Division.

8) SLP/2104, "Spacelab Payload Accommodations Handbook," Preliminary Issue, May 1976, European Space Agency.

9) MCR-73-105, Rev. 1, "Thermal Radiation Analysis System (TRASYS)," NAS9-14318, May 1975, Martin Marietta Aerospace, Denver Division.

10) Robertson, S. J.: "Spacecraft Self-Contamination Due to Back-Scattering of Surface Outgassing," November 1975, Lockheed Missiles and Space Company, Inc.

11) Robertson, S. J.: "Backflow of Outgas Contamination onto Orbiting Spacecraft as a Result of Inter-molecular Collisions," June 1972, Lockheed Missiles and Space Company, Inc.

12) Memo: LSQ/JB/em/885 from J. Bruggemann to Snowdon, Baumann and Frick, European Space Agency, Subject: "Outgassing Rates of Paints/Primers," April 29, 1976.

13) Presentation to NASA on the "European Spacelab Design and Development Effort," Part F: ECS, ESRO/ESTEC, July 1974.

14) "ATM Material Control for Contamination Due to Outgassing," 50M02442 Revision W, March 1, 1972, George C. Marshall Space Flight Center.

15) "Specification - Vacuum Stability Requirements of Polymeric Material for Spacecraft Application," SP-R-0022A, September 9, 1974, Lyndon B. Johnson Space Center.

16) Muraca, R. F. and Wittick, J. S.: "Polymers for Spacecraft Applications," N6740270, September 1967, Stanford Research Institute.

17) Kydd, P. H.: "Total Scattering Cross Sections of H_2O and NH_3," Journal of Chemical Physics, Vol. 37, Number 5, September 1962.

18) Snow, W. R. et al: "Molecular Beam Measurements of Total Collision Cross Sections of H_2O," Journal of Chemical Physics, Vol. 58, Number 6, March 1973.

19) McPherson, D. G.: "ATM Contamination Study," Final Report, F67-06, March 1976, Ball Brothers Research Corporation, Boulder, Colorado.

20) Hirshfelder, J. O., Curtiss, C. F. and Bird, R. B.: Molecular Theory of Gases and Liquids, New York: John Wiley & Sons, Inc. 1954.

21) Scialdone, J. J.: "Self Contamination and Environment of an Orbiting Spacecraft," NASA TND6645, May 1972.

22) Harvey, R. L.: "Spacecraft Self-Contamination by Molecular Outgassing," Technical Note 1975-1, 31 March 1975, Massachusetts Institute of Technology, Lincoln Laboratory.

23) Mirtov, B. A., "Disturbances of Gaseous Medium Caused by Satellite Flight," IGY Annals XII Chapter 5,7 (1957-1958).

24) Technical Letter ESD-EP45-22788 from Thermodynamics Branch, Teledyne Brown Engineering to J. W. Littles, Chief Life Support and Environmental Branch, MSFC, Subject: "JSC/ESA Integrated Orbiter/Spacelab Thermal Model Temperature Data for Spacelab Extreme Design Conditions," April 12, 1976.

25) Memo: EP45 (75-78) from EP41/Mr. Hopson to NA01/Mr. Lee, Subject: Spacelab/Orbiter Payload Bay Thermal Analysis, June 1975.

26) "Payload/Orbiter Contamination Control Requirement Study," Interim Report, MSFC NAS8-31574, MCR-76-7, January 1976, Martin Marietta Aerospace, Denver Division.

27) "Spacelab Contamination Mission Support Plan," MCR-76-271, June 30, 1976, Martin Marietta Aerospace, Denver Division.

28) "Payload/Orbiter Contamination Control Requirement Study - Computer Interface Study," MCR-76-382, July 31, 1976, Martin Marietta Aerospace, Denver Division.

29) Johnson, Francis S.: Satellite Environment Handbook, Second Edition, Stanford University Press, 1965.

30) Contamination Subcontract Study: DOD Space Transportation System (STS), MCR-76-12, January 1976, Martin Marietta Aerospace, Denver Division.

31) "Summarized NASA Payload Descriptions-Sortie Payloads," Level A & B Data, July 1975, George C. Marshall Space Flight Center.

32) Informal Report/Private Communication with J. McGuire, NASA MSFC, Subject: Particle Sightings by the Skylab ATM White Light Coronograph - S052.

33) Witteborn, F.: "The Effect of the Shuttle Contaminant Environment on a Sensitive Infrared Telescope," (Preliminary), Ames Research Center, 1975.

34) Private Communication, Dr. R. M. MacQueen, Principal Investigator for S052, High Altitude Observatory, Boulder, Colorado, October 1975.

35) Van De Hulst: Light Scattering by Small Particles, New York: John Wiley & Sons, Inc. 1957.

36) "Shuttle Infrared Telescope Facility Particle Sighting Study," ARC NAS2-8494, Item ID-4.2, September 1975, Hughes Aircraft Company.

37) Muscari, J. A., and Westcott, P.: "Optical Contamination from Skylab and Gemini Flights," Applied Optics, Vol. 14, pp 2883-2891, December 1975.

38) Robertson, S. J.: "Molecular Scattering of Vernier and Flash Evaporator Plumes from Space Shuttle Orbiter Wings," LMSC-HREC TM D496810, April 1976, Lockheed Missiles and Space Company, Inc.